HYDROGEN-BASED PLASMA ETCH OF COPPER AT LOW TEMPERATURE

A Dissertation
Presented to
The Academic Faculty

by

Fangyu Wu

In Partial Fulfillment
of the Requirements for the Degree
Doctor of Philosophy in the
School of Chemical & Biomolecular Engineering

Georgia Institute of Technology
May 2011

HYDROGEN-BASED PLASMA ETCH OF COPPER AT LOW TEMPERATURE

Approved by:

Dr. Dennis W. Hess, Advisor
School of Chemical & Biomolecular Engineering
Georgia Institute of Technology

Dr. James D. Meindl
School of Electrical & Computer Engineering
Georgia Institute of Technology

Dr. Victor Breedveld
School of Chemical & Biomolecular Engineering
Georgia Institute of Technology

Dr. Elsa Reichmanis
School of Chemical & Biomolecular Engineering
Georgia Institute of Technology

Dr. J. Carson Meredith
School of Chemical & Biomolecular Engineering
Georgia Institute of Technology

Date Approved: Feb 21, 2011

ACKNOWLEDGEMENTS

First of all, I would like to express my sincere gratitude to my advisor Dr. Dennis W. Hess for his invaluable guidance and tremendous support. I always admire his continuous encouragement which helped me to be very creative and innovative at research. He taught me not only how to perform the stressful research work in an extremely productive way, but also how to deal with those negative moods in my PhD life, which is the philosophy of life. As I always say, I can not survive my PhD without Dr. Hess' enormous patience and thoughtful concerns to me. I would also like to thank my committee members, Dr. Victor Breedveld, Dr. J. Carson Meredith, Dr. Elsa Reichmanis and Dr. James D. Meindl for serving on my committee and for providing valuable suggestions.

I am grateful to all the past and present members of Dr. Hess' research group, Dr. Galit Levitin, Dr. Ingu Song, Dr. Lingbho Zhu, Dr. Shantanu C. Pathak, Dr. Yonghao Xiu, Dr. Balamurali Balu, Dr. Ashish Pande, Sonam Sherpa, Lester Li, Michael Casciato, for helping me with ideas and making my graduate life a wonderful learning experience. In particular many thanks to Dr. Levitin for attending my numerous meetings with Dr. Hess and performing a lot of experiments for me; to Dr. Zhu and Dr. Pathak for guiding me to start my first research project on CVD and plasma polymerization; to Dr. Pande for responding to all my trivial problems. In addition, members from other research groups have also been very supportive during my research. Many thanks to Huawei Chu for helping me with AFM and ellipsometry studies, Yan Liu for helping me with UV lamps studies.

As a very important part of my PhD life, I would like to express my great appreciations to the staffs and students who working in the Georgia Tech MiRC cleanroom: Tran-Vinh Nguyen, Gary Spinner, Kevin Martin, William Kimes, Eric Woods, Walter Henderson, Mengli Wang, Xing Gao, Hao Fang. My special thanks go to Tran-Vinh Nguyen for addressing any issues with the ICP reactors, to William Kimes for helping me to set up the MS and OES systems, to Gary Spinner and Kevin Martin for giving permissions to my equipment requests, to Mengli Wang, Xing Gao and Hao Fangy for helping me to be familiar with most of the cleanroom equipments. I would also wish to thank Dr. Nagraj S. Kulkarni and Dr. Ivan Kravchenko for helps during my two-week stay at the Center for Nanophase Materials Sciences (CNMS) in Oak Ridge National Lab (ORNL) to perform the low temperatures studies using their ICP reactor. My sincere thanks go to Dr. Benjamin Schwarz for the donation of OES from Applied Materials.

I would also like to thank my parents and sisters for their constant love and support. Particularly my parents, even though they know nothing about my research work, they always show great interests and happiness to listen to my talks about PhD life, and they are always the strongest supporters through all of the tough times. My family is the sole reason for why I'm doing what I am doing now. Last but important, I am grateful to all my friends from all around the globe for their love and encouragement. Especially, I thank Dr. Xuejia Yan, Dr. Jun Jia, Qiong Guo and Yun Wang who always encouraged me and helped me with those difficult times when I first arrived at Atlanta.

TABLE OF CONTENTS

LIST OF TABLES

LIST OF FIGURES

Page

LIST OF SYMBOLS AND ABBREVIATIONS

RF1	Platen power
RF2	Coil power
ΔH_{dec}^{0}	Standard decomposition enthalpy
ΔH_{298}^{0}	Standard formation enthalpy
$C_{p,m}$	Specific heat capacity
$A_{CuH:Cu}$	Mole ratio of CuH to Cu
ΔT	Temperature increase
IC	Integrated circuit
RC	Resistance-capacitance
rf	radio frequency
ICP	Inductively coupled plasma
CMP	chemical mechanical planarization/polishing
AR	aspect ratios
DI water	De-ionized water
ITRS	International technology roadmap for semiconductors
RIE	Reactive ion etch
ECR	Electron cyclotron resonance
PECVD	plasma enhanced chemical vapor deposition
sccm	standard cubic centimeter per minute
XPS	X-ray photoelectron spectroscopy
SEM	Scanning electron microscope
PVD	Physical vapor deposition

UV	Ultra violet
IR	Infrared radiation
RGA	Residual gas analyzer
MS	Mass spectroscopy
VUV	Vacuum Ultraviolet
DC	Direct current
ER	Etch rate
GD-OES	Glow discharge coupled optical emission spectrometry
OES	Optical emission spectroscopy
ORNL	Oak ridge national laboratory
UHV	Ultra high vacuum
ORNL	Oak ridge national laboratory
FTIR	Fourier transform infrared spectroscopy

SUMMARY

Although copper (Cu) is the preferred interconnect material due to its lower resistivity than aluminum (Al), Cu subtractive etching processes have not been developed at temperatures less than 180 ^{o}C, primarily due to the inability to form volatile etch products at low temperature. The conventional damascene technology avoids the need for subtractive etching of Cu by electroplating Cu into previously etched dielectric trenches/vias, followed by a chemical/mechanical planarization (CMP) process. However, a critical "size effect" limitation has arisen for damascene technology as a result of the continuing efforts to adhere to "Moore's Law". The size effect relates to the fact that the resistivity of damascene-generated lines increases dramatically as the line width approaches the sub-100 nm regime, where feature size is similar to the mean free path of electrons in Cu (40 nm). As a result, an alternative Cu patterning process to that of damascene may offer advantages for device speed and thus operation.

This thesis describes investigations into the development of novel, fully-plasma based etch processes for Cu at low temperatures (10 ^{o}C). Initially, the investigation of a two-step etch process has been studied. This etch approach was based on a previous thermodynamic analysis of the Cu-Cl-H system by investigators at the University of Florida. In the first step, Cu films are exposed to a Cl_2 plasma to preferentially form $CuCl_2$, which is believed to be volatilized as Cu_3Cl_3 by subsequent exposure to a hydrogen (H_2) plasma (second step). Patterning of Cu films masked with silicon dioxide (SiO_2) layers in an inductively coupled plasma (ICP) reactor indicates that the H_2 plasma step in the two-step process is the limiting step in the etch process. This discovery led to

the investigation of a single step Cu etch process using a pure H_2 plasma. Etching of blanket Cu films and Cu film patterning at 10 ^{o}C, display an etch rate ~ 13 nm/min; anisotropic etched features are also observed. Comparison of H_2 plasma etching to sputtering of Cu films in argon (Ar) plasmas, indicates that both a chemical component and a physical component are involved in the etching mechanism. Additional studies using helium plasmas and variation of power applied to the plasma and etching surface demonstrate that the etch rate is controlled by reactive hydrogen species, ion bombardment flux and likely photon flux. Optical Emission Spectroscopy (OES) of the H_2 plasma during the Cu etching process detects Cu emission lines, but is unable to identify specific Cu etch products that desorb from the etching surface. Variation of Cu etch rates as a function of temperature suggests a change in mechanism for the removal of Cu over the temperature of -150 ^{o}C to 150 ^{o}C. OES analyses also suggest that the Cl_2 plasma step in the two-step process can inhibit Cu etching, since the subsequent H_2 (second) plasma step shows a time delay in film removal. Preliminary results of the etching of the SiO_2 mask material in H_2 plasmas with various intentionally introduced contaminants demonstrate the robustness of the H_2 plasma Cu etch process.

CHAPTER 1

INTRODUCTION

1.1 Background

1.1.1 Microelectronics Device Progression and Interconnect Metallization

The silicon-based microelectronics or integrated circuit (IC) industry has had an impressive progression with increasing number of devices, higher functionality and enhanced speed demonstrated by devices and circuits in succeeding generations. Recognition and quantification of this progression resulting from the economics of electronic device fabrication (manufacturing cost per individual component as related to circuit complexity) was formulated 45 years ago by Gordon Moore. His observed trends and predictions, subsequently referred to as "Moore's Law", indicated that the number of components per IC chip doubles every 1.5 to 2 years; indeed this "law" has accurately described the long term trend in the IC industry for more than four decades[1-2]. The ability of the IC industry to adhere to Moore's Law was for many years primarily dependent upon the continued reduction in patterned feature size which allows increased numbers of devices to be fabricated per unit area of silicon. In recent years, adherence to 'Moore's Law' has led to severe requirements on the density of interconnects for devices or circuits with more than one billion transistors.

With this extraordinary number of devices to interconnect, higher circuit speed became a very important factor for improving performance of new generations of ICs. Circuit speed is determined by the time to transport carriers (electrons or holes) within

the transistors and the time for carriers to transport through interconnections between devices. The latter time is called an RC delay, where R is the effective resistance and C the effective capacitance [3-4]. RC delay strongly depends on wire length and material properties [5], However, RC delay does not scale down as the feature size is scaled down; interconnect RC delay increases as interconnect pitch (line width and space) decreases due to the increase in line resistance [6-7]. In deep sub-micron design, RC delay became dominant in determining the overall circuit performance [8].

Reductions in RC delay can be achieved by selecting a material with higher electrical conductivity and by using a dielectric material to isolate the metal interconnect layers that has a low dielectric constant (low-k), or at least a lower k than that of SiO_2 [9]. Thus both the introduction of low-k materials and the replacement of aluminum (Al) by copper (Cu) have taken place. Specifically, the lower electrical resistivity of Cu (1.7 μΩ-cm) compared to that of Al (2.7 μΩ-cm) has been critical in enhancing device performance [10]. This change substantially reduced the RC delay, thereby enabling higher speed operation for the continuously shrinking integrated circuits (ICs).

In addition to RC delay improvements, the enhanced electromigration resistance of Cu relative to Al represents another significant improvement of Cu metallization over Al. Electromigration is a transport phenomenon associated with drift of atoms in a conductor under the influence of an electric field and in the direction of the electron flow [11]. Electromigration is a major cause of reliability limitations for metal lines [3, 12] due to lower Cu grain boundary diffusivities [13]. Indeed, in Al lines, electromigration is controlled by alloying Al with Cu. Due to these advantages, Cu became the preferred choice of conductive material and has essentially replaced Al.

1.1.2. Plasma Etching or Pattern Definition

Plasmas are partially ionized gases that contain chemically active species (e.g., free radicals and excited state atoms/molecules) and energetic radiations: ions, electrons and photons [14-15]. These species are generated by electron impact collisions wherein electrons, accelerated by the radio frequency (rf) field, transfer their energy to molecules or atoms causing excitation, dissociation, and ionization. In addition, ion acceleration into surfaces in contact with the plasma impart energy and thus directionality/anisotropy to the etch process. Plasma etching involves 3 steps: (1) active species are formed by electron collisions; (2) the active species adsorb on the surface and react with the surface to form volatile products; (3) the volatile products leave the surface and are pumped out of the chamber [14]. If any of the three steps does not occur, etching will terminate. Specifically, the limitation experienced in attempts at low temperature plasma etching of Cu has been the inability to form volatile etch products.

Physical and chemical surface processes are essential to plasma etching. Four basic plasma-surface processes involved in etching can be considered as illustrated in Figure 1.1 [15]): sputtering, pure chemical etching, ion energy driven etching and ion-enhanced inhibitor etching. Sputtering is the ejection of atoms from surfaces due to momentum transfer by energetic ion bombardment and has essentially no selectivity to underlying films or mask materials; etch rates are typically low, but sputtering can assist removal of low volatility materials. In pure chemical etching, the etching is highly selective but almost invariably isotropic since chemical reactions rather than ion bombardment control the directionality. Ion energy-driven etching combines chemical

and physical effects of etchant atoms and energetic ions; etch rates generally increase with increasing ion energy although a trade-off exists between anisotropy and selectivity. In ion-enhanced inhibitor etching, precursor molecules from the plasma deposit onto all surfaces, including sidewalls, and thereby inhibit lateral etching while ion-enhancement removes inhibitor species at the trench bottom to allow anisotropic etch profiles [15].

In the work described in this thesis, an inductively coupled plasma (ICP) reactor was used as the primary plasma system. As indicated in Figure 1.2 [15], an ICP has two rf power supplies, one that supplies power to the coil, and thereby generates high density plasmas, and the other that supplies power and thus controls the voltage on the electrode where the substrate/film resides. With these two power supplies, nearly independent control of ion and neutral densities (coil power) and ion energy (electrode power) is possible that permits improved control of the overall etch process.

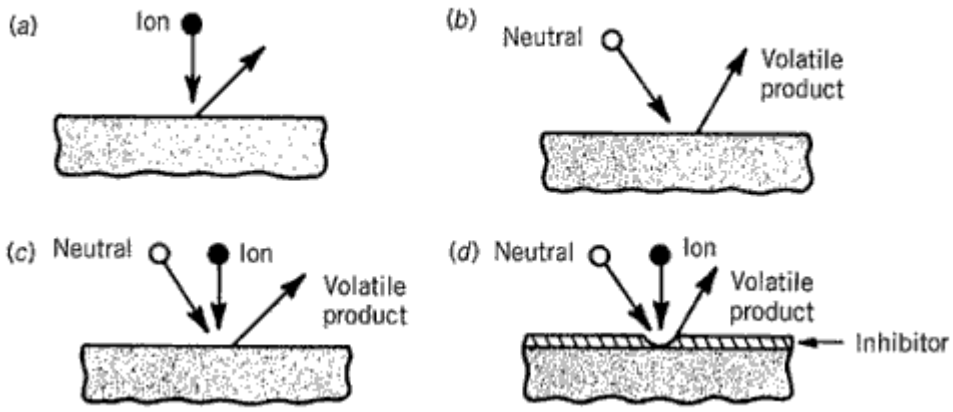

Figure 1.1. Four basic plasma-surface etch processes: (a) sputting; (b) pure chemical etching; (c) ion energy-driven etching; (d) ion-enhanced inhibitor etching [15]

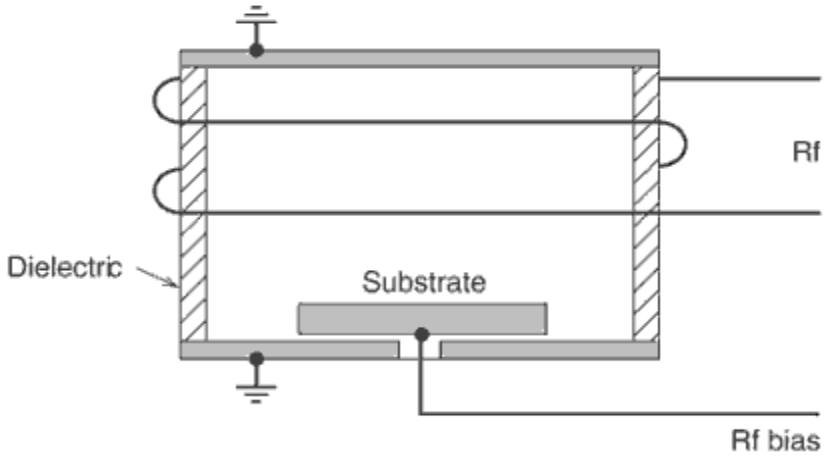

Figure 1.2. Schematic of a cylindrical inductively driven plasma reactor [15]

1.1.3 Current Copper Metallization Technology

Initially, the transition from patterning Al to patterning Cu was unsuccessful. With Al metallization, blanket films are deposited by evaporation or sputtering, and patterns formed by plasma-based etch processes using chlorine-containing gases such as BCl_3 and Cl_2 with photoresist as an etch mask. But unlike Al, Cu did not form volatile halogenated etch products at temperatures below 180 ^oC, which inhibited the subtractive plasma etching of Cu at temperatures compatible with organic resist materials [16]. Even with the implementation of "hard" masks such as SiO_2, difficulties were encountered because considerable sputtering of the mask material occurred as a result of the combined effects of significant ion bombardment energy and flux, and elevated temperature needed to obtain adequate etch rates and anisotropic etch profiles [5]. These restrictions led to the introduction of damascene technology in 1997 [17].

In the damascene process, the need to subtractively pattern or etch Cu is avoided by first plasma etching trenches or vias in a dielectric layer to form the regions where Cu interconnects are to be placed. Cu films are then electroplated into the vias, followed by chemical mechanical planarization/polishing (CMP) removal of the Cu overburden that exists above the dielectric film [18]. Figure 1.3 shows a comparison of subtractive etch processes and the damascene process[19]. The major difference is that the need to plasma etch Cu is obviated by first patterning the dielectric material (normally SiO_2) followed by plating of Cu into the trenches or vias. Thus, the sequence of film patterning and deposition are reversed relative to the subtractive process.

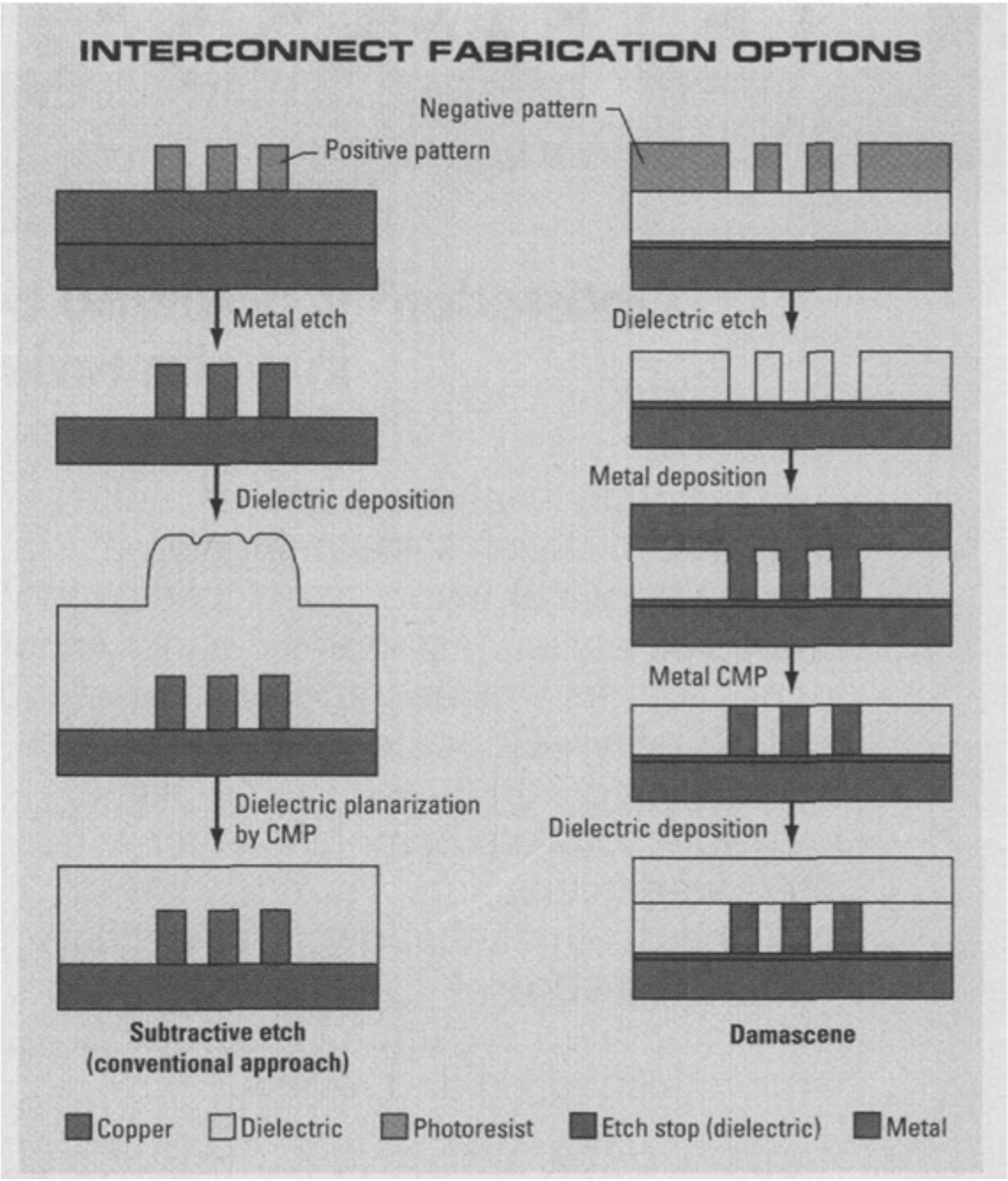

Figure 1.3 Comparison of subtractive etch process and damascene process [19]

Although the damascene approach offers a method to obtain Cu patterns, numerous problems exist with electroplating. For example, “superfilling” of the via or trench is required. “Superfilling” refers to the defect-free filling of trenches or vias that

have vertical walls and high aspect ratios (ARs); that is, superfilling results in a higher deposition rate at the trench bottom than on the trench sides [18]. Thus plating bath additives are necessary to accomplish this mode of filling. Two categories of additives are needed based upon their specific functions: accelerators and inhibitors. Accelerators are typically sulfur-containing organic compounds that preferentially adsorb onto the trench bottom. In comparison, inhibitors are generally polymeric species such as ethylene glycol in the presence of chloride, that suppress deposition rates [20]. Due to the presence of additives, incorporation of impurities into the Cu films from the plating baths is unavoidable, which leads to the inhibition of grain growth during subsequent annealing [13, 18]. In addition, control of the CMP process in terms of uniformity, defect generation, Cu corrosion and impurity incorporation has been problematic [13, 21]. Finally, CMP uses large quantities of chemicals, de-ionized (DI) water, and consumables (e.g., pads, polishing slurries) and therefore has a significant environmental impact [22-23]. It should be noted that the CMP process cannot be eliminated entirely from back end of line IC fabrication sequences due to the need for dielectric planarization. Nevertheless, if an effective subtractive Cu etch process can be developed, Cu polishing will not be required, resulting in the elimination of corrosion and impurity incorporation introduced by the slurry. Therefore, pre-patterned annealing of Cu films should yield larger grain sizes and thus lower film resistivities.

1.1.4 Size Effect Limitations in Damascene Technology

Damascene technology has played an essential role in the initial implementation of Cu metallization. However, a critical limitation in this approach to Cu patterning has

arisen due to the adherence of the IC industry to Moore's Law and thus the reduction of minimum feature sizes, currently (2010) at 45 nm, as described by the International Technology Roadmap for Semiconductors (ITRS) [2]. This limitation is the "size effect " of Cu, a phenomenon in which the electrical resistivity of Cu increases rapidly as lateral dimensions are reduced below 100 nm (displayed in Figure 1.4) , thereby approaching the electron mean free path in Cu (40 nm at 25 ^{o}C) [24-27]. The size effect in electrical resistivity is a critical limitation to future device generations in the IC industry, since this phenomenon increases the voltage drop, signal propagation delay, and Joule heating in narrow lines. As a result of the resistivity increase, device and circuit speed decrease with decreasing pattern or feature size; this effect can also have an adverse effect on the reliability of local interconnects.

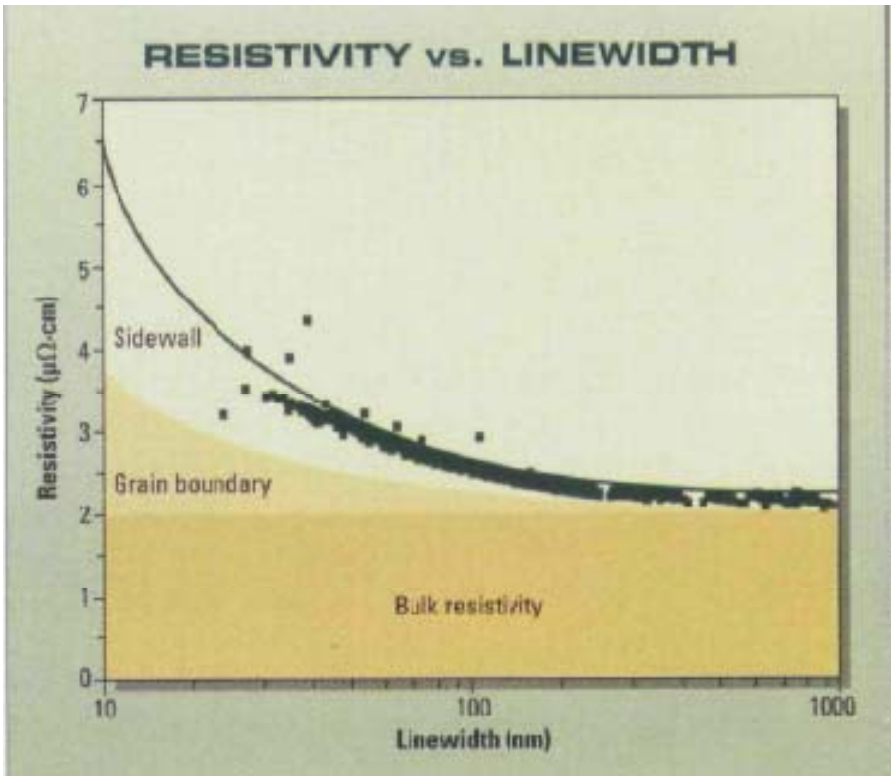

Figure 1.4. Dependence of resistivity of damascene copper lines on line width [27]

The size effect in Cu is caused by electron scattering from both Cu sidewalls and grain boundaries [26, 28]. Thus two approaches exist to reduce or eliminate this size effect: decrease the Cu sidewall/surface roughness and grow larger Cu grains. However, grain growth of Cu in damascene technology is dramatically hindered by the narrow geometries [29] and impurities introduced into Cu that result from CMP and plating processes [30]; that is, grain boundaries are pinned at the sidewalls, thereby limiting grain growth and electroplating is a liquid process where solvents and additives in the bath that permit defect-free filling of narrow, high aspect ratio trenches [31] are incorporated into the Cu film. Therefore, the Cu size effect that causes degradation of current and future device speed cannot be suppressed fully by existing Cu patterning technology. Rather, development of new Cu patterning technologies that mitigate the size effect are required if the past progression of the silicon semiconductor industry (e.g., Moore's Law) is to continue into future device generations.

With the exception of Cu, plasmas are used to define patterns for the films used in IC fabrication. In comparison to damascene technology, subtractive plasma etching begins with a blanket, high purity (sputtered or evaporated instead of plated) and annealed Cu film which therefore has reasonable grain size (~1.5 times the film thickness in the sub-100 nm regime) [29-30, 32]. The resistivity of the blanket, high purity, annealed Cu film should therefore increase only moderately when patterned by plasma etching. An increase in resistivity is expected due to the small line width (< 100 nm) and thus surface scattering that takes place in Cu patterns with widths similar to the electron mean free path. Because plasma-based etching can be used to pattern metal (conducting) films other than Cu, this method of reducing the size effect can be evaluated. Indeed,

clear advantages of subtractive etching compared to a damascene process have been demonstrated for patterned tungsten (W) films in the sub-100 nm regime. Reactive ion etched (RIE) W lines showed a distinctly lower resistivity than did W lines defined by the damascene process, where the resistivities reported were ~13 μΩ-cm for RIE lines vs. 18~23 μΩ-cm for damascene lines [33]. A similar advantage may therefore be expected for Cu. Thus, effective fabrication of future Cu-metallized devices may depend on the development of a plasma-based subtractive etch process.

1.1.5 Approaches to Plasma-based Cu Etching

Halogen-based (specifically chlorine-containing) plasmas have to date been the ones investigated to plasma etch Cu. In large part this has occurred because copper chlorides have the highest volatility of any halogen-containing Cu compound. Furthermore, other conducting films such as Al, W, and heavily doped polycrystalline silicon have been successfully etched by chlorine-based plasmas for many years [34]. The etch mechanism of Cu can be considered a two-step process: (1) formation of Cu halides ($CuCl_x$ or $CuBr_x$); (2) removal or desorption of these Cu halides [35]. However, removal of Cu etch products from the surface is hindered due to the low volatility of Cu halides.

High temperatures (> 180 ^oC) have been generally invoked to enhance desorption of Cu chlorides [35-40]. At such temperatures, photoresist could not be used as a masking material; thus hard masks such as SiO_2 or metals were used. ICP (inductively coupled plasma) or ECR (electron cyclotron resonance) plasma reactors were utilized to achieve high etch rates (up to 500 nm/min); RIE reactors typically yielded relatively low etch

rates (<100 nm/min) even with the addition of N_2 or Ar into the halogen-based plasmas. Addition of Ar or other gases increased the etch rate but did not substantially lower the required high temperatures.

Since Cu etch rates were believed to be limited by desorption of $CuCl_x$ from the etching surface (at lower temperatures), additional energy input to the surface was supplied to accelerate desorption, such as laser impingement or UV photon irradiation. Indeed, photon-enhanced removal of Cu chlorides at temperatures below 100 ^oC by laser [41], UV [42-46], or infrared radiation [47-48] has been reported. These processes are believed to be driven either by local heating to promote thermal evaporation of etch prodcuts, or by non-thermal processes such as electronic excitation. The exact cause of the enhanced etch rates at low temperatures is currently undefined.

Both these approaches to achieve plasma etching of Cu films introduce complexity and control issues into the patterning process. For example, high temperatures greatly limit the choice of mask materials and lead to etch system compatibility issues, while exposure of the etching surface to photons increases etch reactor complexity although more reasonable temperatures are apparently possible. In order to avert problems with product desorption, Cu chlorides formed by chlorine- or bromine-containing plasmas have been removed by immersion of the halogenated Cu layers in dilute HCl solutions; this approach offers an alternative low temperature two-step approach to Cu patterning [49]. Although this method greatly reduced the temperature required to remove the Cu chlorides, and thus permits the use of photoresist as a patterning mask, the combination of vacuum and liquid processes increases the system complexity, reduces the manufacturing throughput, and may lead to process integration

issues. Thus, to date, none of the approaches reported have demonstrated a simple, fully plasma-based Cu etching process that is suitable for future device and IC fabrication.

1.2 Thermodynamic and Kinetic Considerations in Plasma-Based Cu Etching

1.2.1 Theoretical Justification for a Two-Step Plasma Etch Process for Cu

Studies of the interaction of chlorine (without plasma enhancement) with Cu surfaces [50-52] demonstrated that with low Cl_2 exposure doses at 25 °C, a Cu chloride with an average stoichiometry of $CuCl_x$, $0<x<2$, is formed; at high exposure doses, a mixture of CuCl and $CuCl_2$ is observed [52]. In the temperature range of 170 to 200 °C, Cu_3Cl_3 is the gaseous product that is reported to desorb from a CuCl surface layer [50-51]. Furthermore, for a constant exposure dose, the amount of Cu_3Cl_3 desorbed, as detected by mass spectrometry, increases with a decrease in temperature, rising rapidly below 50 °C; that is, Cl_2 reacts much faster with Cu at 30 °C than at 125 °C [50], suggesting that either the reaction is adsorption limited or a high volatility etch product is formed under these conditions.

The above information suggests that (a) Cu can be easily chlorinated to form CuCl and $CuCl_2$, (b) desorption of copper chlorides, including Cu_3Cl_3 can occur, (c) temperatures below 30 °C may give rapid chlorination (chloride formation) rates. With plasma enhancement to generate Cl and supply ion bombardment, anisotropic chlorination may occur to form $CuCl_x$. Although Cu_3Cl_3 can desorb at temperatures < 200 °C, this is still inadequate for implementation of photoresist as a mask material. Such results suggest that if a method can be devised to readily and rapidly convert CuCl or

$CuCl_2$ into a relatively volatile copper etch product, perhaps Cu_3Cl_3 that can be desorbed at T < 50 °C, then combination of this process with a plasma-enhanced chlorination of Cu should allow low temperature, vapor phase Cu etching. This process would represent a paradigm shift in the fabrication of Cu-based interconnects for ICs. This novel approach should also offer a reliable, low contamination level, cost effective, and environmentally benign process that could at least partially mitigate the size effect limitation of the current damascene process for Cu patterning and greatly facilitate continuing advances in IC technology.

A thermochemical analysis was used to investigate various solid-gas volatilization reactions in the Cu-Cl-H system at temperatures < 200 °C [53]. Consideration of the Cu-Cl volatility diagram indicates that under equilibrium conditions, the vapor pressures of gaseous Cu species such as CuCl, $CuCl_2$, and Cu_3Cl_3 are low. In fact, Cu_3Cl_3 does not have sufficient vapor pressure to ensure adequate etch rates significantly below 200 °C, since the vapor pressure is < 10^{-8} atm, consistent with previously reported observations of Cu etching [50-51]. If a reactive gas such as atomic H is introduced into the Cu-Cl system, an equilibrium such as that described by Eqn (1.1) may be operative:

$$3\ CuCl_2\ (c) + 3\ H\ (g) = Cu_3Cl_3\ (g) + 3HCl\ (g) \qquad (1.1)$$

The volatility diagram corresponding to Eqn (1.1) is shown in Figure 1.5, where the metastable equilibrium between solid $CuCl_2$ and gaseous Cu_3Cl_3 is shown and the isobaric lines for different H partial pressures displayed. This figure indicates that even at low partial pressures of H, reasonably high pressures of Cu_3Cl_3 are achievable. In

addition, Eqn (1.1) is exothermic, so that the driving force for reaction (1.1) is favorable [53]. Perhaps the most interesting observation in Figure 1.5 is that the isobaric lines have a negative slope, indicating that the Cu_3Cl_3 partial pressure for a specific partial pressure of H increases as the temperature decreases [53]. Such trends suggest that it may be possible to volatilize Cu_3Cl_3 from $CuCl_2$ at low temperature in the presence of H, and thereby enhance etch rates even at temperatures significantly below 100 ^oC. Although the concentration of H in an H_2 atmosphere at reasonable temperatures is extremely small, plasma dissociation of H_2 will increase the H partial pressure substantially, and thus may enhance Cu_3Cl_3 removal rates.

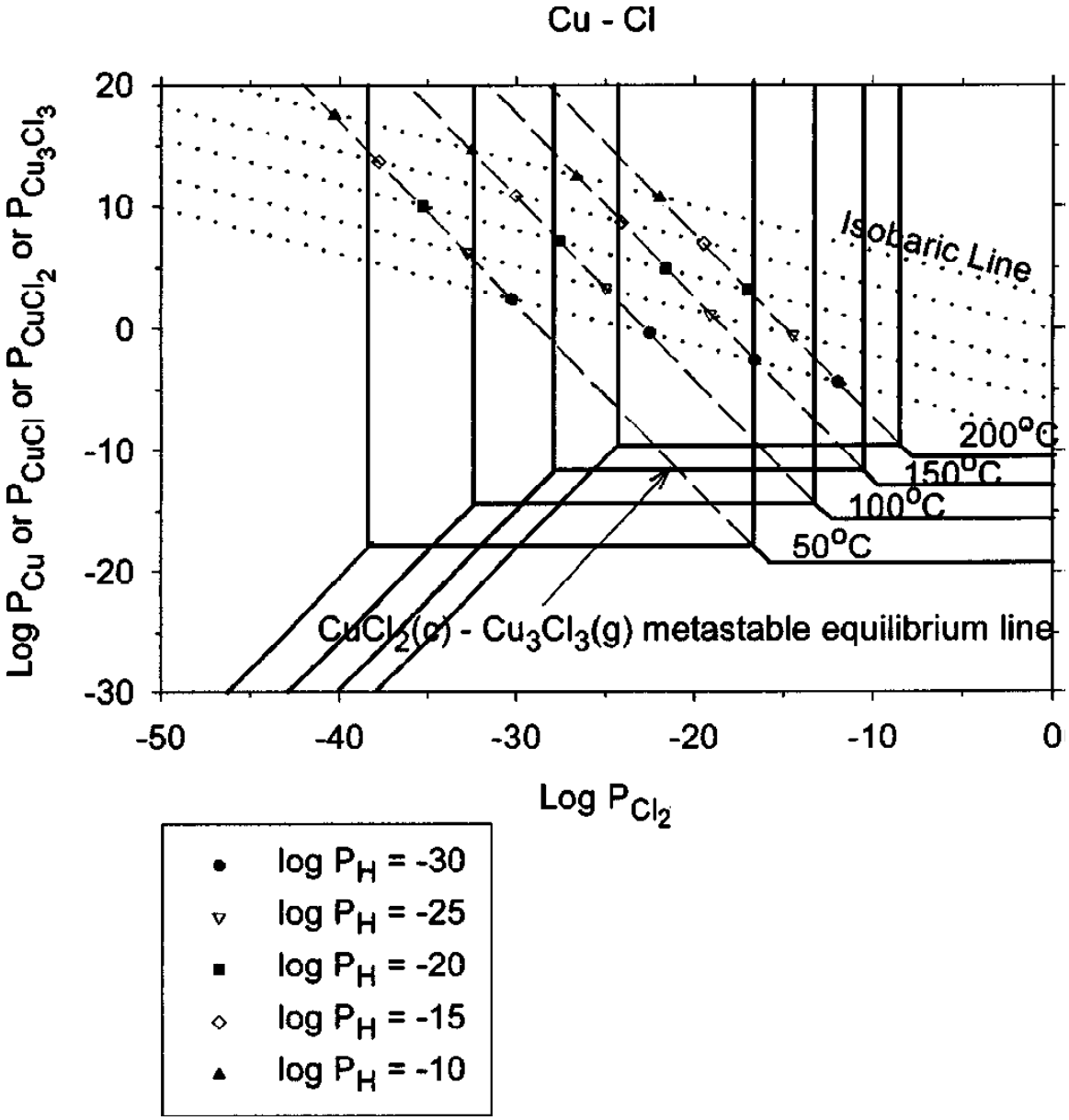

Figure 1.5. Volatility diagram for the Cu-Cl system showing the isobaric lines for various partial pressures of H (in atm) for the reaction $3CuCl_2(c) + 3H(g) = Cu_3Cl_3(g) + 3HCl(g)$ [53].

1.2.2 Two-Step Plasma Etch Process for Cu

Based upon the above thermodynamic analysis, a novel two-step plasma etching scheme was proposed to address the problem of low-temperature, plasma-assisted dry

etching of copper [53]. The conceptual process, illustrated in Figure 1.6, consists of two steps, which will require a number of cycles in order to remove thick (probably >10 nm) Cu films. In the first step, Cu is chlorinated at low temperature in a Cl_2 plasma with $CuCl_2$ preferentially formed over CuCl on the etching surface. In the second step, the $CuCl_2$ layer is exposed to an H_2 plasma which according to Eqn (1.1) promotes the reaction of $CuCl_2$ with H atoms to form Cu_3Cl_3; if the volatility of this product sufficient, Cu_3Cl_3 can then evaporate from the surface [53]. These two steps can be repeated an appropriate number of times as needed to obtain the desired etch depth as shown schematically in Figure 1.6.

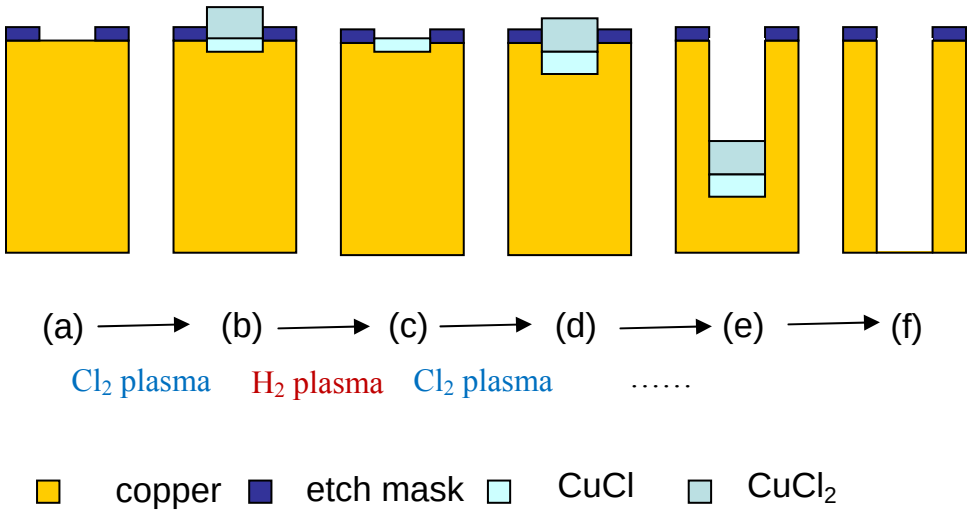

Figure 1. 6. Proposed two-step plasma etching process [53]to pattern or etch a copper feature: (a) a resist pattern creation; (b) exposure to a chlorine plasma for a specified time to convert a certain thickness of Cu to CuCl and $CuCl_2$, assuming anisotropic growth with a $CuCl_2$ layer on top of CuCl; (c) $CuCl_2$ layer removal with a hydrogen plasma using the $CuCl_2$-Cu_3Cl_3 reaction described by Eqn (1.1); (d) process shown in (b) is repeated; (e) after a number of cycles involving the two sequential steps shown in (b) and (c) ; (f) completion of etch after the necessary number of cycles.

The goal of this thesis is to evaluate the possibility of using plasmas, particularly those of chlorine and hydrogen, to etch patterns in copper films at temperatures below 50 ^{o}C, based upon previous thermodynamic analyses of the Cu-Cl-H system. Our particular interests are identification of the rate controlling step in this process and the generation of mechanistic insight for such low temperature copper etch processes. Since anisotropy, etch selectivity to mask materials and underlying adhesive layers (e.g., Ti) and edge roughness are important aspects of a successful etch process, these issues will also be investigated. If successful, this novel approach to copper pattern definition could supply an attractive alternative to the conventional damascene process for future IC device fabrication.

1.3 Thesis Objectives and Organization

The brief introduction in this chapter describes the motivation and background related to low temperature plasma-based etching of copper films. In the following chapters, details regarding the studies performed are described. In particular, the specific objectives of this thesis project are:

(1) Investigate approaches to design a low temperature plasma etch process for Cu;

(2) Gain insight into the mechanisms involved in this plasma etch process;

(3) Investigate the feasibility of such a low temperature plasma etch process by evaluating characteristics required for the fabrication of device geometries such as adequate etch rate, selectivity, and anisotropy;

(4) Compare the advantages of this low temperature plasma etch process to the current damascene method for Cu patterning.

Chapter 2 describes the investigation of a two-step plasma etching process for Cu that involves Cu chlorination followed by reduction to form a more volatile etch product. *Chapter 3* describes a novel low temperature plasma etching process for Cu inspired by mechanistic investigations of the two-step process; this new process uses only one step, a H_2 plasma. *Chapter 4* describes the effect of various plasma parameters on the physics and chemistry involved in Cu etching. *Chapter 5* utilizes optical emission spectroscopy and temperature control to gain insight into the mechanism of the H_2 plasma etching process. *Chapter 6* investigates the effect of H_2 plasmas on SiO_2 masks during the Cu etch process, and evaluates the effect of various contaminants present in the etch reactor on SiO_2 etch rates. *Chapter 7* presents an overall summary and conclusions obtained from this project and offers recommendations for future research.

1.4 References:

[1] G. E. Moore, "Cramming More Components onto Integrated Circuits," *Electronics,* vol. 38, pp. 114-117, April 19 1965.

[2] *International technology roadmap for semiconductors 2008 update*, 2008.

[3] R. Rosenberg, D. C. Edelstein, C. K. Hu, and K. P. Rodbell, "Copper metallization for high performance silicon technology," *Annual Review of Materials Science,* vol. 30, pp. 229-262, 2000.

[4] M. Morgen, E. T. Ryan, J.-H. Zhao, C. Hu, T. Cho, and P. S. Ho, "Low dielectric constant materials for ULSI interconnects," *Annual Review of Materials Science,* vol. 30, pp. 645-680, 2000.

[5] R. Doering and Y. Nishi, *Handbook of semiconductor manufacturing technology*, 2nd ed. Boca Raton: CRC Press, 2008.

[6] M. T. Bohr, "Interconnect scaling--the real limiter to high performance ULSI," *Solid State Technology,* vol. 39, p. 105, 1996.

[7] M. T. Bohr and Y. A. El-Mansy, "Technology for advanced high-performance microprocessors," *IEEE Transactions on Electron Devices* vol. 45, pp. 620-625, 1998.

[8] L. Tsu-Chang and J. Cong, "The new line in IC design," *Spectrum, IEEE,* vol. 34, pp. 52-58, 1997.

[9] R. H. Havemann and J. A. Hutchby, "High-performance interconnects: an integration overview," *Proceedings of the IEEE,* vol. 89, pp. 586-601, 2001.

[10] D. R. Lide, *CRC Handbook of Chemistry and Physics*, 84th ed. Boca Raton: CRC Press, 2003.

[11] P. G. Slade, *Electrical contacts: principles and applications*. New York: Marcel Dekker, 1999.

[12] J. R. Black, "Electromigration-A brief survey and some recent results," *Electron Devices, IEEE Transactions on,* vol. 16, pp. 338-347, 1969.

[13] P. Singer, "Copper Challenges for the 45 nm Node," *Semiconductor International,* vol. 27, pp. 40-46, 05 2004.

[14] A. Grill, *Cold plasma in materials fabrication: from fundamentals to applications*. Piscataway, NJ: IEEE Press, 1994.

[15] M. A. Lieberman and A. J. Lichtenberg, *Principles of plasma discharges and materials processing*, 2nd ed. Hoboken, N.J.: Wiley-Interscience, 2005.

[16] C. Steinbruchel, "Patterning of copper for multilevel metallization: reactive ion etching and chemical-mechanical polishing," *Applied Surface Science,* vol. 91, pp. 139-146, 1995.

[17] D. Edelstein, J. Heidenreich, R. Goldblatt, W. Cote, C. Uzoh, N. Lustig, P. Roper, T. McDevitt, W. Motsiff, A. Simon, J. Dukovic, R. Wachnik, H. Rathore, R. Schulz, L. Su, S. Luce, and J. Slattery, "Full copper wiring in a sub-0.25 um CMOS ULSI technology," in *Technical Digest., IEEE international Electron Devices Meeting*, 1997, pp. 773-776.

[18] P. C. Andricacos, C. Uzoh, J. O. Dukovic, J. Horkans, and H. Deligianni, "Damascene copper electroplating for chip interconnections," *IBM Journal of Research and Development,* vol. 42, p. 567, 1998.

[19] L. Peters, "Pursuing the perfect low-k dielectric," *Semiconductor International,* vol. 21, pp. 64-74, 1998.

[20] M. Datta, "Electrochemical processing technologies in chip fabrication: challenges and opportunities," *Electrochimica Acta,* vol. 48, pp. 2975-2985, Sep 30 2003.

[21] R. Bajaj, A. Zutshi, R. Surana, M. Naik, and T. Pan, "Integration challenges for CMP of copper," *Mrs Bulletin,* vol. 27, pp. 776-778, Oct 2002.

[22] B. Maag, D. Boning, and B. Voelker, "Assessing the Environmental Impact of Copper CMP," *Semiconductor International,* vol. 23, p. 101, 10 2000.

[23] J. H. Golden, R. Small, L. Pagan, C. Shang, and S. Ragavan, "Evaluating and Treating CMP Wastewater," *Semiconductor International,* vol. 23, p. 85, 10 2000.

[24] A. Mallikarjunan, S. Sharma, and S. P. Murarka, "Resistivity of Copper Films at Thicknesses Near the Mean Free Path of Electrons in Copper Minimization of the Diffuse Scattering in Copper," *Electrochemical and Solid-State Letters,* vol. 3, pp. 437-438, 2000.

[25] H. D. Liu, Y. P. Zhao, G. Ramanath, S. P. Murarka, and G. C. Wang, "Thickness dependent electrical resistivity of ultrathin (<40 nm) Cu films," *Thin Solid Films,* vol. 384, pp. 151-156, 2001.

[26] W. Steinhogl, G. Schindler, G. Steinlesberger, M. Traving, and M. Engelhardt, "Comprehensive study of the resistivity of copper wires with lateral dimensions of 100 nm and smaller," *Journal of Applied Physics,* vol. 97, p. 023706, 2005.

[27] W. Steinhoegl, G. Schindler, and M. Engelhardt, "Unraveling the Mysteries Behind Size Effects in Metallization Systems. (cover story)," *Semiconductor International,* vol. 28, pp. 34-38, 05 2005.

[28] W. Zhang, S. H. Brongersma, T. Clarysse, V. Terzieva, E. Rosseel, W. Vandervorst, and K. Maex, "Surface and grain boundary scattering studied in beveled

polycrystalline thin copper films," *Journal of Vacuum Science & Technology B: Microelectronics and Nanometer Structures,* vol. 22, pp. 1830-1833, 2004.

[29] W. Wu, D. Ernur, S. H. Brongersma, M. Van Hove, and K. Maex, "Grain growth in copper interconnect lines," *Microelectronic Engineering,* vol. 76, pp. 190-194, 2004.

[30] W. Zhang, S. H. Brongersma, N. Heylen, G. Beyer, W. Vandervorst, and K. Maex, "Geometry Effect on Impurity Incorporation and Grain Growth in Narrow Copper Lines," *Journal of The Electrochemical Society,* vol. 152, pp. C832-C837, 2005.

[31] P. M. Vereecken, R. A. Binstead, H. Deligianni, and P. C. Andricacos, "The chemistry of additives in damascene copper plating," *IBM Journal of Research and Development,* vol. 49, pp. 3-18, Jan 2005.

[32] N. Artunc and Z. Z. Ozturk, "Influence of grain-boundary and surface scattering on the electrical resistivity of single-layered thin copper films," *Journal of Physics: Condensed Matter,* p. 559, 1993.

[33] M. Traving, G. Schindler, and M. Engelhardt, "Damascene and subtractive processing of narrow tungsten lines: Resistivity and size effect," *Journal of Applied Physics,* vol. 100, pp. 094325-4, 2006.

[34] R. A. Powell, *Dry etching for microelectronics*. Amsterdam: North-Holland Physics Pub., 1984.

[35] C. Y. Nakakura and E. I. Altman, "Bromine adsorption, reaction, and etching of Cu(100)," *Surface Science,* vol. 370, pp. 32-46, Jan 1 1997.

[36] B. J. Howard and C. Steinbruchel, "Reactive Ion Etching of Copper with Bcl3 and Sicl4 - Plasma Diagnostics and Patterning," *Journal of Vacuum Science & Technology a-Vacuum Surfaces and Films,* vol. 12, pp. 1259-1264, Jul-Aug 1994.

[37] A. Bertz, T. Werner, N. Hille, and T. Gessner, "Effects of the Biasing Frequency on Rie of Cu in a Cl-2-Based Discharge," *Applied Surface Science,* vol. 91, pp. 147-151, Oct 1995.

[38] S. K. Lee, S. S. Chun, C. Y. Hwang, and W. J. Lee, "Reactive ion etching mechanism of copper film in chlorine-based electron cyclotron resonance plasma," *Japanese Journal of Applied Physics Part 1-Regular Papers Short Notes & Review Papers,* vol. 36, pp. 50-55, Jan 1997.

[39] J. W. Lee, Y. D. Park, J. R. Childress, S. J. Pearton, F. Sharifi, and F. Ren, "Copper dry etching with Cl-2/Ar plasma chemistry," *Journal of The Electrochemical Society,* vol. 145, pp. 2585-2589, Jul 1998.

[40] M. Armacost, P. D. Hoh, R. Wise, W. Yan, J. J. Brown, J. H. Keller, G. A. Kaplita, S. D. Halle, K. P. Muller, M. D. Naeem, S. Srinivasan, H. Y. Ng, M. Gutsche, A. Gutmann, and B. Spuler, "Plasma-etching processes for ULSI semiconductor circuits," *IBM Journal of Research & Development,* vol. 43, p. 39, 01 1999.

[41] H. Tang and I. P. Herman, "Anomalous Local Laser Etching of Copper by Chlorine," *Applied Physics Letters,* vol. 60, pp. 2164-2166, Apr 27 1992.

[42] K. S. Choi and C. H. Han, "Low-temperature plasma etching of copper films using ultraviolet irradiation," *Japanese Journal of Applied Physics Part 1-Regular Papers Short Notes & Review Papers,* vol. 37, pp. 5945-5948, Nov 1998.

[43] K. S. Choi and C. H. Han, "Low temperature copper etching using an inductively coupled plasma with ultraviolet light irradiation," *Journal of The Electrochemical Society,* vol. 145, pp. L37-L39, Mar 1998.

[44] M. S. Kwon, J. Y. Lee, K. S. Choi, and C. H. Han, "Reaction characteristics between Cu thin film and RF inductively coupled Cl-2 plasma without/with UV irradiation," *Japanese Journal of Applied Physics Part 1-Regular Papers Short Notes & Review Papers,* vol. 37, pp. 4103-4108, Jul 1998.

[45] Y. B. Hahn, S. J. Pearton, H. Cho, and K. P. Lee, "Dry etching mechanism of copper and magnetic materials with UV illumination," *Materials Science and Engineering B,* vol. 79, pp. 20-26, 2001.

[46] K. Myoung Seok and L. Jeong Yong, "Reaction Mechanism of Low-Temperature Cu Dry Etching Using an Inductively Coupled Cl[sub 2]/N[sub 2] Plasma with Ultraviolet Light Irradiation," *Journal of The Electrochemical Society,* vol. 146, pp. 3119-3123, 1999.

[47] N. Hosoi and Y. Ohshita, "Lower-Temperature Plasma-Etching of Cu Films Using Infrared Radiation," *Applied Physics Letters,* vol. 63, pp. 2703-2704, Nov 8 1993.

[48] Y. Ohshita and N. Hosoi, "Lower Temperature Plasma-Etching of Cu Using Ir Light Irradiation," *Thin Solid Films,* vol. 262, pp. 67-72, Jun 15 1995.

[49] Y. Kuo and S. Lee, "Room-temperature copper etching based on a plasma-copper reaction," *Applied Physics Letters,* vol. 78, pp. 1002-1004, Feb 12 2001.

[50] H. F. Winters, "The etching of Cu(100) with Cl[sub 2]," *Journal of Vacuum Science & Technology A: Vacuum, Surfaces, and Films,* vol. 3, pp. 786-790, 1985.

[51] H. F. Winters, "Etch products from the reaction on Cl[sub 2] with Al(100) and Cu(100) and XeF[sub 2] with W(111) and Nb," *Journal of Vacuum Science & Technology B: Microelectronics and Nanometer Structures,* vol. 3, pp. 9-15, 1985.

[52] W. Sesselmann and T. J. Chuang, "The interaction of chlorine with copper : I. Adsorption and surface reaction," *Surface Science,* vol. 176, pp. 32-66, 1986.

[53] N. S. Kulkarni and R. T. DeHoff, "Application of Volatility Diagrams for Low Temperature, Dry Etching, and Planarization of Copper," *Journal of The Electrochemical Society,* vol. 149, pp. G620-G632, 2002.

CHAPTER 2

PATTERNING OF CU FILMS BY A TWO-STEP PLASMA ETCHING PROCESS AT LOW TEMPERATURE

2.1 Introduction

As described by the International Technology Roadmap for Semiconductors (ITRS) [1], the semiconductor industry has followed Moore's Law for more than four decades. Adherence to Moore's Law has placed severe requirements on the device density needed for increasingly complex higher speed integrated circuits (ICs). In order to meet the speed requirements for current and future generations of ICs, Cu has virtually replaced aluminum as the interconnect material of choice due to the lower electrical resistivity relative to aluminum (1.7 μΩ-cm compared to 2.7 μΩ-cm); this change has led to a substantial reduction in the resistance-capacitance (RC) delay.

Initially, the transition to Cu metallization was difficult, since no effective subtractive plasma-based etch process for Cu was available at temperatures below 180˚C, primarily due to the low volatility of Cu etch products such as $CuCl_x$. As a result, IBM introduced damascene technology in the 1990s to allow pattern formation in Cu films [2]. In the damascene approach, subtractive etching of Cu is avoided by electroplating Cu into plasma-etched dielectric trenches or vias, followed by chemical mechanical planarization/polishing (CMP) to remove the Cu overburden. Although many of the problems related to the development and implementation of the Cu damascene process have been overcome, a significant constraint has arisen for this technology when feature dimensions fall below 50 nm. This constraint is due to the "size effect " in Cu, a

phenomenon in which the electrical resistivity of Cu increases rapidly as lateral dimensions are reduced below 100 nm thereby approaching the electron mean free path in Cu (40 nm at 25 ^{o}C) [3-6]. The size effect in electrical resistivity is a critical limitation to future device generations since it increases the voltage drop, signal propagation delay, and Joule heating in narrow lines. Two primary contributors to this size effect exist: sidewall scattering and grain boundary scattering of electrons [5, 7]. Due to the intrinsic limitations of damascene technology, it is unlikely that the size effect can be mitigated for current Cu patterning technology. That is, the grain growth that occurs during normal annealing processes is dramatically hindered by the narrow geometries [8] and impurities [9] incorporated into grain boundaries during Cu electroplating.

However, annealing of blanket, high purity (non-electroplated) Cu films results in extensive grain growth due to the semi-infinite dimensions of the thin film and the lack of impurities in the deposited film[7, 9]. As a result, the resistivity of blanket-deposited and annealed Cu films that are subsequently patterned to < 100 nm line widths is expected to increase only moderately. Thus, development of a plasma-based, dry, subtractive etch process that can be implemented following annealing of a blanket deposited Cu film of semi-infinite dimensions is highly desirable for future device generations.

Most Cu plasma etch studies to date have invoked halogen-based plasmas, although the low volatility of Cu chloride etch products has been well-recognized. In order to remove etch products from the halogenated Cu surface, several different approaches have been explored. High temperatures (>180 ^{o}C) have been used for the etch process [10-20], although this greatly limited the selection of a mask material and led to etch system compatibility issues. In addition, photo-assisted removal of etch products has

been investigated; these approaches include laser[21], UV[22-28], or infrared radiation [29-30], suggesting that excitation of the Cu surface by photons can facilitate desorption of Cu chlorides relative to thermally enhanced desorption. In an alternative low temperature two-step approach to plasma-based etching of Cu, plasmas of Cl_2, HCl or HBr have been used to chlorinate or brominate Cu films at room temperature. Removal of the $CuCl_x$ or $CuBr_x$ layer was achieved by immersion in a dilute HCl solution [31-36]. Although this method greatly reduced the temperature required to remove Cu chlorides, the combination of vacuum and liquid process increases the system complexity and reduces the manufacturing throughput; in addition, rough sidewalls can result from this method. Thus, none of the approaches reported has conclusively demonstrated a fully plasma-based Cu etching process that is suitable for future device fabrication.

Recently, we developed a low temperature two-step Cu plasma etching process[37] that is based on a thermochemical analysis of solid-gas volatilization reactions in the Cu-Cl-H system[38]. In the first step, the Cu film is chlorinated in a Cl_2 plasma at low temperatures to preferentially form $CuCl_2$ relative to CuCl[39]. In the second step, a hydrogen plasma is used to convert $CuCl_2$ into Cu_3Cl_3 which is more volatile than $CuCl_2$ or CuCl[40]. However, to date, Cu patterning has not been demonstrated using this low temperature process. In this chapter, we describe the patterning of Cu films by this novel two-step plasma etching process, and investigate the etching mechanism.

There have been a limited number of H_2 plasma-related approaches to Cu etching and removal of Cu compounds reported to date. One of the approaches used a Cl_2/H_2 plasma to etch Cu films at ~200 ^oC. The Cu etch rate displayed a maximum at 20% Cl_2

and 80% H_2. The authors speculated that the reason for this behavior involved two competitive processes: decreased flux of active species to the surface and nonlinear desorption of reaction products under ion bombardment [41]. In another study, a H_2 plasma was used to reduce a mixture of Cu salts and oxides that contained 7.3% Cl [42]. This investigation was performed in order to clean oxidized Cu surfaces. From these studies, we conclude that a H_2 plasma may play an important role in the removal of Cu chlorides. As a result, the experiments described below investigate the etching and patterning of Cu films by the two-step plasma etch process reported previously [37], and study the role of a H_2 plasma in this etch process.

2.2 Experimental

2.2.1 Cu Sample Preparation

100nm thick Cu films were deposited by e-beam evaporation (CVC E-Beam Evaporator) onto silicon wafers that had been coated with 20 nm of titanium to promote Cu adhesion to silicon.

Both blanket and masked Cu films were investigated in these plasma etch atmospheres. Masked Cu films invoked SiO_2 (126nm) as the mask layer. The SiO_2 film was deposited in a Plasma Therm PECVD (plasma enhanced chemical vapor deposition) system with 400 sccm SiH_4 and 900 sccm N_2O as precursors; the substrate electrode was heated to 250 ^{o}C, the power applied to the electrode was 25 W, and the pressure was maintained at 900 mtorr during the deposition process. Mask patterns were generated by fluorine-based plasma etching in an inductively coupled plasma (ICP) reactor (Plasma Therm SLR); the etch gas was a mixture of 25 sccm Ar, 2 sccm O_2, 14 sccm CF_4 and 6

sccm C_4F_6, The power applied to the ICP coil (RF2) was 100 W, whereas the power applied to the substrate (RF1) was 200W, while the process pressure was maintained at 5mtorr.

2.2.2 Plasma Etching of Cu by a Two-step Process

Plasma etching of thin Cu films was performed within the same ICP reactor as that used to pattern the SiO_2 mask. Several cycles of the two-step plasma etching process (Cl_2 plasma followed by H_2 plasma) were required to completely etch the 100nm Cu film. In all experiments the substrate temperature was maintained at 10 °C by use of a chiller connected to the substrate electrode. Initial studies used a two-step etch process that consisted of a 2 min Cl_2 plasma followed by a 2 min H_2 plasma; both Cl_2 and H_2 gas flow rates were 10 standard cubic centimeters per minute (sccm) and the reactor pressure was maintained at 20 mtorr. The power applied to the ICP coil (RF2) was 500 W, whereas the power applied to the substrate (RF1) was 150W. In order to improve the etch rates and pattern fidelity and reduce the time needed for the etch process, RF1 for the Cl_2 plasma and the H_2 plasma was tuned between 50 and 150W; in addition, the Cl_2 plasma exposure time was shortened to 30sec. Addition of argon into the hydrogen plasma resulted in improved etch profiles and higher etch rates.

2.2.3 Post Etch Characterization

After Cu etching, the hard masks were removed by a dilute HF solution (1:50). Some samples were cleaned using an ultrasonic bath of DI water to remove post-etch residues.

Chemical analysis of the films and surfaces before and after plasma etching was performed using X-ray photoelectron spectroscopy (XPS). XPS spectra were collected using a Physical Electronics (PHI) Model 1600 XPS system equipped with a monochromator. Cu film patterns were examined with a scanning electron microscope (SEM, Zeiss SEM Ultra60). Thickness changes of the Cu layer were determined from SEM images.

2.3 Results and Discussion

2.3.1 Etch results for 100nm blanket Cu film

100nm thick Cu films were etched using five cycles of the two-step plasma etch process; each cycle consisted of a 2 min chlorine plasma and a 2 min hydrogen plasma. Conditions for both plasmas were: RF1=150 W, RF2=500 W, 20 mtorr total pressure, 10 sccm flow rate for each gas. XPS spectra of Cu 2p peaks for samples before and after the etch process cycles are shown in Figure 2.1. The spectrum of the untreated sample displays four characteristic peaks for Cu. The binding energy range of 930-937 eV contains the Cu2p3 peak, composed of two individual peaks: 932.59 eV and 934.67 eV, corresponding to Cu_2O and CuO, respectively [43]. The area ratios under these two peaks are 32.08% and 67.92%, which indicates that Cu (II) is the primary species present at the surface. In comparison, the XPS spectrum of a sample exposed to 5 etch cycles, showed no detectable Cu peaks; thus, 5 cycles completely remove a 100nm blanket Cu film. These results indicate that the etch rate for the two step sequence is at least 20 nm/cycle under the specified etch conditions.

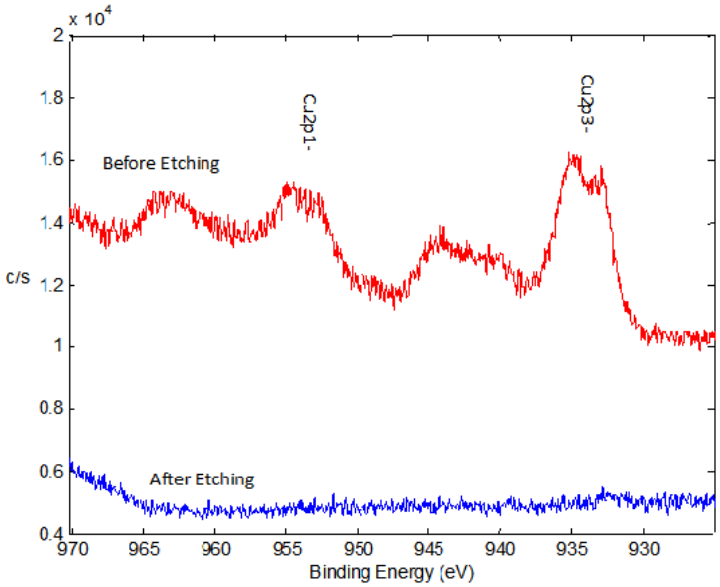

Figure 2.1. XPS spectra of 100nm blanket Cu films showing Cu 2p peaks before and after etching: 5 cycles of (2 min Cl_2 plasma + 2 min H_2 plasma).

2.3.2 Role of Cl_2 Plasma and H_2 Plasma

In order to investigate the effects of chlorine and hydrogen plasmas on Cu surfaces and compare these experimental results to those predicted by a thermochemical analysis [38], we performed XPS measurements on samples exposed to a 2 min chlorine plasma, and on samples exposed to 1 cycle of the two-step etch process (2 min chlorine plasma followed by 2 min hydrogen plasma). These spectra are compared to that of an untreated Cu sample in Figure 2.2. After a 2 min chlorine plasma treatment, a Cu Cu2p3 peak is observed at 934.08eV which corresponds to $CuCl_2$, while no Cu Cu2p3 corresponding to CuCl was observed; this observation indicates that $CuCl_2$ is preferentially formed under this plasma chlorination condition. After 1 cycle of the two-step etch process, the Cu Cu2p3 was split into a 932.52eV peak and 934.74eV peak,

which correspond to CuCl and $CuCl_2$ respectively[44]. Compared to the unetched surface, the peak area ratio of $CuCl_2$ dropped from nearly 100% to 31.78%. This result is consistent with plasma chlorination of a Cu film to form $CuCl_2$ on the film surface and formation of CuCl beneath the surface. A subsequent H_2 plasma generates H atoms that can react with $CuCl_2$ to form Cu_3Cl_3 as predicted previously [38]. Since Cu_3Cl_3 has much higher volatility than either CuCl or $CuCl_2$ [40], essentially only CuCl should remain on the surface, in agreement with the XPS spectra shown in Figure 2.2. However, it is conceivable that CuCl could form during the H_2 plasma treatment step. At present, we are unable to differentiate between such reactions and the reduction of $CuCl_2$ to form Cu_3Cl_3 which desorbs during the H_2 plasma step and leaves the less fully-chlorinated CuCl layer which is detected by XPS.

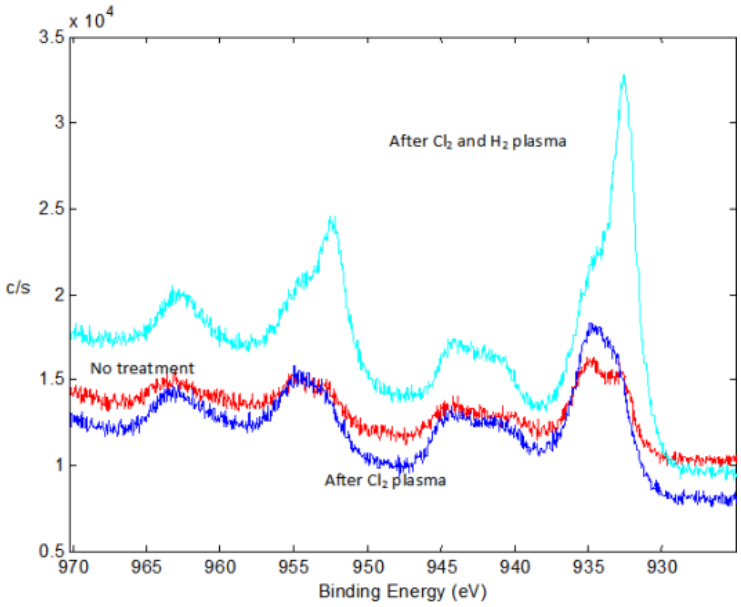

Figure 2.2. XPS spectra of 100nm blanket Cu films showing Cu 2p peaks before and after a) 2 min Cl_2 plasma; b) 2 min Cl_2 plasma + 2 min H_2 plasma.

For the studies described in this chapter, the length of the H_2 plasma step was fixed at 2 min. This time was selected because our studies indicated that the H_2 plasma step is the rate-determining step for the two-step etch process. Therefore, we have used a longer plasma exposure time for H_2 than for Cl_2 (30 sec). However, we also investigated both 5 min and 1 min H_2 plasma treatment times. The longer time showed no apparent improvement in copper chloride removal rate, while the shorter time resulted in an overall decrease in removal rate, since more cycles were needed to etch through a specific Cu film thickness. As a result, we fixed the H_2 plasma treatment time to 2 min.

2.3.3 Patterning of 100nm Cu Films with a SiO_2 Mask

2.3.3.1 SEM results of chlorination step and hydrogen treatment step

Studies to gain insight into the roles of chlorine and hydrogen plasmas in patterning Cu with this two-step etch process using a SiO_2 mask have been performed. Figure 2.3a shows a cross sectional SEM of a 100 nm Cu film etched with 2.5 cycles of two-step etch process (two cycles plus one additional Cl_2 step) where the first etch step invoked a 30 sec Cl_2 plasma and the second step invoked a 2 min H_2 plasma (the purpose of changing chlorination time from 2 min to 30 sec will be discussed later in this section). Figure 2.3b shows a cross sectional SEM of a 100 nm Cu film patterned using 3 cycles of this two-step etch process (30 sec Cl_2 plasma + 2 min H_2). Figure 2.3a indicates that Cu plasma chlorination occurs rapidly as indicated previously [39]; this process thereby converts a significant depth of Cu (~80 nm) to $CuCl_x$ which increases the film volume (and thus thickness) due to the conversion [39]. The subsequent H_2 plasma then removes ~50 nm of the $CuCl_x$ layer in 2 minutes (Figure 2.3b). As a result, the total thickness of

the chlorinated Cu layer will be greater than 100 nm since a volume (e.g., thickness) increase occurs during the chlorination step. Due to the low mass of hydrogen ion species, sputtering is not likely to be the sole mechanism for hydrogen-assisted removal of $CuCl_x$. Rather, a chemical-assisted etching process is believed to control the etching.

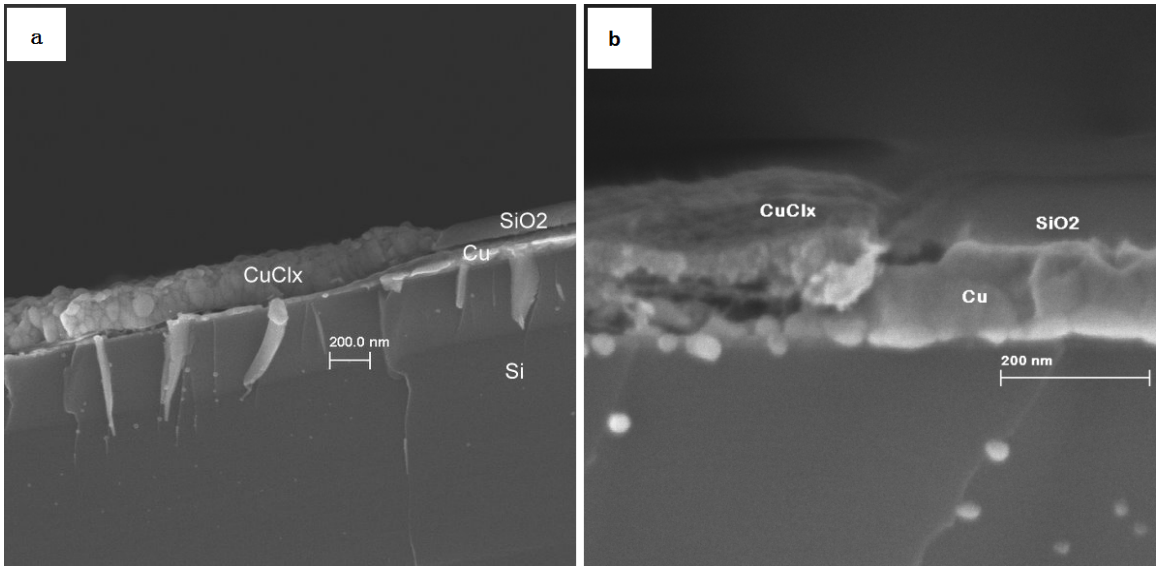

Figure 2.3. Cross sectional SEMs of SiO_2 masked 100nm Cu film: (a) after 2 cycles of two-step etch process plus 30 sec Cl_2 plasma (b) after 3 cycles of two-step etch process. The two-step etch process includes 30 sec Cl_2 plasma (RF1=100 W) and 2 min H_2 plasma (RF1=150 W), 20 mtorr, 10 sccm flow rate for both gases, RF2=500 W.

2.3.3.2 Effects of chlorination step time

A comparison of Cu patterns formed using both 30 sec and 2 min Cl_2 plasma steps is shown in Figure 2.4; these results indicate that the longer the chlorination time, the more extensive the undercut, as is evident from comparison of Figures 2.4a and 2.4b. Since Cu chlorination is not the rate determining step in the etch process, all subsequent patterning studies were performed with the Cl_2 plasma step at 30 sec, in order to

minimize lateral (sidewall) chlorination introduced by the longer chlorination time. Only the H_2 plasma parameters were subsequently changed, while the ICP power (RF2) and temperature were fixed at 500 W and 10 ^oC, respectively.

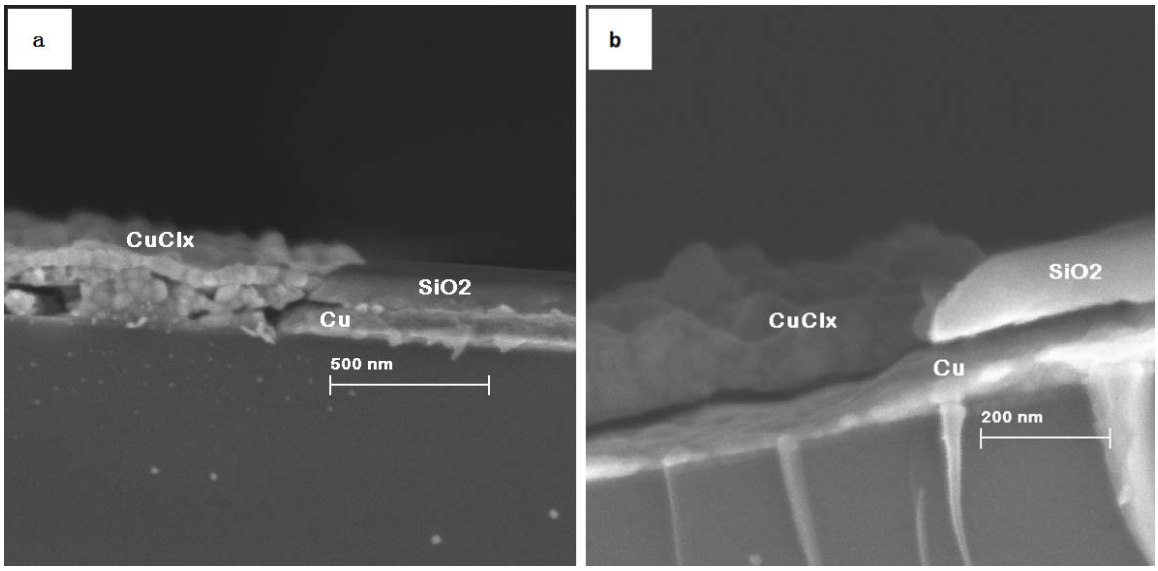

Figure 2.4. Cross sectional SEMs of SiO_2 masked 100nm Cu film after 2 cycles of two-step etch process. The two-step etch process includes (a) 2 min (b) 30 sec Cl_2 plasma (RF1=100 W) and 2 min H_2 plasma (RF1=150 W), 20 mtorr, 10 sccm flow rate for both gases, RF2=500 W.

2.3.3.3 Issues with two-step plasma etch of Cu

Two major limitations observed with this two-step Cu patterning process are rough pattern edges and sidewall/edge residue (Figure 2.5a). Both of these are difficult to avoid due to the high reactivity of Cu with chlorine. Residues likely arise because Cu edges beneath the SiO_2 mask are chlorinated leading to volume expansion due to the $CuCl_x$ formed. Furthermore, when adhesion of the mask to the Cu surface is inadequate, chlorination occurs at the interface, thereby lifting the mask and creating residues at the

Cu edge. In addition, re-deposition of plasma etch products may enhance the residue observed since the volatility of Cu_3Cl_3 is limited. Residual hydrogen species at the edges may also react with chlorine to form HCl which can react with Cu. In order to minimize lateral Cu chlorination, we reduced the chlorination time to 30 sec and have varied the H_2 plasma parameters in order to reduce the sidewall roughness while maintaining a reasonable etch rate.

Applied substrate power (RF1) during the H_2 step was decreased from 150 to 50 W; this improved the edge roughness as can be seen by comparison of Figures 2.5b and 2.5c. A higher RF1 power (150 W) yields a higher hydrogen ion energy, which therefore increases the amount of energy transferred to the Cu film. This process results in enhanced sputtering; some of the sputtered Cu or $CuCl_x$ redeposited on the sidewalls. In addition to this enhanced sputtering, further chlorination can occur on the sidewall and so enhance undercut. These processes degraded the edge definition. However, the reduced RF1 also decreased the etch rate from 10 nm/cycle to 8 nm/cycle and therefore requires more cycles to completely etch through 100nm of Cu; indeed, residues are observed in the etched area (Figure 2.5c). More etch cycles increase the total chlorination time and thus yields additional undercutting and increases the etch residue.

Since argon is an effective sputter etching gas, an Ar/H_2 plasma with a ratio of 45 sccm Ar: 5 sccm H_2 was used in the second step of the two-step etch process. Although only 10% H_2 was present, the etch rate was much higher than that without Ar, which is consistent with enhanced energy input to the surface. In addition, the residence time decreased due to the increased total flow rate (50 sccm instead of 10 sccm) and constant pressure. The shorter residence time improves the desorption rate of etch products by

removing the desorbed species from the surface, thereby enhancing the local concentration gradient and so the etch rate. RF1 was 150 W and RF2 was kept at 500 W. Under these conditions, the time required to etch through a 100 nm Cu film dropped dramatically, because the etch rate doubled relative to using pure H_2 in the second step. Figure 2.5d displays a much improved sidewall roughness and no visible etch residue. Furthermore, only 6 etch cycles were needed to completely remove the copper film. The etch process for Cu removal is not completely physical (sputtering), since pure Ar in the second step did not effectively remove the $CuCl_x$ layers as shown in Figure 2.5e. Furthermore, Figure 2.5f indicates that a pure Ar plasma (without the previous chlorination step) could not effectively remove Cu films. However, use of an Ar/H_2 plasma in the second step of the low temperature process resulted in pattern definition with little to no residue in the etched areas. Clearly, H atoms generated from the H_2 plasma play an important role in removal of the $CuCl_x$ layer, perhaps through formation of Cu_3Cl_3, where removal is facilitated by Ar^+ bombardment. We should also note that H_2 addition may change the chemistry and physics of the Ar plasma, and thereby alter the Cu etch process. However, further discussion of this possibility is beyond the scope of the current chapter.

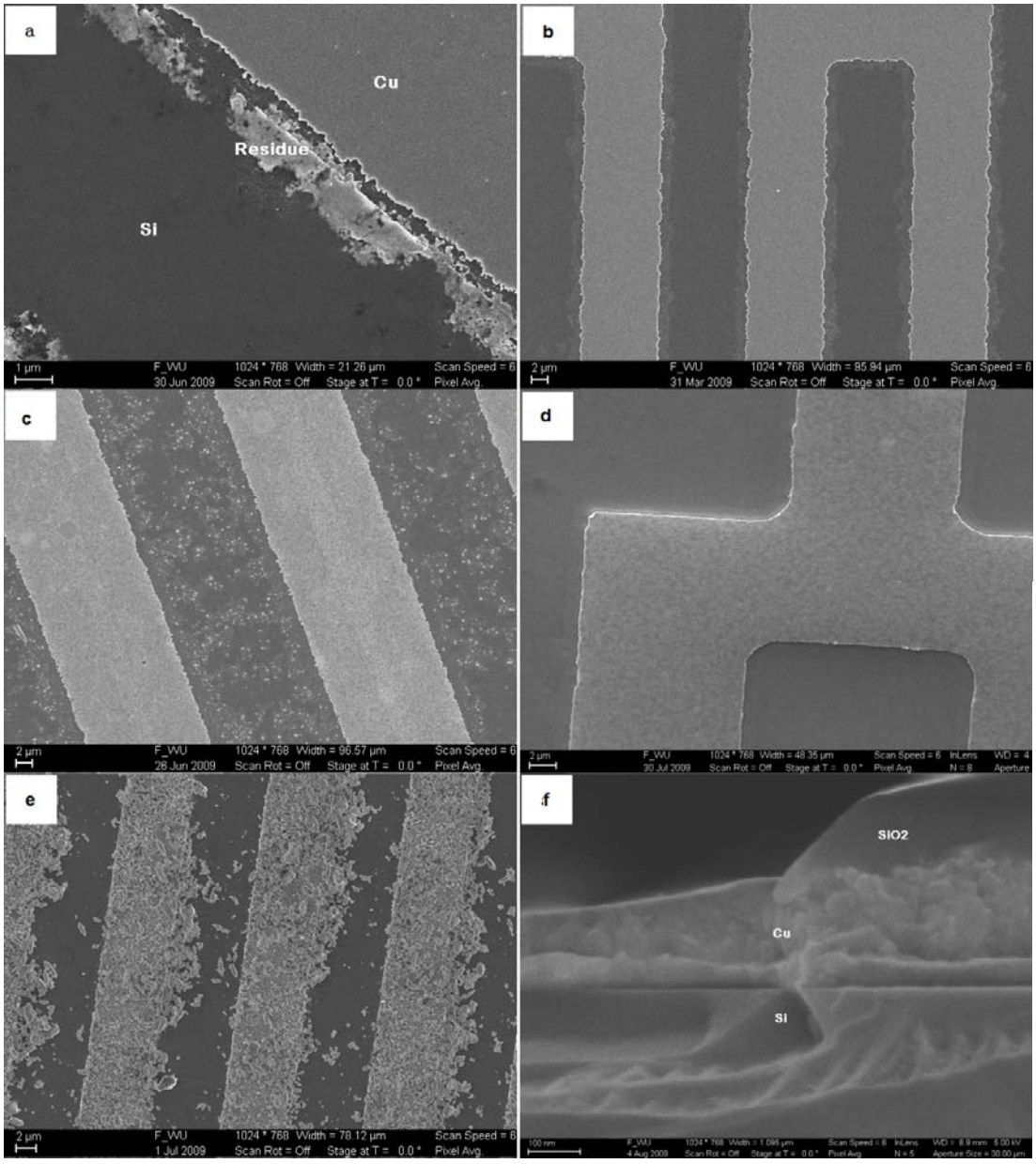

Figure 2.5. SEM images of SiO_2 masked 100nm Cu film after certain cycles of the two-step etch process. The 30 sec Cl_2 plasma is always under the same condition: RF1=150 W, 10 sccm flow rate. Both plasmas have the same 20 mtorr pressure and RF2=500 W, 10^0C. (a) 10 cycles, H_2 plasma: RF1=100 W, 10 sccm; (b) 10 cycles, H_2 plasma: RF1=150 W, 10 sccm; (c) 12 cycles, H_2 plasma: RF1=50 W, 10 sccm; (d) 6 cycles, (45 sccm Ar + 5 sccm H_2) plasma, RF1=150 W); (e) 4 cycles, 50 sccm Ar plasma, RF1=150 W; (f) 8 min Ar plasma (without previous chlorination), 50 sccm, RF1=150 W.

2.4 Conclusion:

A two-step plasma etch process for Cu has been developed and successfully utilized to pattern Cu thin films at low temperature (10 ^{o}C) in an ICP system. This two-step etch process includes a chlorine plasma followed by a hydrogen plasma. The Cl_2 plasma formed $CuCl_x$ on the surface of Cu films while the H_2 plasma assisted removal of the $CuCl_x$ layer, and this process is believed to be at least partially chemically controlled. Cu patterns were generated by invoking SiO_2 as a mask layer. Two major limitations were observed during the patterning process: rough pattern edges and sidewall/edge residues. In order to address these issues, plasma parameters were altered. Shorter chlorination time, lower applied substrate power, lower residence time and the addition of Ar to the second (H_2) step all improved the pattern definition while allowing reasonable etch rates.

Our work indicates that the hydrogen plasma plays a key role in this two-step Cu etching process, although the mechanism is not yet established. XPS analysis of the Cu surface before and after chlorination as well as after hydrogen treatment has been performed; results agreed with the original prediction: in the first step, Cu is chlorinated to preferably form $CuCl_2$, while in the second step, $CuCl_x$ layer is partially removed by a H_2 plasma. These conclusions are consistent with cross-sectional SEM images of patterned Cu films. The initial predictions are based on a previous thermodynamic analysis of the solid-gas Cu-Cl-H system [38], which indicated that in the presence of H atoms, $CuCl_2$ will be reduced to form Cu_3Cl_3, and that Cu_3Cl_3 has sufficient volatility to

be removed from the Cu surface. Further investigations into the etch mechanism of this two-step process and into approaches to reduce the current edge roughness are underway.

2.5 References:

[1] *International technology roadmap for semiconductors 2008 update*, 2008.

[2] R. Rosenberg, D. C. Edelstein, C. K. Hu, and K. P. Rodbell, "COPPER METALLIZATION FOR HIGH PERFORMANCE SILICON TECHNOLOGY," *Annual Review of Materials Science,* vol. 30, pp. 229-262, 2000.

[3] A. Mallikarjunan, S. Sharma, and S. P. Murarka, "Resistivity of Copper Films at Thicknesses Near the Mean Free Path of Electrons in Copper Minimization of the Diffuse Scattering in Copper," *Electrochemical and Solid-State Letters,* vol. 3, pp. 437-438, 2000.

[4] H. D. Liu, Y. P. Zhao, G. Ramanath, S. P. Murarka, and G. C. Wang, "Thickness dependent electrical resistivity of ultrathin (<40 nm) Cu films," *Thin Solid Films,* vol. 384, pp. 151-156, 2001.

[5] W. Steinhogl, G. Schindler, G. Steinlesberger, M. Traving, and M. Engelhardt, "Comprehensive study of the resistivity of copper wires with lateral dimensions of 100 nm and smaller," *Journal of Applied Physics,* vol. 97, p. 023706, 2005.

[6] W. Steinhoegl, G. Schindler, and M. Engelhardt, "Unraveling the Mysteries Behind Size Effects in Metallization Systems. (cover story)," *Semiconductor International,* vol. 28, pp. 34-38, 05 2005.

[7] W. Zhang, S. H. Brongersma, T. Clarysse, V. Terzieva, E. Rosseel, W. Vandervorst, and K. Maex, "Surface and grain boundary scattering studied in beveled polycrystalline thin copper films," *Journal of Vacuum Science & Technology B: Microelectronics and Nanometer Structures,* vol. 22, pp. 1830-1833, 2004.

[8] W. Wu, D. Ernur, S. H. Brongersma, M. Van Hove, and K. Maex, "Grain growth in copper interconnect lines," *Microelectronic Engineering,* vol. 76, pp. 190-194, 2004.

[9] W. Zhang, S. H. Brongersma, N. Heylen, G. Beyer, W. Vandervorst, and K. Maex, "Geometry Effect on Impurity Incorporation and Grain Growth in Narrow Copper Lines," *Journal of The Electrochemical Society,* vol. 152, pp. C832-C837, 2005.

[10] B. J. Howard and S. Ch, "Reactive ion etching of copper with BCl[sub 3] and SiCl[sub 4]: Plasma diagnostics and patterning," 1994, pp. 1259-1264.

[11] B. J. Howard and S. Ch, "Reactive ion etching of copper in SiCl[sub 4]-based plasmas," *Applied Physics Letters,* vol. 59, pp. 914-916, 1991.

[12] B. J. Howard and C. Steinbruchel, "Reactive Ion Etching of Copper with Bcl3 and Sicl4 - Plasma Diagnostics and Patterning," *Journal of Vacuum Science & Technology a-Vacuum Surfaces and Films,* vol. 12, pp. 1259-1264, Jul-Aug 1994.

[13] C. Steinbruchel, "Patterning of copper for multilevel metallization: reactive ion etching and chemical-mechanical polishing," *Applied Surface Science,* vol. 91, pp. 139-146, 1995.

[14] A. Bertz, T. Werner, N. Hille, and T. Gessner, "Effects of the Biasing Frequency on Rie of Cu in a Cl-2-Based Discharge," *Applied Surface Science,* vol. 91, pp. 147-151, Oct 1995.

[15] M. Markert, A. Bertz, and T. Gessner, "Mechanism studies of Cu RIE for VLSI interconnections," *Microelectronic Engineering,* vol. 37-8, pp. 127-133, Nov 1997.

[16] M. Markert, A. Bertz, T. Gessner, Y. Ye, A. Zhao, and D. Ma, "High throughput, high quality dry etching of copper/barrier film stacks," *Microelectronic Engineering,* vol. 50, pp. 417-423, 2000.

[17] S. K. Lee, S. S. Chun, C. Y. Hwang, and W. J. Lee, "Reactive ion etching mechanism of copper film in chlorine-based electron cyclotron resonance plasma," *Japanese Journal of Applied Physics Part 1-Regular Papers Short Notes & Review Papers,* vol. 36, pp. 50-55, Jan 1997.

[18] C. Y. Nakakura and E. I. Altman, "Bromine adsorption, reaction, and etching of Cu(100)," *Surface Science,* vol. 370, pp. 32-46, Jan 1 1997.

[19] J. W. Lee, Y. D. Park, J. R. Childress, S. J. Pearton, F. Sharifi, and F. Ren, "Copper dry etching with Cl-2/Ar plasma chemistry," *Journal of The Electrochemical Society,* vol. 145, pp. 2585-2589, Jul 1998.

[20] M. Armacost, P. D. Hoh, R. Wise, W. Yan, J. J. Brown, J. H. Keller, G. A. Kaplita, S. D. Halle, K. P. Muller, M. D. Naeem, S. Srinivasan, H. Y. Ng, M. Gutsche, A. Gutmann, and B. Spuler, "Plasma-etching processes for ULSI semiconductor circuits," *IBM Journal of Research & Development,* vol. 43, p. 39, 01 1999.

[21] H. Tang and I. P. Herman, "Anomalous Local Laser Etching of Copper by Chlorine," *Applied Physics Letters,* vol. 60, pp. 2164-2166, Apr 27 1992.

[22] K. S. Choi and C. H. Han, "Low-temperature plasma etching of copper films using ultraviolet irradiation," *Japanese Journal of Applied Physics Part 1-Regular Papers Short Notes & Review Papers,* vol. 37, pp. 5945-5948, Nov 1998.

[23] K. S. Choi and C. H. Han, "Low temperature copper etching using an inductively coupled plasma with ultraviolet light irradiation," *Journal of The Electrochemical Society,* vol. 145, pp. L37-L39, Mar 1998.

[24] C. Kang-Sik and H. Chul-Hi, "Low Temperature Copper Etching Using an Inductively Coupled Plasma with Ultraviolet Light Irradiation," *Journal of The Electrochemical Society,* vol. 145, pp. L37-L39, 1998.

[25] M. S. Kwon, J. Y. Lee, K. S. Choi, and C. H. Han, "Reaction characteristics between Cu thin film and RF inductively coupled Cl-2 plasma without/with UV irradiation," *Japanese Journal of Applied Physics Part 1-Regular Papers Short Notes & Review Papers,* vol. 37, pp. 4103-4108, Jul 1998.

[26] Y. B. Hahn, S. J. Pearton, H. Cho, and K. P. Lee, "Dry etching mechanism of copper and magnetic materials with UV illumination," *Materials Science and Engineering B,* vol. 79, pp. 20-26, 2001.

[27] K. H. Jang, W. J. Lee, H. R. Kim, and G. Y. Yeom, "Etching of copper films for thin film transistor liquid crystal display using inductively coupled chlorine-based plasmas," *Japanese Journal of Applied Physics Part 1-Regular Papers Short Notes & Review Papers,* vol. 43, pp. 8300-8303, Dec 2004.

[28] K. Myoung Seok and L. Jeong Yong, "Reaction Mechanism of Low-Temperature Cu Dry Etching Using an Inductively Coupled Cl[sub 2]/N[sub 2] Plasma with Ultraviolet Light Irradiation," *Journal of The Electrochemical Society,* vol. 146, pp. 3119-3123, 1999.

[29] N. Hosoi and Y. Ohshita, "Lower-Temperature Plasma-Etching of Cu Films Using Infrared Radiation," *Applied Physics Letters,* vol. 63, pp. 2703-2704, Nov 8 1993.

[30] Y. Ohshita and N. Hosoi, "Lower Temperature Plasma-Etching of Cu Using Ir Light Irradiation," *Thin Solid Films,* vol. 262, pp. 67-72, Jun 15 1995.

[31] Y. Kuo and S. Lee, "Room-temperature copper etching based on a plasma-copper reaction," *Applied Physics Letters,* vol. 78, pp. 1002-1004, Feb 12 2001.

[32] Y. Kuo and S. Lee, "A new, room-temperature, high-rate plasma-based copper etch process," *Vacuum,* vol. 74, pp. 473-477, 2004.

[33] Y. Kuo and S. Lee, "A Novel Plasma-Based Copper Dry Etching Method," *Japanese Journal of Applied Physics,* vol. 39, pp. L188-L190, 2000.

[34] S. Lee and Y. Kuo, "Chlorine plasma/copper reaction in a new copper dry etching process," *Journal of The Electrochemical Society,* vol. 148, pp. G524-G529, Sep 2001.

[35] S. Lee and Y. Kuo, "Hydrogen bromide plasma-copper reaction in a new copper etching process," *Thin Solid Films,* vol. 457, pp. 326-332, 2004.

[36] S. H. Lee and Y. Kuo, "A new hydrogen chloride plasma-based copper etching process," *Japanese Journal of Applied Physics Part 1-Regular Papers Short Notes & Review Papers,* vol. 41, pp. 7345-7352, Dec 2002.

[37] P. A. Tamirisa, G. Levitin, N. S. Kulkarni, and D. W. Hess, "Plasma etching of copper films at low temperature," *Microelectronic Engineering,* vol. 84, pp. 105-108, 2007.

[38] N. S. Kulkarni and R. T. DeHoff, "Application of Volatility Diagrams for Low Temperature, Dry Etching, and Planarization of Copper," *Journal of The Electrochemical Society,* vol. 149, pp. G620-G632, 2002.

[39] W. Sesselmann and T. J. Chuang, "The interaction of chlorine with copper : I. Adsorption and surface reaction," *Surface Science,* vol. 176, pp. 32-66, 1986.

[40] M. Guido, G. Balducci, G. Gigli, and M. Spoliti, "Mass Spectrometric Study of the Vaporization of Cuprous Chloride and the Dissociation Energy of Cu[sub 3]Cl[sub 3], Cu[sub 4]Cl[sub 4], and Cu[sub 5]Cl[sub 5]," *The Journal of Chemical Physics,* vol. 55, pp. 4566-4572, 1971.

[41] A. M. Efremov, A. I. Izgorodin, V. S. Ochenkov, and V. I. Svettsov, "Spectroscopic study of copper etching in plasma of a glow discharge in a chlorine- hydrogen mixture," *Khimiya i Khimicheskaya Tekhnologiya,* vol. 50, pp. 69-73, 2007.

[42] M. J. Alcayde, L. Robbiola, J. Esteve, M. Puges, and S. Borros, "Hydrogen cold plasma reduction in a restoration conservation protocol for metallic archaeological heritage," *Afinidad,* vol. 62, pp. 513-519, Sep-Oct 2005.

[43] J. Haber, T. Machej, L. Ungier, and J. Ziolkowski, "ESCA studies of copper oxides and copper molybdates," *Journal of Solid State Chemistry,* vol. 25, pp. 207-218, 1978.

[44] C. Battistoni, G. Mattogno, E. Paparazzo, and L. Naldini, "An XPS and Auger study of some polynuclear copper compounds," *Inorganica Chimica Acta,* vol. 102, pp. 1-3, 1985.

CHAPTER 3

LOW TEMPERATURE ETCHING OF CU BY HYDROGEN-BASED PLASMAS

3.1 Introduction

The resistivity of interconnect materials is the primary determinant of integrated circuit (IC) speed for current and future devices [1-2]. Patterns are normally generated in these materials by plasma-assisted (subtractive) etching. However, due to the inability to form volatile Cu etch products during halogen-based plasma etching [3], damascene technology was introduced to avoid the need for Cu plasma etching [4]. Although damascene technology played an essential role in the initial implementation of Cu metallization, a critical limitation has arisen due to the adherence of the IC industry to Moore's Law [5] and thus the reduction of minimum feature sizes. This limitation is the "size effect " of Cu, where the electrical resistivity of Cu increases rapidly as lateral dimensions are reduced below 100 nm, thereby approaching the electron mean free path in Cu (40 nm at 25 ^{0}C) [6-9].

Two approaches exist to reduce or eliminate the Cu size effect: decrease the Cu sidewall/surface roughness and grow larger Cu grains. However, grain growth of Cu in damascene technology is dramatically hindered by the narrow geometries [10] and impurities introduced into Cu that result from chemical mechanical planarization/polishing (CMP) and plating processes [11-12]. Therefore, development of new Cu patterning technologies that mitigate the size effect are required for future device generations. Subtractive etching may offer a viable approach. Indeed, etched tungsten

(W) lines showed a distinctly lower resistivity than did W lines defined by the damascene process, where the resistivities reported were ~13 μΩ-cm for plasma etched lines vs. 18~23 μΩ-cm for damascene lines [13]. A similar advantage may therefore be expected for Cu.

Halogen-based (specifically chlorine-containing) plasmas have to date been the ones investigated to plasma etch Cu but removal of Cu etch products from the surface is hindered due to the relatively low volatility of Cu halides. Thus, high temperatures (>180 ^{0}C) have been generally invoked to enhance desorption of Cu chlorides [14-19]. Alternatively, photon-enhanced removal of Cu chlorides at temperatures below 100 ^{0}C by laser [20], UV [21], or infrared radiation [22] has been reported. Both approaches introduce complexity and control issues into the patterning process. Cu halide product desorption has been averted by plasma chlorination or bromination of Cu followed by removal of the halides by immersion in dilute HCl solutions, thereby offering an alternative low temperature two-step approach to Cu patterning [23]. However, this method requires a combination of vacuum and liquid process and so increases the system complexity, reduces the manufacturing throughput, and may lead to process integration issues.

In Chapter 2, we developed a low temperature (10 ^{0}C) two-step Cu plasma etching process [24] based on a thermochemical analysis of solid-gas volatilization reactions in the Cu-Cl-H system [25]. The Cu film is first chlorinated in a Cl_2 plasma to preferentially form $CuCl_2$ relative to CuCl [26]. In the second step, a hydrogen plasma is used to convert $CuCl_2$ into a product with improved volatility, presumably Cu_3Cl_3 [27]. Although this sequence represents an improvement relative to current approaches to

plasma-based Cu etching, the process requires an etch sequence that will reduce overall etch rate and thus throughput. Our Cu patterning and etching mechanism studies for this two-step process indicated that the H_2 plasma treatment (2^{nd} step) is rate-limiting and a critical component in establishing etch pattern fidelity [28]. Thus in this chapter, we describe studies that demonstrate the ability to etch Cu films in a pure H_2 or a H_2-based plasma at low temperatures. This surprising result offers a straightforward approach to patterning Cu using a simple plasma (vacuum) single step process, thereby greatly improving manufacturability and process control.

3.2 Experimental

3.2.1 Cu Sample Preparation

Copper films of 100 or 300 nm thickness were deposited by e-beam evaporation (CVC E-Beam Evaporator) onto silicon wafers that had been coated with 20 nm of titanium to promote Cu adhesion to silicon. Electroplated Cu films (145 nm electroplated Cu films grown from an 80 nm physical vapor deposited (PVD) seed layer followed by annealing at 200 ^{0}C in forming gas for 30 sec) were also studied. Since no differences in etch properties were observed, the results reported in this chapter are from e-beam deposited Cu films. Cu-coated substrates were sectioned into etch samples ~1 cm^2.

Masked Cu films invoked SiO_2 (~150 nm) as the mask layer. The SiO_2 film was deposited in a Plasma Therm PECVD (plasma enhanced chemical vapor deposition) system with 400 sccm SiH_4 and 900 sccm N_2O as reactants; the substrate electrode was heated to 250 ^{0}C, the power applied to the electrode was 25 W, and the pressure was

maintained at 900 mtorr during the deposition process. Mask patterns were generated by fluorine-based plasma etching in an inductively coupled plasma (ICP) reactor (Plasma Therm ICP): the etch gas was a mixture of 25 sccm Ar, 2 sccm O_2, 14 sccm CF_4 and 6 sccm C_4F_6, RF1 (power applied to the platen) was 200 W and RF2 (power applied to the coil) was 100 W, while the process pressure was maintained at 5 mtorr.

3.2.2 H_2 Plasma Etching of Cu

Plasma etching of thin Cu films was performed within the same ICP reactor. The substrate temperature was maintained at ~10 ^{0}C using a water cooled chiller connected to the substrate electrode. The H_2 gas flow rate was 50 standard cubic centimeters per minute (sccm) and the reactor pressure was maintained at 20 mtorr. The radio frequency power applied to the ICP coil (RF2) was 500 W, whereas the power applied to the substrate (RF1) was 100W. Both blanket and masked Cu films were investigated in these plasma etch atmospheres.

3.2.3 Post Etch Characterization

Chemical analysis of the films and surfaces before and after plasma etching was performed using X-ray photoelectron spectroscopy (XPS). XPS spectra were collected using a Thermo Scientific K-Alpha XPS. Cu film patterns were examined with a scanning electron microscope (SEM, Zeiss SEM Ultra60). Thickness changes of the Cu layer were determined from SEM images and a Wyko Profilometer.

3.3 Results and Discussion

3.3.1 H_2 Plasma Etching of Cu

Plasma etching of 100 nm Cu films was performed in an inductively coupled plasma (ICP) reactor. Figure 3.1a shows a scanning electron microscope (SEM) image of an SiO_2-masked Cu film prior to etching; Figure 3.1b indicates that an 8 min H_2 plasma completely removed the 100 nm copper film (above a 20 nm Ti adhesion layer) under the conditions RF1 (platen power) = 100 W, RF2 (coil power) = 500 W, with flow rate and pressure 50 sccm and 20 mtorr, respectively. The temperature of the substrate electrode was assumed to be the same as that of the chiller (10 ^{0}C); clearly this is not the Cu surface temperature, but substantial temperature excursions (> 20 ^{0}C) are unlikely over the etch time (normal 8 min) and conditions used. Figure 3.1b also shows that etching terminated at the Ti adhesion layer (confirmed by further etching), indicating that etch selectivity of Cu over Ti is possible. In addition, the Cu profile is anisotropic, although the sidewall surface is rough. This result demonstrates the feasibility of etching Cu with a pure H_2 plasma at low temperatures.

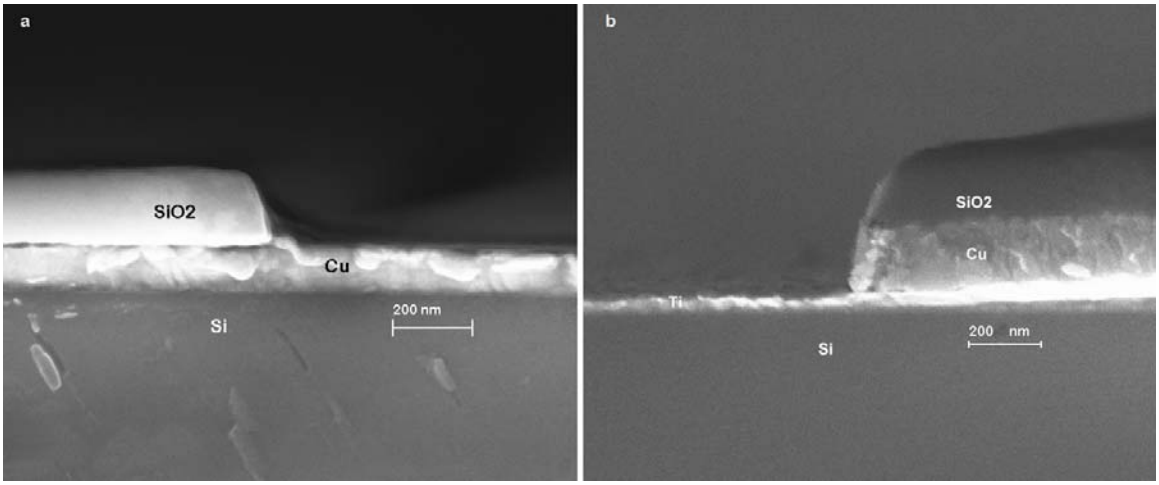

Figure 3.1. Cross sectional SEM of SiO_2 masked 100 nm Cu films: (a) before; (b) after 8 min of H_2 plasma etching under the conditions RF1=100 W, RF2=500 W, 20 mtorr pressure, 50 sccm flow rate and 10 ^oC electrode temperature

3.3.2 XPS Studies of Cu Surfaces after H_2 Plasma Etch

Etch studies on blanket Cu samples were performed to gain additional insight into this H_2 plasma etching process. X-ray photoelectron spectroscopy (XPS) was used to probe blanket Cu surfaces before and after an 8 min H_2 etch cycle. Figure 3.2 shows that the untreated sample displays four characteristic peaks for Cu, but Ti is not detected since the sampling depth of XPS is < 10 nm; after the H_2 plasma treatment, Cu peaks are not apparent which indicates removal of the Cu film by the H_2 plasma at least to the detectability limit of XPS. The appearance of Ti peaks after the etch process indicates that a H_2 plasma does not substantially etch Ti under these etch conditions.

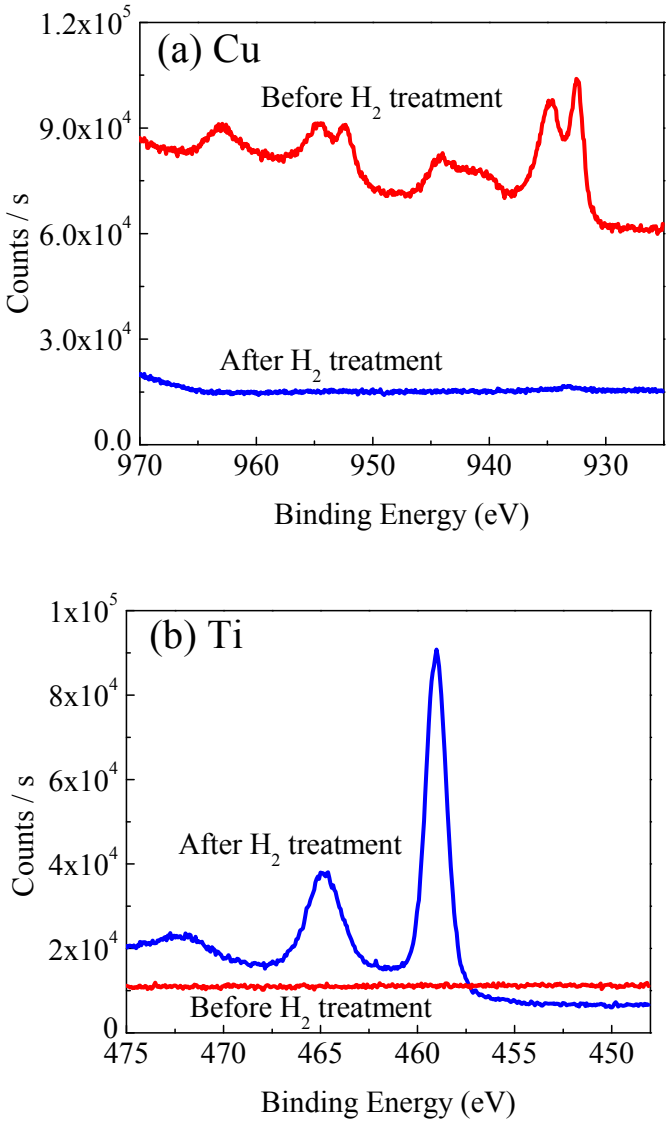

Figure 3.2. Cu (a) and Ti (b) 2p spectra (XPS) of 100 nm blanket Cu films before and after an 8 min (pure) H_2 plasma treatment. Atomic percentages of the surface before and after the H_2 treatment are (Cu2p: 15.92, O1s: 35.81, C1s: 48.26 %) and (Ti2p: 16.47, O1s: 48.12, C1s 28.31, F1s: 2.91, N1s: 4.18 %), respectively. The carbon and oxygen detected are from exposure of the surfaces to air after etching. The small amount of F on the Ti surface after H_2 etch arose from the reactor chamber where a fluorine-based plasma is used to etch the SiO_2 mask in patterning studies.

This result is unexpected since copper hydrides are not predicted to have significant volatility (this issue is discussed in the following paragraphs), and H_2 should

not efficiently sputter Cu due to the low molecular (or atomic) weight. We also note that the same H_2 etching capability was observed on electroplated Cu samples (145 nm electroplated Cu on 80 nm physical vapor deposited seed layer), which indicates that this phenomenon is not unique to e-beam evaporated Cu films. In order to gain additional insight into the role of ion bombardment in this Cu plasma etching process, argon was used as a Cu etchant to allow comparison of this more efficient sputter gas to results obtained with H_2.

3.3.3 H_2/Ar Cu Plasma Etching

Figure 3.3 shows cross sectional SEM images of masked Cu samples after 8 min of etching using different H_2: Ar ratios, where Figures 3b and 3d are cross-sectional images of a 100 nm Cu film etched for 8 min in a 1:1 H_2:Ar plasma and in an Ar plasma, respectively. Both etch runs were performed with RF1=100 W, RF2=500 W, 20 mtorr pressure, and an electrode chiller temperature of 10 ^{0}C. The gas flows were: 50 sccm Ar for Ar plasma, 25 sccm H_2 plus 25 sccm Ar for H_2/Ar plasma. Figure 3.3d demonstrates that under these conditions, Ar is able to etch Cu, albeit at a low rate of < 4 nm/min; this represents a pure sputter rate for Cu. However, significant ablation of the SiO_2 mask is apparent, consistent with the ability of Ar ion bombardment to remove materials by momentum transfer. However, the H_2/Ar plasma (Figure 3.3b) displays a much improved etch result compared to Ar (Figure 3.3d) and an improvement relative to that of a pure H_2 plasma (Figure 3.3a) , with a smoother etched surface and higher etch rate (~ 16 nm/min under the conditions used). These results indicate that the mechanism involved in the H_2 plasma etching of Cu has a chemical component. The fact that directional etching with no

discernible undercutting of the SiO_2 mask is observed in a H_2 plasma suggests that a physical (sputtering) component due to ion bombardment is also involved.

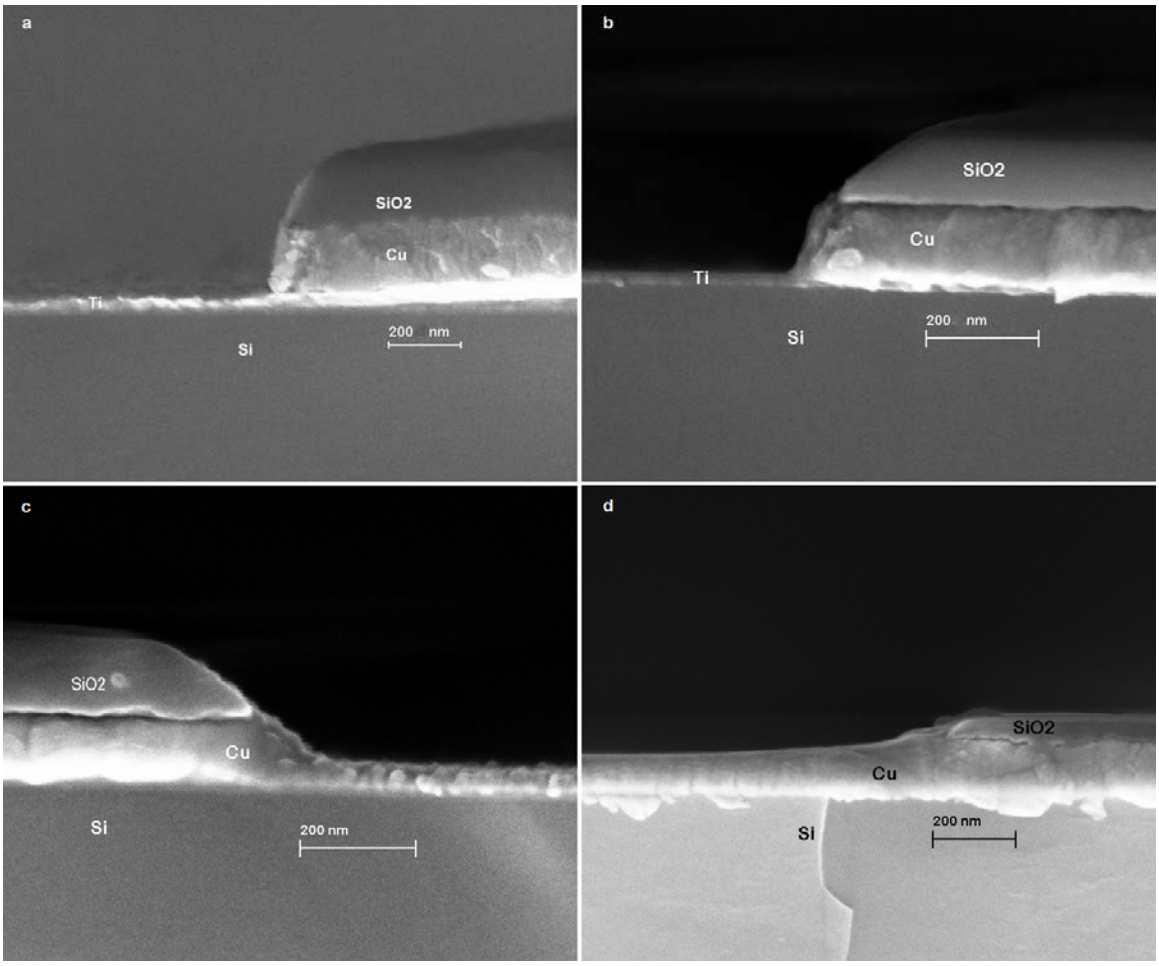

Figure 3.3. Cross sectional SEM images of SiO_2 masked 100 nm Cu films: after 8 min plasma Cu etching with flows of (a) 50 sccm H_2 (b) 25 sccm H_2 + 25 sccm Ar (c) 10 sccm H_2 + 40 sccm Ar (d) 50 sccm Ar. Other etch conditions were RF1=100 W, RF2=500 W, 20 mtorr pressure, and 10 ^oC electrode temperature.

Because Ar ion bombardment should assist in the removal of Cu etch products due to the high atomic weight and thus momentum transfer, the effect of different H_2/Ar plasma mixtures was investigated. Clearly, in Figure 3.3, the etch profile anisotropy

(sidewall angle) degrades with increasing Ar concentration. Also, the etch rate of Cu relative to SiO_2 increases and then decreases as the Ar concentration increases. Specifically, the etch rates for these different ratios were 13, 16, 10 and 4 nm/min respectively as determined from SEM images of samples whose patterns were only partially etched. These observations indicate that an optimum combination of chemical and physical effects exists for efficient Cu etching. Enhanced ion bombardment assists desorption, but the presence of hydrogen, probably H, is critical to effective etching. Finally, the increased sidewall slope that results from increasing Ar concentration (Figs. 3.3a-d) is consistent with increased sputter rate of the SiO_2 mask which yields sloped sidewalls [29]. These results confirm our conclusion regarding the importance of a chemical component in the plasma-assisted etching of Cu in H_2-based plasmas.

Preliminary effects of temperature changes were also investigated by increasing the substrate temperature from 10 ^{0}C to 40 ^{0}C in 15 ^{0} increments. H_2 plasma etch conditions were the same as those of previous etch studies, although 300 nm thick Cu samples were used to allow etch depths to be measured by profilometry and thereby obtain etch rates. Over this small temperature regime, etch rates (roughly measured from SEM images) were not affected by temperature; etch rates for all experiments were ~13 nm/min. Due to equipment limitations, higher temperatures were not possible with this reactor system; further studies are underway using other plasma reactors. These observations indicate that at least over the narrow range of temperatures investigated, H_2 plasma-based etching of Cu films offers a wide temperature control window for implementation of a manufacturable etch process. Possible reasons for the volatilization of Cu in these low temperature processes are discussed in the following paragraphs.

Hydrogen, especially in the atomic form, has a high chemical reactivity and lattice mobility; indeed, H embrittlement of Cu is an important source of Cu degradation [30]. In a plasma environment, H^+ or H^- can react with film material and release H into the solid, which can cause the formation of defects or highly metastable phases [31]. Introduction of hydrogen into f.c.c metals has resulted in microstructure changes; specifically with copper, micro bubbles may be generated [30]. These observations suggest that Cu hydrides may form as a result of plasma exposure. However, thermodynamic calculations indicate that the vapor pressures of Cu hydrides (CuH, CuH_2 or other CuH_x species) are too low to substantially enhance vapor phase Cu removal or etching [25]. Because we observed that the Cu etch rate in a pure H_2 plasma was higher than that for the two-step etch process (chlorination followed by hydrogen treatment) [28], alternate mechanisms for Cu etch product desorption must be considered.

In a H_2 plasma, the Cu surface is bombarded by ions and electrons, as well as UV and visible photons; these particles and photons supply energy to the Cu surface and can enhance etch product removal. Indeed, photodesorption of metal atoms have been reported upon exposure of alkali metals such as Na, K, and Cs to photons [32]; specifically, desorption of sodium atoms was detected even with 40 mW/cm^2 cw laser exposure, where the excitation wavelength was 514 nm [33]. As indicated by the atomic spectrum of hydrogen [34], intense atomic lines in the UV wavelength range of 90 - 120 nm will be present in the H_2 plasma. Although CuH is reported to be thermally unstable, even at 0 ^0C [35], more recent studies suggest that in the presence of a high hydrogen pressure or high hydrogen activity, CuH might be formed [36]. It is also likely that this reaction may be promoted by the presence of H (e.g., from the plasma atmosphere) which

can react with Cu. If sufficient stability of CuH is achieved, desorption of this product may be enhanced by ion and/or photon bombardment. Therefore, photon-assisted desorption of products such as CuH may be important in Cu removal using H_2 plasmas.

These observations are consistent with reports of photon-enhanced removal of copper chloride etch products using UV [21] or even IR radiation [22]. In these studies, UV irradiation was believed to promote the surface reaction between Cu and chlorine by lowering the activation energy of Cu to preferentially form specific Cu chlorides (CuCl or $CuCl_2$). However, our studies [28] as well as those of previous investigators [26], have demonstrated that Cu chlorination occurs rapidly and thus should not limit Cu removal rates. Thus, the enhanced etch rates of Cu in chlorine plasmas due to photon irradiation as demonstrated in previous studies may have resulted from photon assisted etch product removal rather than from reaction rate enhancement. Such observations combined with the high energy photon emission that occurs in H_2 plasmas [34] and the reduced removal rates with Ar which is known to be an effective sputter gas, suggest that UV enhanced desorption of Cu etch products in a H_2 plasma is plausible.

3.4 Conclusion

The surprising results in this study showed that thin Cu films (blanket and SiO_2 masked) were etched in a H_2 plasma at temperatures below room temperature, with an anisotropic profile and high selectivity over Ti. Etch rate variation of pure Ar and H_2/Ar plasmas indicated that chemical and physical components were involved in the etch process. Although the etch mechanism is not yet understood, these preliminary studies

suggest that chemical effects and ion bombardment play a role in the low temperature H_2-based Cu etch process, and photon enhancement may be involved as well.

3.5 References:

[1] M. T. Bohr, "Interconnect scaling--the real limiter to high performance ULSI," *Solid State Technology,* vol. 39, p. 105, 1996.

[2] M. T. Bohr and Y. A. El-Mansy, "Technology for advanced high-performance microprocessors," *IEEE Transactions on Electron Devices* vol. 45, pp. 620-625, 1998.

[3] C. Steinbruchel, "Patterning of copper for multilevel metallization: reactive ion etching and chemical-mechanical polishing," *Applied Surface Science,* vol. 91, pp. 139-146, 1995.

[4] D. Edelstein, J. Heidenreich, R. Goldblatt, W. Cote, C. Uzoh, N. Lustig, P. Roper, T. McDevitt, W. Motsiff, A. Simon, J. Dukovic, R. Wachnik, H. Rathore, R. Schulz, L. Su, S. Luce, and J. Slattery, "Full copper wiring in a sub-0.25 um CMOS ULSI technology," in *Technical Digest., IEEE international Electron Devices Meeting*, 1997, pp. 773-776.

[5] G. E. Moore, "Cramming More Components onto Integrated Circuits," *Electronics,* vol. 38, pp. 114-117, April 19 1965.

[6] A. Mallikarjunan, S. Sharma, and S. P. Murarka, "Resistivity of Copper Films at Thicknesses Near the Mean Free Path of Electrons in Copper Minimization of the Diffuse Scattering in Copper," *Electrochemical and Solid-State Letters,* vol. 3, pp. 437-438, 2000.

[7] H. D. Liu, Y. P. Zhao, G. Ramanath, S. P. Murarka, and G. C. Wang, "Thickness dependent electrical resistivity of ultrathin (<40 nm) Cu films," *Thin Solid Films,* vol. 384, pp. 151-156, 2001.

[8] W. Steinhogl, G. Schindler, G. Steinlesberger, M. Traving, and M. Engelhardt, "Comprehensive study of the resistivity of copper wires with lateral dimensions of 100 nm and smaller," *Journal of Applied Physics,* vol. 97, p. 023706, 2005.

[9] W. Steinhoegl, G. Schindler, and M. Engelhardt, "Unraveling the Mysteries Behind Size Effects in Metallization Systems. (cover story)," *Semiconductor International,* vol. 28, pp. 34-38, 05 2005.

[10] W. Wu, D. Ernur, S. H. Brongersma, M. Van Hove, and K. Maex, "Grain growth in copper interconnect lines," *Microelectronic Engineering,* vol. 76, pp. 190-194, 2004.

[11] W. Zhang, S. H. Brongersma, N. Heylen, G. Beyer, W. Vandervorst, and K. Maex, "Geometry Effect on Impurity Incorporation and Grain Growth in Narrow Copper Lines," *Journal of The Electrochemical Society,* vol. 152, pp. C832-C837, 2005.

[12] P. M. Vereecken, R. A. Binstead, H. Deligianni, and P. C. Andricacos, "The chemistry of additives in damascene copper plating," *IBM Journal of Research and Development,* vol. 49, pp. 3-18, Jan 2005.

[13] M. Traving, G. Schindler, and M. Engelhardt, "Damascene and subtractive processing of narrow tungsten lines: Resistivity and size effect," *Journal of Applied Physics,* vol. 100, pp. 094325-4, 2006.

[14] B. J. Howard and C. Steinbruchel, "Reactive Ion Etching of Copper with Bcl3 and Sicl4 - Plasma Diagnostics and Patterning," *Journal of Vacuum Science & Technology a-Vacuum Surfaces and Films,* vol. 12, pp. 1259-1264, Jul-Aug 1994.

[15] A. Bertz, T. Werner, N. Hille, and T. Gessner, "Effects of the Biasing Frequency on Rie of Cu in a Cl-2-Based Discharge," *Applied Surface Science,* vol. 91, pp. 147-151, Oct 1995.

[16] S. K. Lee, S. S. Chun, C. Y. Hwang, and W. J. Lee, "Reactive ion etching mechanism of copper film in chlorine-based electron cyclotron resonance plasma," *Japanese Journal of Applied Physics Part 1-Regular Papers Short Notes & Review Papers,* vol. 36, pp. 50-55, Jan 1997.

[17] C. Y. Nakakura and E. I. Altman, "Bromine adsorption, reaction, and etching of Cu(100)," *Surface Science,* vol. 370, pp. 32-46, Jan 1 1997.

[18] J. W. Lee, Y. D. Park, J. R. Childress, S. J. Pearton, F. Sharifi, and F. Ren, "Copper dry etching with Cl-2/Ar plasma chemistry," *Journal of The Electrochemical Society,* vol. 145, pp. 2585-2589, Jul 1998.

[19] M. Armacost, P. D. Hoh, R. Wise, W. Yan, J. J. Brown, J. H. Keller, G. A. Kaplita, S. D. Halle, K. P. Muller, M. D. Naeem, S. Srinivasan, H. Y. Ng, M. Gutsche, A. Gutmann, and B. Spuler, "Plasma-etching processes for ULSI semiconductor circuits," *IBM Journal of Research & Development,* vol. 43, p. 39, 01 1999.

[20] H. Tang and I. P. Herman, "Anomalous Local Laser Etching of Copper by Chlorine," *Applied Physics Letters,* vol. 60, pp. 2164-2166, Apr 27 1992.

[21] Y. B. Hahn, S. J. Pearton, H. Cho, and K. P. Lee, "Dry etching mechanism of copper and magnetic materials with UV illumination," *Materials Science and Engineering B,* vol. 79, pp. 20-26, 2001.

[22] Y. Ohshita and N. Hosoi, "Lower Temperature Plasma-Etching of Cu Using Ir Light Irradiation," *Thin Solid Films,* vol. 262, pp. 67-72, Jun 15 1995.

[23] Y. Kuo and S. Lee, "Room-temperature copper etching based on a plasma-copper reaction," *Applied Physics Letters,* vol. 78, pp. 1002-1004, Feb 12 2001.

[24] P. A. Tamirisa, G. Levitin, N. S. Kulkarni, and D. W. Hess, "Plasma etching of copper films at low temperature," *Microelectronic Engineering,* vol. 84, pp. 105-108, 2007.

[25] N. S. Kulkarni and R. T. DeHoff, "Application of Volatility Diagrams for Low Temperature, Dry Etching, and Planarization of Copper," *Journal of The Electrochemical Society,* vol. 149, pp. G620-G632, 2002.

[26] W. Sesselmann and T. J. Chuang, "The interaction of chlorine with copper : I. Adsorption and surface reaction," *Surface Science,* vol. 176, pp. 32-66, 1986.

[27] M. Guido, G. Balducci, G. Gigli, and M. Spoliti, "Mass Spectrometric Study of the Vaporization of Cuprous Chloride and the Dissociation Energy of Cu[sub 3]Cl[sub 3], Cu[sub 4]Cl[sub 4], and Cu[sub 5]Cl[sub 5]," *The Journal of Chemical Physics,* vol. 55, pp. 4566-4572, 1971.

[28] F. Wu, G. Levitin, and D. W. Hess, "Patterning of Cu Films by a Two-Step Plasma Etching Process at Low Temperature," *Journal of The Electrochemical Society,* vol. 157, pp. H474-H478, 2010.

[29] B. Chapman, *Glow discharge processes: sputtering and plasma etching*. New York: Wiley, 1980.

[30] A. Zielinski, "Effect of Hydrogen on Internal-Friction of Some Fcc Metals," *Acta Metallurgica Et Materialia,* vol. 38, pp. 2573-2582, Dec 1990.

[31] S. M. Myers, M. I. Baskes, H. K. Birnbaum, J. W. Corbett, G. G. DeLeo, S. K. Estreicher, E. E. Haller, P. Jena, N. M. Johnson, R. Kirchheim, S. J. Pearton, and M. J. Stavola, "Hydrogen interactions with defects in crystalline solids," *Reviews of Modern Physics,* vol. 64, p. 559, 1992.

[32] J. C. Miller and R. F. Haglund, "Laser ablation : mechanisms and applications : proceedings of a workshop, held in Oak Ridge, Tennessee, USA, 8-10 April, 1991," in *Lecture Notes in Physics*. vol. 389 Berlin: Springer-Verlag, 1991, pp. 77-81.

[33] W. Hoheisel, K. Jungmann, M. Vollmer, R. Weidenauer, and F. Träger, "Desorption stimulated by laser-induced surface-plasmon excitation," *Physical Review Letters,* vol. 60, p. 1649, 1988.

[34] C. Candler, *Atomic Spectra and the Vector Model*, 2nd ed. Princeton, N. J.: Van Nostrand, 1964.

[35] N. P. Fitzsimons, W. Jones, and P. J. Herley, "Studies of copper hydride. Part 1.—Synthesis and solid-state stability," *Journal of the Chemical Society, Faraday Transactions* vol. 91, pp. 713-718, 1995.

[36] R. Burtovyy, E. Utzig, and M. Tkacz, "Studies of the thermal decomposition of copper hydride," *Thermochimica Acta,* vol. 363, pp. 157-163, 2000.

CHAPTER 4

MECHANISTIC CONSIDERATIONS OF LOW TEMPERATURE HYDROGEN-BASED PLASMA ETCHING OF CU

4.1 Introduction

We discussed the low temperature (10 ^{o}C) two-step Cu plasma etching process [1] that is based on a thermochemical analysis of solid-gas volatilization reactions in the Cu-Cl-H system [2] in Chapter 2. In the first step, the Cu film is chlorinated in a Cl_2 plasma at low temperatures to preferentially form $CuCl_2$ relative to CuCl [3]. In the second step, a hydrogen plasma is used to convert $CuCl_2$ into a product with improved volatility, presumably Cu_3Cl_3, which is more volatile than $CuCl_2$ or CuCl [4]. Our Cu patterning and etching mechanism studies of this new process indicated that the H_2 plasma treatment for Cu chloride removal is the rate-limiting step and a critical component in establishing etch pattern fidelity [5]. Most importantly, these studies also demonstrated that a pure H_2 plasma can etch a Cu film at these low temperatures [6], which was discussed in Chapter 3. This surprising result offers a simple approach to patterning Cu using a single step plasma (vacuum) process, thereby greatly improving manufacturability and process control. In addition, if damascene processes are no longer required for Cu patterning, the need for large concentrations of reactive liquid chemicals for CMP as well as chemical recycling or disposal of these chemicals can be eliminated. The advantages of this process promise significant cost reduction and environmental improvements for current Cu etching technology. Thus in this chapter, we describe the factors that control low

temperature H_2-based plasma etching of Cu films and offer preliminary mechanistic information regarding this process.

4.2 Experimental

4.2.1 Cu sample preparation

100 or 300 nm thick Cu films were deposited by e-beam evaporation (CVC E-Beam Evaporator) onto (100) silicon wafers that had been coated with 20 nm of titanium to promote Cu adhesion to silicon. Electroplated Cu films (145 nm electroplated Cu films grown from an 80 nm physical vapor deposited (PVD) seed layer followed by annealing at 200 ^{o}C in forming gas for 30 sec) were also studied. Since no differences in etch properties were observed, the results reported in this chapter are from e-beam deposited Cu films. Cu-coated substrates were sectioned into etch samples ~1 cm^2.

Both blanket and masked Cu films were investigated in these plasma etch atmospheres. Masked Cu films invoked SiO_2 (~150 nm) as the mask layer. The SiO_2 film was deposited in a Plasma Therm PECVD (plasma enhanced chemical vapor deposition) system with 400 sccm SiH_4 and 900 sccm N_2O as precursors; the substrate electrode was heated to 250 ^{o}C, the power applied to the electrode was 25 W, and the pressure was maintained at 900 mtorr during the deposition process. Mask patterns were generated by fluorine-based plasma etching an inductively coupled plasma (ICP) reactor (Plasma Therm SLR): the etch gas was a mixture of 25 sccm Ar, 2 sccm O_2, 14 sccm CF_4 and 6 sccm C_4F_6, RF1 (power applied to the platen) was 200 W and RF2 (power applied to the coil) was 100 W, while the process pressure was maintained at 5 mtorr.

4.2.2 Plasma Etching of Cu

For nearly all results presented, plasma etching of thin Cu films was performed in an inductively coupled plasma (ICP) reactor (Plasma Therm SLR). However, due to the inability to strike a plasma in the Plasma Therm SLR reactor when power was not applied simultaneously to both the coil and platen, several experiments were performed in an STS SOE ICP reactor, to investigate etch processes at either zero platen power or zero coil power. The substrate temperature was maintained at ~10 ^{o}C using a water cooled chiller connected to the substrate electrode. The H_2 gas flow rate was 50 standard cubic centimeters per minute (sccm) and the reactor pressure was maintained at 20 mtorr. The radio frequency power applied to the ICP coil (RF2) was varied from 300-700 W, whereas the power applied to the substrate (RF1) was varied between 25 and 200 W. After Cu etching, the hard masks were removed by a dilute HF:H_2O solution (1:50).

In order to gain further insight into the etch mechanism, plasmas of two noble gases, Ar and He, were used to pattern Cu thin films. In addition, their respective H_2 mixture plasmas (H_2/Ar and H_2/He plasmas) were investigated. All of these etch gases were used under the same conditions as those for the H_2 plasma, except that with the H_2/Ar (or H_2/He) plasmas, the total flow rate was fixed at 50 sccm while the gas ratio (H_2 : Ar or H_2 : He) was varied.

4.2.3 Plasma Diagnostics and Post Etch Analysis

During the etching process, the plasma atmosphere was analyzed with a residual gas analyzer (RGA); the RGA was an AccuQuad Model 300D. Chemical analysis of the

films and surfaces before and after plasma etching was performed using X-ray photoelectron spectroscopy (XPS). XPS spectra were collected with a Thermo Scientific K-Alpha XPS system. Cu film patterns were examined with a scanning electron microscope (SEM, Zeiss SEM Ultra60). Thickness changes of the Cu layer were determined from SEM images, as well as Wyko Profilometer and Dektak 150 Profilometer measurements.

4.3 Results and Discussion

4.3.1 Chemical Etch Considerations: Mass Spectroscopy

Initially, masked Cu samples were etched with a pure H_2 plasma [6]; this yielded an anisotropic profile but rough sidewall surfaces, as discussed in Chapter 3. These preliminary results indicate that sputtering alone cannot account for Cu removal in this etch process, due to the low molecular (or atomic) weight of H_2 (H) and thus the minimal momentum of impinging ions. Indeed, argon was investigated as a Cu etchant to gain further insight into the role of ion bombardment in the H_2 plasma etch process [6]. However, pure Ar was not an efficient etch gas for Cu, with a much lower Cu removal rate (~4 nm/min) than that of H_2 (13 nm/min) and greatly enhanced sputtering of the SiO_2 etch mask. These observations suggest that the Cu etch mechanism involves a chemical component in addition to a physical (sputtering) component in the H_2 plasma. Furthermore, alteration of the H_2/Ar plasma mixture resulted in varying Cu etch rates and sidewall angles, indicating that control of feature/edge profile is possible and that effective etching may depend on an optimal combination of chemical and physical components [6].

The results of H_2-based Cu etching suggest that Cu hydrides are likely etch products due to the efficient removal observed. However none of the reported Cu hydrides have significant volatility [7-8]. Etchant/product gases from the plasma were sampled through a port on the side of the vacuum chamber using mass spectroscopy in an attempt to detect possible etch product molecules. The mass spectra were taken 1 min, 3 min and 5 min after H_2 plasma ignition for the etching of blanket 100 nm Cu samples with the etch conditions used to generate the patterns shown in Figure 3.1b. The spectra indicate the presence of H, O, N, C (C^+, CO^+, CO_2^+) in the plasma atmosphere, but no Cu-containing peaks were observed. These results indicate that the specific etch products formed do not have sufficient vapor pressure and/or are too reactive at surfaces in the chamber and tubing to allow the products to reach the detector. Clearly, re-deposition occurs either within the chamber or in the tubing leading to the detector. Further evaluation of possible Cu etch product re-deposition was carried out by performing H_2 plasma etching of Cu films on 4-inch diameter silicon substrates. In these investigations, both masked and blanket Cu layers were studied; results were analogous to those for the 1 cm^2 samples, demonstrating that re-deposition onto the wafer surface is not apparent when etching larger Cu areas. This observation indicates that Cu etch product volatility is sufficient to minimize re-deposition even when etching large areas under the conditions studied.

4.3.2 Chemical Etch Considerations: Possible Etch Products

Atomic hydrogen has a high chemical reactivity and both atomic and molecular hydrogen have high lattice mobility; indeed, hydrogen embrittlement of Cu is well-

known [9]. In a plasma environment, H^+ or $H^\cdot$ can form defects or metastable phases in the exposed solids by reacting with film material [10]. Various interactions of hydrogen atoms with f.c.c metals have been noted, including irreversible microstructural changes such as hydride or microbubble formation in copper [9]. However, the vapor pressures of Cu hydrides (CuH, CuH_2 or other CuH_x species) appear to be too low to substantially enhance vapor phase Cu removal based on thermodynamic calculations [2]. Although vapor pressure data as a function of temperature for most copper compounds are not available, the melting points (Table 4.1) can give insight into the relative volatility of these compounds. At high temperatures (~200 ^oC) and with atomic H exposure, themodynamic analyses of the Cu-Cl-H system indicated that a reasonable vapor pressure of CuH is expected [2]. Atomic hydrogen is prevalent in a plasma environment; however, the vapor pressure of CuH is not predicted to be higher than that of Cu_3Cl_3 [2]. Furthermore, CuH is reported to be thermally unstable even at 0 ^oC [7] and can decompose into small Cu particles especially in the presence of trace amounts of oxygen [11]. Because we observed that the Cu etch rate in a pure H_2 plasma was higher than that for the two-step etch process (chlorination followed by hydrogen treatment) [5], alternate mechanisms for Cu etch product desorption must be considered.

Table 4.1 Comparison of melting points of copper compounds [12].

Copper Compounds	Melting Point
CuCl	426 ^{o}C
$CuCl_2$	498 ^{o}C (anhydrous)
CuH	Thermally unstable (decomposes <100 ^{o}C) [7]
CuH_2	Unstable to decomposition [8]
Cu_2O	1235 ^{o}C
CuO	1201 ^{o}C

4.3.3 Physical Etch Considerations: Photon-Enhanced Etching

In a H_2 plasma, the Cu surface is exposed to ions, electrons and plasma-emitted photons. As shown in Table 4.2, these photons have relatively short wavelengths and thus can impart significant energy to the Cu film. High energy UV photons combined with energetic ion bombardment and the chemical reaction of $H^{\cdot}$ with Cu can all contribute to the removal of Cu during the etching process. Indeed, photodesorption of metal atoms has been reported for alkali metals such as Na, K, and Cs [13]. Table 4.2 lists the atomic emission lines in the UV region for H, Ar , He and Cl. Clearly, intense atomic lines in the UV wavelength range are present in H_2 (90~120 nm), Ar (80~100 nm) and He plasmas (50~60 nm). The energy of the most intense H and Ar lines (indicated by an asterisk in Table 4.2) is substantially higher than that of Cl, but much lower than that of He; in fact, He plasmas have been used as a source of VUV photons [14]. If photons play a role in the plasma etching of Cu, then a He plasma may display higher etch rates than are observed with an Ar plasma, since both are noble gases (no chemical component in the

etch process) even though He has a lower atomic weight than does Ar and thereby imparts less momentum to the etching surface relative to Ar.

Table 4.1 Atomic emission lines (in angstroms) of H_2, Ar, He and Cl in the high energy regime (from Grotrian Diagrams) [15].

H	Ar	He	Cl
972.54	876.06	537.024	1201.4
1025.83*	894.30	584.331*	1347.3/1351.7/1363.5
1215.68	1048.22*	591.420	1379.6/1389.9/1396.5*
	1066.66		

* Highest intensity emission line for the specific atom.

In order to compare Cu removal using Ar and He plasmas, Cu etching was performed in a pure He plasma under the same plasma conditions as those used to generate the etch profile in Figure 3.1b. Figure 4.1a shows a cross-sectional SEM image of a SiO_2 masked 100 nm Cu film after an 8 min He plasma treatment. Despite the fact that Ar should be a more efficient sputter etch gas than He due to the higher atomic weight and so enhanced momentum transfer, the Cu etch rate in the He plasma is higher than that of Ar (~10 nm/min vs. 4 nm/min). In addition, the DC bias (corresponding approximately to the ion energy) on the wafer platen for the He plasma was essentially the same as that of Ar plasma (230 V) under these plasma conditions. This observation is consistent with shorter wavelength and thus higher energy photon emission from the He plasma relative to that from the Ar plasma. However, both the He etch rate and the anisotropy were degraded relative to those obtained with H_2-based plasmas (Figure 4.1b) due to the ablation of SiO_2, resulting in a Cu edge profile similar to that generated by the

Ar etch. In addition, H_2/He plasma mixtures displayed the same trend as did the H_2/Ar plasmas, except that mixtures with He showed higher etch rates. Again, such observations indicate the importance of a chemical component in H_2 plasma etching of Cu and suggest that photon enhancement may offer an additional physical component to that of ion bombardment-enhanced etching, since both He and Ar are noble gases, but differ substantially in atomic weight and emission lines.

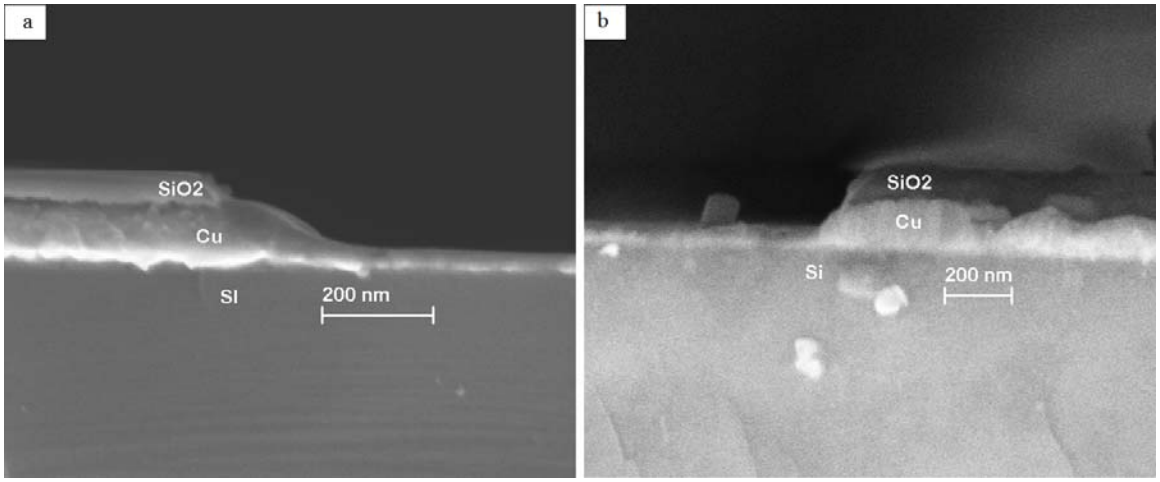

Figure 4.1. Cross sectional SEMs of SiO_2 masked 100 nm Cu films (a) after 8 min of He plasma; (b) after 4 min of H_2 plasma treatment. Plasma etching was performed under the conditions RF1 = 100 W, RF2 = 500 W, 20 mtorr pressure, 50 sccm flow rate and 10 ^{o}C electrode temperature.

Photodesorption is not unique to alkali metals, since photon-enhanced removal of chloride etch products using UV [16-20]or even IR [21-22] exposure has been reported for the chlorine-based plasma etching of Cu. In these studies, local heating was deemed a minor contributor to the etch mechanism [19] especially with IR exposure; rather, a non-thermal (photochemical) mechanism seemed more plausible since etch rate changed with wavelength [22]. Similarly, UV photon emission from the H_2 plasma may have analogous effects to those observed in laser exposure studies irregardless of whether the etch

products are copper chlorides or other copper species. Combined with the counter-intuitive sputtering results described above and the high energy photon emission that occurs in different plasma atmospheres, UV enhanced desorption of Cu etch products may play a role in H_2-based plasma etching of Cu.

4.3.4 Physical Etch Considerations: Ion Bombardment

The ICP reactor has two power supplies, one for coil power (for plasma generation), and the other for platen power (to accelerate ions); both ion bombardment and photon impingement will be influenced by power from these two rf sources. Therefore the Cu etch rate and the corresponding DC bias of H_2 plasmas under different platen powers (RF1, Figure 4.2a) and coil powers (RF2, Figure 4.2b) were investigated. When changing the platen power, coil power was kept constant (500 W); likewise, when changing coil power, the platen power was kept constant (100 W). As is evident in Figure 4.2a, Cu etch rates were nearly linear with platen power up to 100 W, with smaller increases at higher applied powers. This trend essentially followed changes in DC bias, which indicates the importance of ion energy in this Cu etch process. Figure 4.2b demonstrates that an increase in coil (plasma) power resulted in an increase in Cu etch rate, apparently due to an increase in the flux of plasma moieties such as ions, neutral species and photons to the Cu surface, and a reduction in DC bias as expected at a constant plasma power.

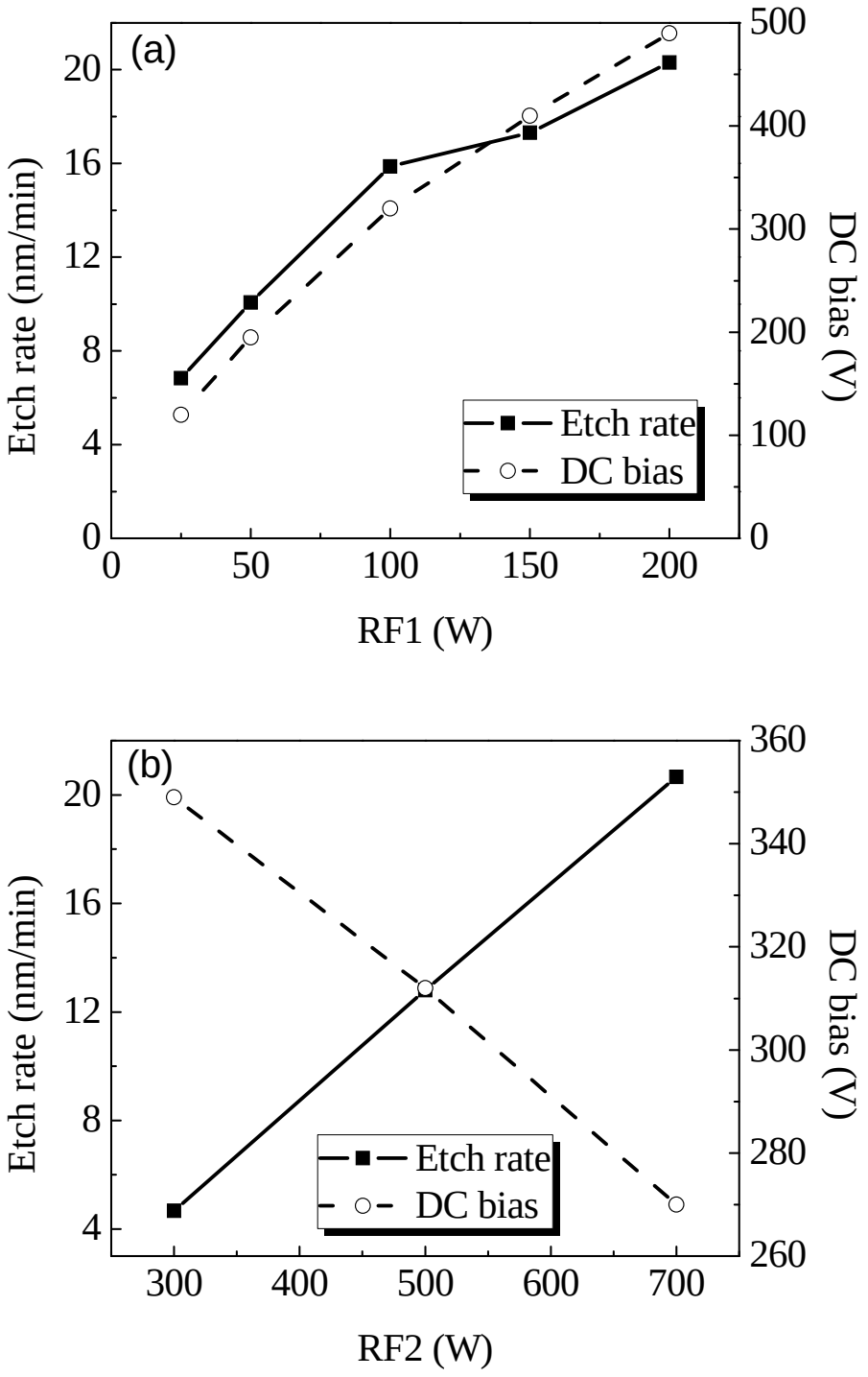

Figure 4.2. Cu etch rates in H_2 plasma vs. (a) platen power (RF1) when RF2 = 500 W; (b) coil power (RF2) when RF1 = 100 W. Other plasma etching conditions were: 20 mtorr pressure, 50 sccm flow and 10 ^{o}C electrode temperature.

This trend is beneficial with respect to lowered mask ablation and mitigation of possible plasma damage from the etch process. Indeed, higher ion energy increased SiO_2 mask ablation and thus degraded the etch profile anisotropy. Figure 4.3 shows the Cu (~180 nm) edge profile before and after a 8 min H_2 plasma when RF2 = 700 W. Higher coil power yields higher etch rate (~20 nm/min) relative to that for RF2 = 500 W as shown in Figure 3.1b, but no obvious enhancement of SiO_2 mask ablation was observed for higher coil power (RF2). Such results are consistent with an increased ion flux for the process with higher plasma generation power. These observations further confirm that ion bombardment flux is an important consideration in the low temperature Cu etch process.

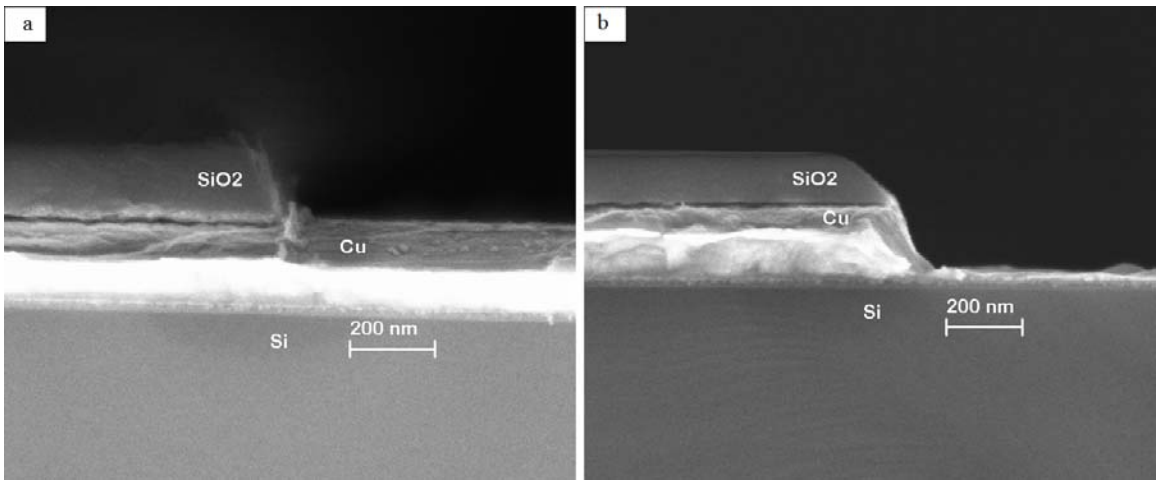

Figure 4.3. Cross sectional SEMs of SiO_2 masked 180 nm Cu films before (a) and after (b) 8 min of H_2 plasma under the conditions RF1 = 100 W, RF2 = 700 W, 20 mtorr pressure, 50 sccm flow rate and 10 ^{o}C electrode temperature.

4.3.5 Differentiation between Physical and Chemical Considerations

In order to gain additional insight into the relative contributions of ion bombardment and chemical reactions to the etch mechanism, preliminary studies at zero

platen power and zero coil power (with the other power supply kept constant) were performed. Because of the inability to strike a plasma without platen power in the Plasma Therm ICP reactor, these experiments were performed in an STS SOE ICP reactor. These initial studies used the same pressure as well as platen and coil powers as those used in the Plasma Therm reactor; due to the different reactor configuration/size, and the inability to cool the platen to 10^{o}C, the Cu etch rates obtained were different. That is, for this preliminary investigation, reactor power conditions were not adjusted in an attempt to obtain identical etch rates in the two reactors. Figure 4.4 shows etch rates and the corresponding DC bias under the indicated power settings. Application of power to both the coil and platen yields the highest etch rate. With zero platen power (RF1= 0W) but the same coil power (RF2=500 W), the Cu etch rate is near zero, while with zero coil power (RF2=0W) but the same platen power (RF1=100W), the Cu etch rate is ~36% of the etch rate when power is supplied to both coil and platen. These results indicate that ion bombardment is critical to Cu etching in H_2 plasmas, but ion bombardment and chemical reaction are contributors to the etch rates achieved.

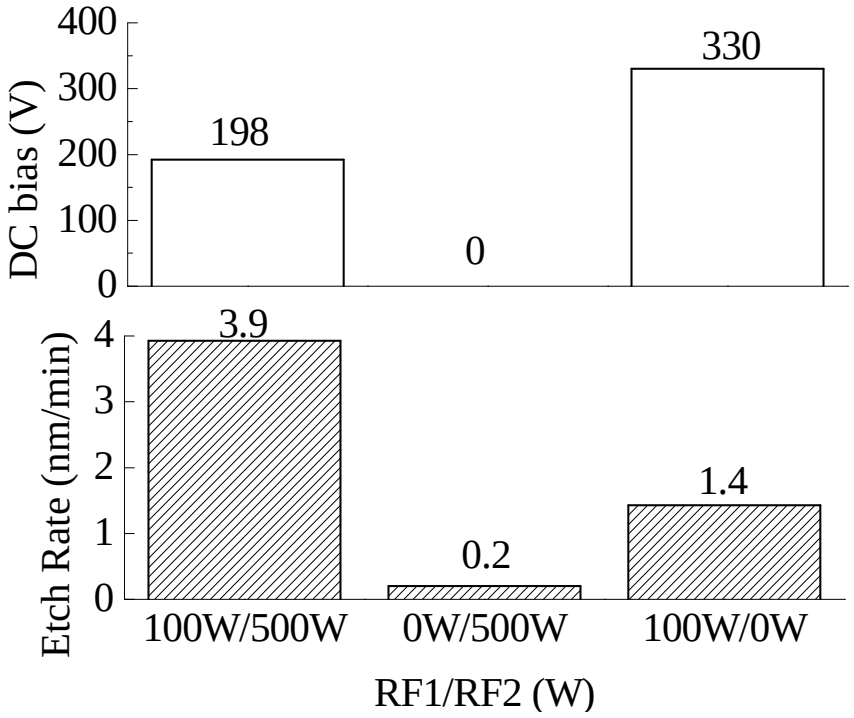

Figure 4.4.Cu etch rates and corresponding DC bias in H_2 plasma with typical power supplies (RF1=100W, RF2=500W) , zero platen power (RF1=0 W) and zero coil power (RF2=0 W);other parameters are: 20 mtorr pressure, 50 sccm H_2 flow rate, 20 ^oC electrode temperature in a STS SOE ICP reactor.

4.3.6 Photodesorption Considerations in Cu Etching

Laser-induced desorption and ablation can be considered an extreme example of photodesorption, wherein photoexcitation is converted into kinetic energy, leading to the ejection of atoms, ions and molecules [23]. Although the H_2 or He plasma emission in this study does not possess the high intensity of a laser source, our etch results with Ar and He etchants suggest that UV photons may be a contributor to low temperature H_2 plasma etching of Cu films. Therefore, we offer that possibility that the H_2 plasma Cu

etch process may be considered a combined result of Cu hydride formation, ion bombardment and photon impingement.

Further evidence for photon enhancement of plasma etch processes arises from a reported “hydrogen effect” in glow discharge coupled optical emission spectrometry (GD-OES) or mass spectrometric (MS) analysis of solids, wherein the sputter rate of sample solids changed with the addition of H_2 to an Ar plasma [24]. In particular for Cu, addition of a small amount (less than 1%) of H_2 resulted in an intensity increase for Cu I emission lines while quenching Cu II emission lines [25]. An accurate interpretation of these changes in the emission spectrum is not possible since emission intensities are not necessarily proportional to sputter rate or discharge current. However, this observation offers strong evidence that H_2 addition changes both the nature of the noble gas plasma and the sputter rate of Cu.

4.4. Conclusions

Hydrogen-based ICP plasmas can etch Cu at temperatures below room temperature; with SiO_2 as a mask, pattern definition with $> 80^o$ sidewall slope can be achieved. Our results indicate that both physical and chemical components are involved in the etch mechanism. Comparison of Cu etch results among Ar, He and H_2 plasmas suggests that photon enhancement contributes to the etch process. Both platen and coil powers influence Cu etch rates and mask ablation which confirms the importance of ion bombardment in the etch process. The overall plasma-based low temperature Cu etch process appears to be controlled by a combination of UV photon impingement, ion bombardment and H interaction with Cu surfaces.

4.5 References:

[1] P. A. Tamirisa, G. Levitin, N. S. Kulkarni, and D. W. Hess, "Plasma etching of copper films at low temperature," *Microelectronic Engineering,* vol. 84, pp. 105-108, 2007.

[2] N. S. Kulkarni and R. T. DeHoff, "Application of Volatility Diagrams for Low Temperature, Dry Etching, and Planarization of Copper," *Journal of The Electrochemical Society,* vol. 149, pp. G620-G632, 2002.

[3] W. Sesselmann and T. J. Chuang, "The interaction of chlorine with copper : I. Adsorption and surface reaction," *Surface Science,* vol. 176, pp. 32-66, 1986.

[4] M. Guido, G. Balducci, G. Gigli, and M. Spoliti, "Mass Spectrometric Study of the Vaporization of Cuprous Chloride and the Dissociation Energy of Cu[sub 3]Cl[sub 3], Cu[sub 4]Cl[sub 4], and Cu[sub 5]Cl[sub 5]," *The Journal of Chemical Physics*, vol. 55, pp. 4566-4572, 1971.

[5] F. Wu, G. Levitin, and D. W. Hess, "Patterning of Cu Films by a Two-Step Plasma Etching Process at Low Temperature," *Journal of The Electrochemical Society*, vol. 157, pp. H474-H478, 2010.

[6] F. Wu, G. Levitin, and D. W. Hess, "Low Temperature Etching of Cu by Hydrogen-Based Plasmas," *ACS Applied Materials & Interfaces,* vol. 2, pp. 2175–2179, 2010.

[7] N. P. Fitzsimons, W. Jones, and P. J. Herley, "Studies of copper hydride. Part 1.—Synthesis and solid-state stability," *Journal of the Chemical Society, Faraday Transactions* vol. 91, pp. 713-718, 1995.

[8] E. V. Lavrov, J. Weber, and F. Borrnert, "Copper dihydrogen complex in ZnO," *Physical Review B,* vol. 77, p. 155209, Apr 2008.

[9] A. Zielinski, "Effect of Hydrogen on Internal-Friction of Some Fcc Metals," *Acta Metallurgica Et Materialia,* vol. 38, pp. 2573-2582, Dec 1990.

[10] S. M. Myers, M. I. Baskes, H. K. Birnbaum, J. W. Corbett, G. G. DeLeo, S. K. Estreicher, E. E. Haller, P. Jena, N. M. Johnson, R. Kirchheim, S. J. Pearton, and M. J. Stavola, "Hydrogen interactions with defects in crystalline solids," *Reviews of Modern Physics,* vol. 64, p. 559, 1992.

[11] J. C. Warf and W. Feitknecht, "Zur Kenntnis des Kupferhydrids, insbesondere der Kinetik des Zerfalls," *Helvetica Chimica Acta,* vol. 33, pp. 613-639, 1950.

[12] D. R. Lide, *CRC Handbook of Chemistry and Physics*, 84th ed. Boca Raton: CRC Press, 2003.

[13] J. C. Miller and R. F. Haglund, "Laser ablation : mechanisms and applications : proceedings of a workshop, held in Oak Ridge, Tennessee, USA, 8-10 April, 1991," in *Lecture Notes in Physics*. vol. 389 Berlin: Springer-Verlag, 1991, pp. 77-81.

[14] D. Dictus, M. R. Baklanov, V. Pikulev, S. De Gendt, C. Vinckier, W. Boullart, and S. Vanhaelemeersch, "Unusual Modification of CuCl or CuBr Films by He Plasma Exposure Resulting in Nanowire Formation," *Langmuir,* vol. 26, pp. 2014-2020, 2009.

[15] C. Candler, *Atomic Spectra and the Vector Model,* 2nd ed. Princeton, N. J.: Van Nostrand, 1964.

[16] K. S. Choi and C. H. Han, "Low-temperature plasma etching of copper films using ultraviolet irradiation," *Japanese Journal of Applied Physics Part 1-Regular Papers Short Notes & Review Papers,* vol. 37, pp. 5945-5948, Nov 1998.

[17] K. S. Choi and C. H. Han, "Low temperature copper etching using an inductively coupled plasma with ultraviolet light irradiation," *Journal of The Electrochemical Society,* vol. 145, pp. L37-L39, Mar 1998.

[18] M. S. Kwon, J. Y. Lee, K. S. Choi, and C. H. Han, "Reaction characteristics between Cu thin film and RF inductively coupled Cl-2 plasma without/with UV irradiation," *Japanese Journal of Applied Physics Part 1-Regular Papers Short Notes & Review Papers,* vol. 37, pp. 4103-4108, Jul 1998.

[19] Y. B. Hahn, S. J. Pearton, H. Cho, and K. P. Lee, "Dry etching mechanism of copper and magnetic materials with UV illumination," *Materials Science and Engineering B,* vol. 79, pp. 20-26, 2001.

[20] K. Myoung Seok and L. Jeong Yong, "Reaction Mechanism of Low-Temperature Cu Dry Etching Using an Inductively Coupled Cl[sub 2]/N[sub 2] Plasma with Ultraviolet Light Irradiation," *Journal of The Electrochemical Society,* vol. 146, pp. 3119-3123, 1999.

[21] N. Hosoi and Y. Ohshita, "Lower-Temperature Plasma-Etching of Cu Films Using Infrared Radiation," *Applied Physics Letters,* vol. 63, pp. 2703-2704, Nov 8 1993.

[22] Y. Ohshita and N. Hosoi, "Lower Temperature Plasma-Etching of Cu Using Ir Light Irradiation," *Thin Solid Films,* vol. 262, pp. 67-72, Jun 15 1995.

[23] J. C. Miller, *Laser ablation and desorption*. San Diego: Academic Press, 1998.

[24] A. Martín, A. Menéndez, R. Pereiro, N. Bordel, and A. Sanz-Medel, "Modifying argon glow discharges by hydrogen addition: effects on analytical characteristics of optical emission and mass spectrometry detection modes," *Analytical and Bioanalytical Chemistry*, vol. 388, pp. 1573-1582, 2007.

[25] V.-D. Hodoroaba, V. Hoffmann, E. B. M. Steers, and K. Wetzig, "Emission spectra of copper and argon in an argon glow discharge containing small quantities of hydrogen," *Journal of Analytical Atomic Spectrometry*, vol. 15, pp. 951-958, 2000.

CHAPTER 5

TEMPERATURE EFFECTS AND OPTICAL EMISSION SPECTROSCOPY STUDIES OF HYDROGEN-BASED PLASMA ETCHING OF COPPER

5.1 Introduction

The two-step plasma etch process for Cu was discussed in Chapter 2. Based upon the discovery that the H_2 plasma step was the limiting step in this etch process, the feasibility of the H_2 plasma etching of Cu was described in Chapter 3 and preliminary mechanistic studies were discussed in Chapter 4. Results demonstrated clearly that H_2 plasma-based etching of Cu at low temperature (~10 ^oC) must contain a chemical as well as a physical component, but no direct evidence regarding the etch product was offered. In this chapter, optical emission spectroscopy (OES) studies, wherein light emission from the plasma is analyzed, are described. Although temperature is expected to affect the volatility of Cu_3Cl_3 [1-2] in the two-step etch process (Chapter 2), ICP platen cooling limitations precluded our ability to investigate these effects at Georgia Tech. By employing the ICP reactor at Oak Ridge National Laboratory (ORNL), OES was used to investigate the etch products from both the single step H_2 plasma Cu etch and the two-step plasma etch process. Results from these investigations offer insight into the etch products present in the plasma atmosphere.

Optical diagnostic techniques use photons to interrogate chemical and physical characteristics of plasmas. In particular, specific chemical moieties and their concentrations within the plasma can be determined without altering or modifying the plasma [3]. Excited state species generated primarily by electron impact, decay into lower energy levels and thus emit a photon of energy equal to the difference in energy between the emitting and final state, which is the "fingerprint" of the chemical species present in the plasma. OES is deceptively simple, requiring only a monochromator and detector. Establishment of the species present in the plasma is reasonably straight-forward; however, quantification of species concentrations is difficult since emission intensity is generally not an accurate indicator of relative etchant concentration since the emission intensity also depends on the electron energy distribution function.

5.2 Experimental

5.2.1 Cu Sample Preparation

100 nm (sample A) and 200 nm (sample B) thick Cu films were deposited by e-beam evaporation (CVC E-Beam Evaporator) onto (100) silicon wafers that had been coated with 20 nm of titanium to promote Cu adhesion to silicon. Four inch diameter Cu-coated silicon substrates were used for OES studies or were sectioned into small samples ~1 cm^2 for etch studies.

Both blanket and masked Cu films were studied; masked films used SiO_2 (~150 nm) as the mask layer. The SiO_2 film was deposited in a Plasma Therm PECVD (plasma enhanced chemical vapor deposition) system with 400 sccm (standard cubic centimeters per minute) SiH_4 and 900 sccm N_2O as precursors; the substrate electrode was heated to

250 ^{o}C, the power applied to the electrode was 25 W, and the pressure was maintained at 900 mtorr during the deposition process. Mask patterns were generated by fluorine-based plasma etching in a Plasma Therm SLR ICP (inductively coupled plasma) reactor; the etch gas was a mixture of 5 sccm Ar, 28 sccm CO_2, and 15 sccm C_4F_8 , RF1 (power applied to the platen) was 80 W and RF2 (power applied to the coil) was 400 W, while the process pressure was maintained at 5 mtorr.

5.2.2 Plasma Etching of Cu

Plasma etching of thin Cu films was performed in an ICP reactor (Oxford Plasmalab System 100 ICP-RIE) located at Oak Ridge National Laboratories. The substrate temperature was varied between -150 and 150 ^{o}C at 50 ^{o}C intervals by using a liquid nitrogen cooled chiller and a built-in heater connected to the substrate electrode.

Two types of plasma etch processes were performed: single step H_2 plasma etch [4] and two-step plasma etch (Cl_2 plasma step followed by H_2 plasma step) [1]. For the former process, the H_2 gas flow rate was 60 sccm and the reactor pressure was maintained at 20 mtorr. The radio frequency power applied to the ICP coil (RF2) was 1800 W, whereas the power applied to the substrate (RF1) was 100 W. The two-step etch process consisted of either a 1 min or 30 sec Cl_2 plasma to chlorinate Cu, followed by a 2 min H_2 plasma for etch product removal. For the Cl_2 step, the Cl_2 gas flow was 10 sccm, the reactor pressure was 20 mtorr, and RF1 and RF2 were 100 W and 1800W, respectively. For the H_2 plasma, the corresponding plasma conditions were 60 sccm H_2, 20 mtorr, RF1=150 W, RF2=1800 W. The use of 150 W (rather than 100 W) for RF1 was to allow direct comparison of the results in this chapter to those described in Chapter 2.

Limited temperature variation studies in a Plasma Therm ICP reactor (located at Georgia Tech), which was employed in the studies described previously [1, 4]) were also performed to serve as a comparison with the temperature studies carried out in the Oxford Plasmalab System 100 ICP-RIE reactor (at ORNL). The plasma parameters used in the Plasma Therm ICP (Georgia Tech) are RF1=100 W, RF2=500 W, 50 sccm H_2 flow rate and 20 mtorr pressure. The electrode temperature was varied between 10 and 40 ^oC.

5.2.3 Post Etching Treatment and Characterization

After Cu etching, the SiO_2 mask layer was removed with a dilute HF: H_2O solution (1:50). Cu film patterns were examined with a scanning electron microscope (SEM, Zeiss SEM Ultra60). Thickness changes of the Cu layer were determined from SEM images, Wyko Profilometer and Dektak 150 Profilometer data. Chemical analysis of the films and surfaces before and after plasma etching was performed using X-ray photoelectron spectroscopy (XPS). XPS spectra were collected using a Thermo Scientific K-Alpha XPS system. Optical emission spectra (OES) of plasmas during the etch processes were obtained with a Verity SD2048DL Spectrography system.

5.3 Results and Discussion

5.3.1 Single step H_2 Plasma Etching of Cu

5.3.1.1 Effect of Temperature on Etch Rate

Cu etch rates were determined by measuring the etch depth of masked Cu samples (1 cm^2 size) after 10 min of H_2 plasma treatment under the conditions RF1= 100 W, RF2= 1800 W, 20 mTorr pressure and 60 sccm H_2 flow rate; etch rates are plotted in Figure 5.1 as a function of electrode temperature. As indicated in Figure 5.1, in the temperature range from -150 ^oC to 10 ^oC, Cu etch rates increased monotonically, which is consistent with higher temperatures favoring evaporation of Cu etch products. That is, the ion bombardment flux and energy during the plasma etch process do not change with temperature; therefore, enhanced sputtering at higher temperatures is not the likely cause of the etch rate increase displayed in Figure 5.1. Rather, such etch rate trends with temperature confirm that a strong chemical component is present in the H_2 plasma etch process [4]. It is also interesting that even at -150 ^oC, a measurable etch rate is observed with pure H_2 suggesting that the etch product is volatile or is easily sputtered.

At temperatures above 10 ^oC, a reduction in etch rate occurs. Since this trend is reproducible and is consistent with optical emission data which will be discussed later in this paper, the variation may be related to etch product instability over a certain temperature range. Specifically, if Cu hydrides are the etch products, decomposition should occur readily [5] and may affect the ability to desorb or sputter etch products from the surface. DC bias voltages for the different temperatures were essentially constant (-240 to -250 V). This observation is consistent with the fact that since the pressure and power values did not change, no substantial change in ion energy and flux should occur. These facts again suggest that the temperature effects on etch rates are related to chemical reactions between Cu and H and the ability to desorb etch products. Such results are consistent with our previous studies which indicate that pure physical sputtering using Ar

plasmas is ineffective in etching Cu under the conditions used in this study, thereby offering more evidence to the importance of chemistry in this etch process.

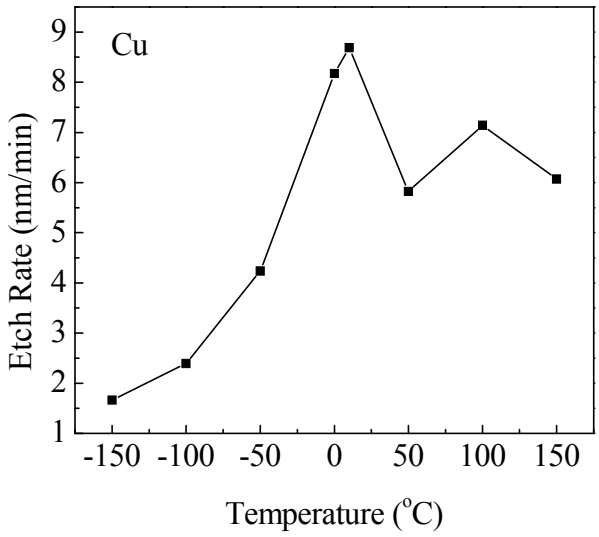

Figure 5.1 Cu etch rate vs. electrode temperature. Etch conditions were RF1= 100 W, RF2= 1800 W, 20 mTorr pressure, 60 sccm H_2 flow rate.

5.3.1.2 OES Analysis of H_2 Plasmas

Optical emission spectroscopy (OES) diagnostics of hydrogen plasmas during the etching of blanket Cu samples (4'' wafers) are shown in Figure 5.2 for pure H_2 plasma etching of Cu at 10 ^{o}C. The hydrogen Balmer series (370~660 nm) lines are prominent in the spectrum, with high intensity atomic H lines at 656.5 nm (H_α) and 486.1 nm (H_β) [6]. Cu resonance lines at 324.7 nm and 327.4 nm are also evident [7]. To a first approximation, the emission intensities may be considered indicative of changes in Cu etch rates, since as reported previously, Cu emission intensity (324.7 nm) was linearly proportional to the sputtering rate of a Cu target in diode and triode systems [8]. Because

CuH_x is a likely etch product, emission from a Cu hydride species is expected. However, no CuH lines are detected (most intense would appear at 428 nm [9]). Furthermore, no emission lines from either CuO (most intense at 605.9 nm and 445.7 nm) or CuOH (535 to 555 nm) [9] are evident. Indeed, the volatility of these Cu compounds is quite low and therefore emission intensities will also be low for species such as CuO and CuOH. The other possible etch product (CuH_2) is reported to be unstable [10] and so should undergo dissociation upon electron impact collision. In this case, Cu emission will be evident, but H emission cannot be differentiated from the etch gas background. Currently, we can only state that Cu species are in the gas phase during the etch process, but the etch product that desorbs from the surface is unknown.

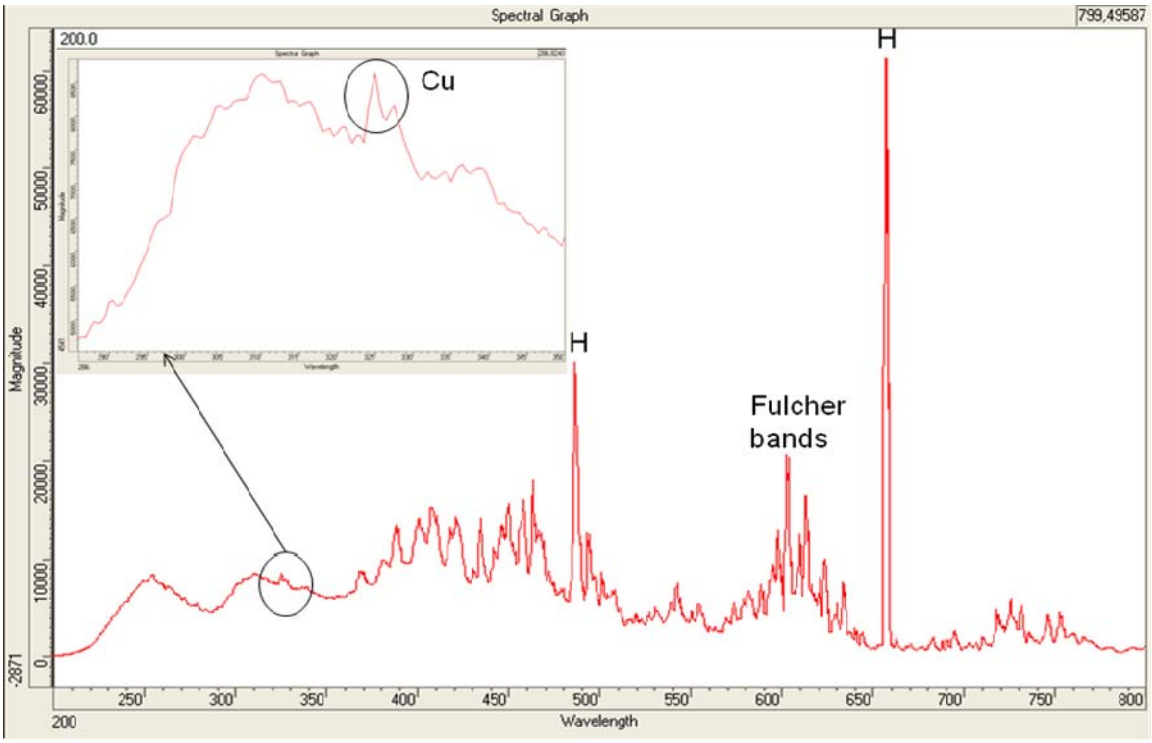

Figure 5.2 Optical emission spectrum of the H_2 plasma etching of Cu (4'' blanket Cu film). Plasma conditions were RF1= 100 W, RF2= 1800 W, 20 mTorr pressure, 60 sccm H_2 flow rate and 10 ^{o}C.

5.3.1.3 Cu Emission Line Intensity as a Function of Temperature

Because the intensities of the two Cu emission lines should be related to Cu etch rates, the average emission intensities during the sampling time of these two Cu lines are plotted as a function of electrode temperature in Figure 5.3, where OES data are from the etching of 4'' blanket Cu films at temperatures between -150 ^{o}C and 150 ^{o}C. Since the resolution of the OES system is 0.5 nm, the emission lines at 325 nm and 327.5 nm in our spectrum correspond to the 324.7 nm and 327.4 nm Cu peaks reported previously [7]. The absence of OES data at -150 ^{o}C and -100 ^{o}C is due to the inability of the OES system to detect such low Cu emission intensities. Comparison of Figures 5.1 and 5.3 indicates that the Cu etch rate trend essentially tracks the Cu emission intensity trend. Since the data shown in these figures were taken on different samples (data in Figure 5.1 are from SiO_2 masked 1 cm^2 samples while data in Figure 5.3 are from 4'' blanket Cu samples), these results offer strong evidence that the changes in Cu etch rates above 10 ^{o}C are not due to experimental error or to an uncontrolled etch process. Although the reason for such behavior is currently unclear, the results suggest an alteration in etch mechanism at 10 ^{o}C, perhaps due to a change in the specific etch product that desorbs.

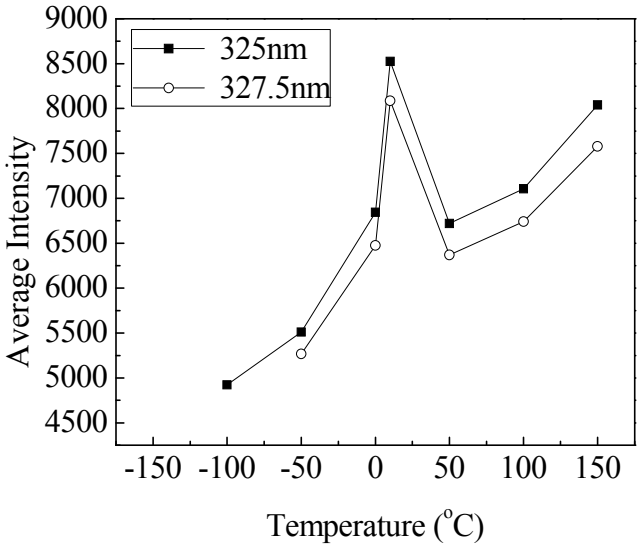

Figure 5.3 Average intensities of the two atomic Cu lines (325nm and 327.5 nm) from OES during H_2 plasma etching of Cu (4'' blanket Cu film) at temperatures from -150 ^{o}C to 150 ^{o}C; etch conditions were RF1= 100 W, RF2= 1800 W, 20 mTorr pressure, 60 sccm H_2 flow rate.

Reports of CuH decomposition indicate that CuH decomposes exothermally. CuH can decompose slowly at 0 ^{o}C [5], but decomposition is rapid above 50 ^{o}C [11]; above 100 ^{o}C decomposition is nearly instantaneous [5], although the majority of the decomposition occurs between 110 ^{o}C and 145 ^{o}C [11]. Because of the local heating induced by ion bombardment and exothermic decomposition, the surface temperature will be greater than that of the electrode set-point temperature. This enhanced energy input to the surface and concomitant temperature rise may cause decomposition of CuH so that sputtering becomes the primary mechanism for Cu removal. That is, there may be a "critical" temperature such as 10 ^{o}C in our experiments, where below this temperature, Cu removal from the etching surface is controlled by CuH (or other copper hydride) desorption, while above that temperature, Cu removal occurs primarily by sputtering, thereby reducing the removal rate. This assumption is consistent with the Cu etch rate

behavior shown in Figures 5.1 and 5.3, although currently, no direct evidence for this mechanism can be offered. As will be discussed in the following chapter, F or other contaminants from the reactor chamber may also affect Cu etch rates. Thus, the specific change of mechanism proposed is currently speculative.

Little information regarding the CuH decomposition enthalpy is available. Nevertheless, if we assume that the enthalpy of CuH formation and decomposition (ΔH^0_{dec}) are the same, the standard formation enthalpy $\Delta H^0_{298} = +21.3 kJ / mol$ [12] can be used as the standard decomposition enthalpy. In addition, we will assume that the specific heat capacity of bulk Cu applies to thin films: $C_{p,m} = 24.47 J \cdot mol^{-1} \cdot K^{-1}$ (at 25 °C). However, it is likely that not all the Cu surface atoms are hydrogenated; that is, there is only a fraction of CuH in the total number of moles of Cu present. Since the atomic ratio of H:Cu has been reported to be between 0.15 and 0.25 for a solution-prepared CuH substrate [11], we will assume that the mole ratio of CuH generated by the H_2 plasma at the Cu surface (CuH: Cu, designated by $A_{CuH:Cu}$ on surface) is 0.2. A simple calculation of the temperature increase as the result of exothermic decomposition (assuming that all energy released contributes to the temperature increase) is then given by:

$$\Delta T = \frac{\Delta H^0_{dec} \times A_{CuH:Cu}}{C_{p,m} \times (1 + A_{CuH:Cu})} \tag{5.1}$$

This simple estimation yields a temperature increase ΔT of 145K (with 25 ^{o}C CuH formation data, [12]). Although this value is certainly an approximation, this offers some idea of the temperature rise due to heating by thermal decomposition of CuH. Of

course, the temperature may be still higher than this when ion and electron bombardment-induced heating is considered. Of course, if the CuH: Cu ratio is higher or lower than 0.2, the temperature rise could be greater or less than 145 ^{o}C, respectively.

5.3.1.4 Temperature Effects Observed in the Plasma Therm ICP Reactor System

In order to obtain confirmation of the Cu etch rate trends with temperature that were observed in the Oxford Plasmalab etch system, a few temperature studies were performed in a different ICP reactor. Specifically, the Plasma Therm ICP reactor at Georgia Tech [4] has been employed despite the fact that the controllable temperature range in this reactor ranges only from 10 to 40 ^{o}C. Nevertheless, this temperature range falls within the etch rate transition regime shown in Figure 5.1. Electrode temperature effects have been described previously [4], where our preliminary data suggested that no change in etch rate with temperature over the range of 10 ^{o} to 40 ^{o}C was evident. However, those preliminary data arose by estimation of etch rates from Cu thickness changes via SEM images (with etch masks still on the surface). Of course, the accuracy of measuring small changes in Cu thickness using SEM images is poor, especially when considering nm scale differences. The measurements performed in the current study invoked a profilometer which has a resolution <2.5 nm, to determine the etch rate. Furthermore, the measurements were performed after removal of the mask material, further improving the accuracy.

Experiments were performed in the Plasma Therm reactor at three electrode temperatures: 10, 25 and 40 ^{o}C; all the other plasma parameters remained constant: RF1= 100 W, RF2= 500 W, 20 mTorr pressure and 50 sccm H_2 flow rate. Masked Cu samples

were the same as those utilized to generate the data displayed in Figure 5.1; etch rate results are shown in Figure 5.4. Over this small temperature range, a noticeable drop in etch rates (~1.7 nm/min) occurred, while the etch rates at 25 ^{o}C and 40 ^{o}C were essentially constant (10.7 and 10.9 nm/min) when the experimental error involved in profilometer measurements is considered. These observations are consistent with those in the Oxford Plasmalab reactor over virtually the same temperature range (Figure 5.1). Such results indicate that this etch rate phenomenon is not specific to a particular etch reactor, but is characteristic of the etch process.

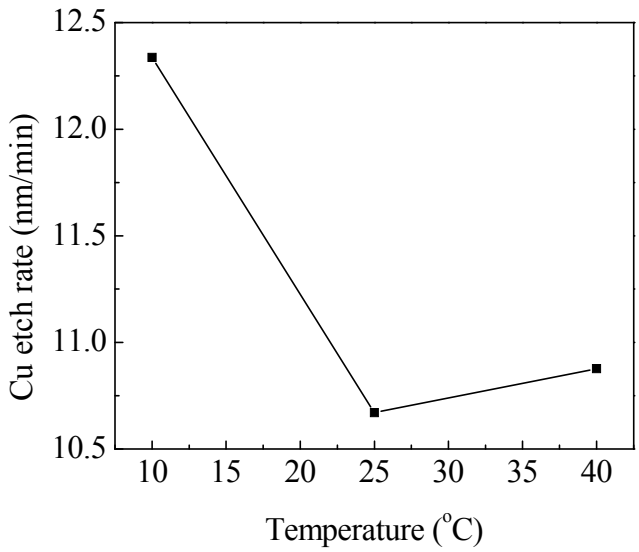

Figure 5.4 Cu etch rate vs. electrode temperature (Plasma Therm ICP reactor). Etch conditions were RF1= 100 W, RF2= 500 W, 20 mTorr pressure, 50 sccm H_2 flow rate.

5.3.2 Two-step Plasma Etching of Cu

5.3.2.1 OES of Cl_2 Plasma in the Two-step Process

As described previously [1], Cu can be etched by a two-step plasma etching sequence composed of a Cl_2 plasma chlorination step followed by a H_2 plasma step to remove the chlorinated layer. In order to investigate the removal of Cu using this two-step process, a 200 nm blanket Cu film on a 4'' silicon wafer was subjected to one cycle of the two-step process: 30 sec of Cl_2 plasma followed by a 2 min H_2 plasma. Optical emission spectra were recorded during both plasma steps. Figure 5.5 shows Cl_2 plasma emission spectra obtained at etch temperatures of 0 ^oC and -100 ^oC. The OES displays molecular-chlorine bands at 256, 307 nm and Cl_2^+ lines in the blue-green (380~600 nm) and atomic-chlorine lines in the near-IR (725.5, 7415, 754.5 nm) regions [7, 9]. The intensities of the molecular chlorine emission lines at the two etch temperatures are similar, but the intensities of the atomic chlorine lines are higher at lower temperature (-100 ^oC). This result is primarily due to the reduced recombination rate of chlorine atoms on surfaces at lower temperature [13]. It is important to note that no Cu or CuCl bands (most intense at 435.8 nm [7]) were observed in the Cl_2 plasma, which indicates that the chlorination step does not contribute significantly to the direct removal of Cu from the etching surface.

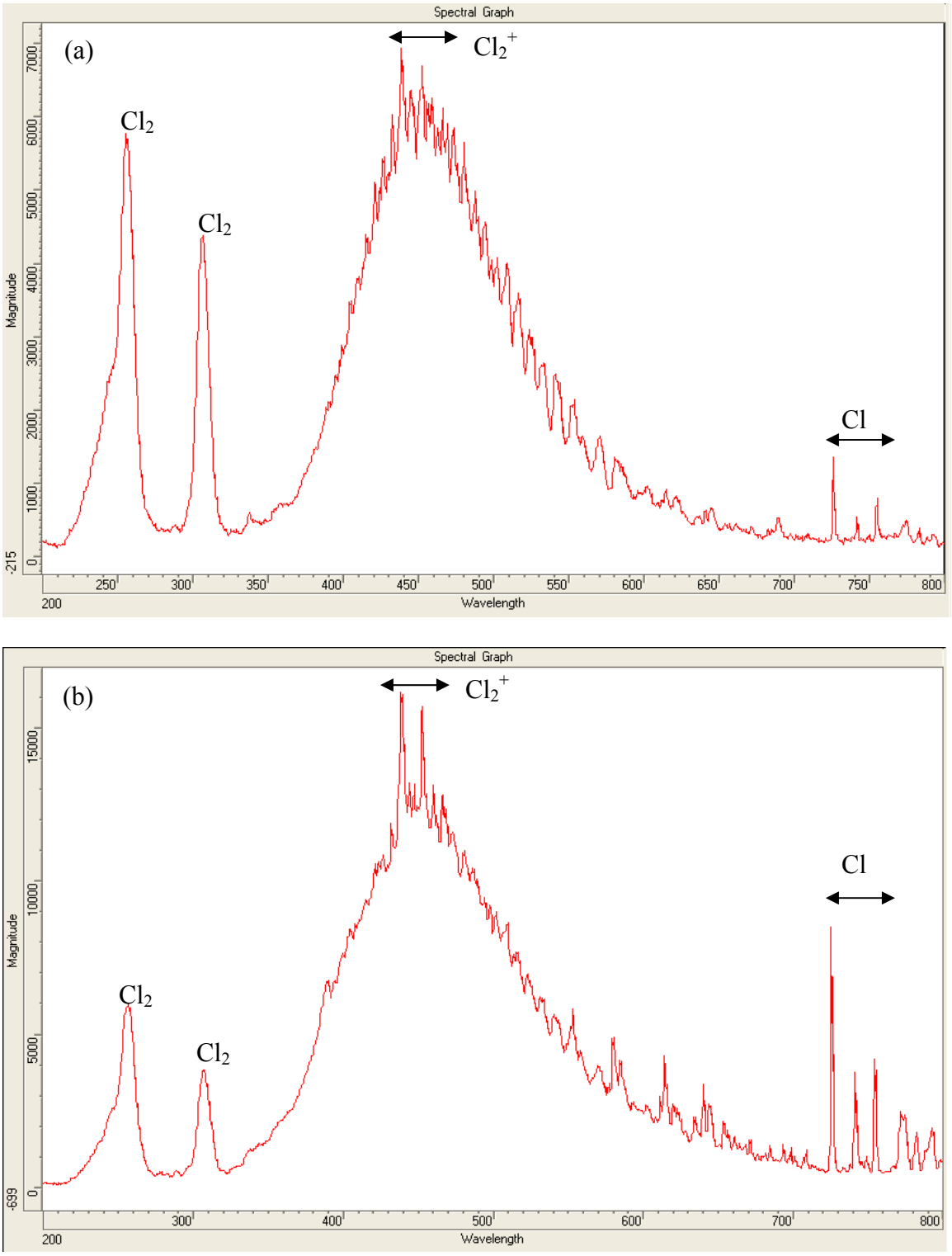

Figure 5.5 Optical emission spectra of Cl_2 plasma at (a) 0 ^oC and (b) -100 ^oC; plasma conditions are: 10 sccm Cl_2, 20mtorr, RF1=100 W and RF2=1800 W on 4'' blanket Cu samples (200 nm thick).

5.3.2.2 OES of H_2 Plasma in the Two-step Process

Figure 5.6 shows the optical emission spectrum from the second step (H_2 plasma) in the two-step process on the same 4'' Cu sample. The emission bands are essentially the same as those in the single step H_2 plasma process (Figure 5.2) except that the relative intensities for those bands are different primarily due to the higher platen power (RF1= 150 W for the H_2 plasma in two-step process). No Cl_2, Cl or CuCl lines were detected, and only atomic Cu lines (325, 327.5 nm) appeared. These observations indicate that chlorine species are either not involved or play a minor role in the removal of Cu from the etching surface. Since both H and Cl are present during the H_2 plasma step but no Cl emission lines are detected, HCl is likely formed. However, the most intense emission for HCl^+ is at 324.6 nm [9], which overlaps with the 324.7 atomic Cu line, and thereby precludes unambiguous identification in the current OES system due to the resolution possible (0.5 nm). A plot of the average intensities of the two Cu peaks (325 nm & 327.5 nm) during the sampling time of the H_2 plasma step is shown as a function of temperature in Figure 5.7 (no data are plotted at -150 ^oC due to the low Cu emission intensities). Analogous to the results in Figure 5.3, Cu emission intensities go through a maximum and then decrease as a function of temperature, with the maximum intensity and presumably etch rate, near 10 ^oC.

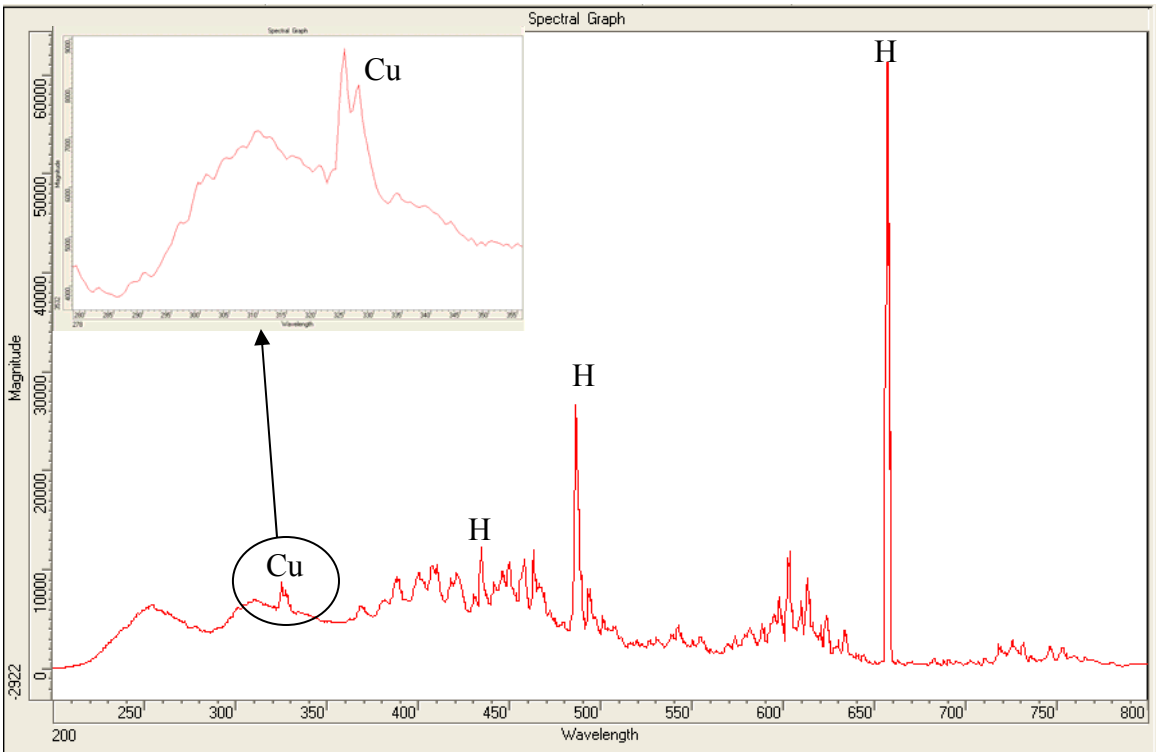

Figure 5.6 Optical emission spectrum of the H_2 plasma step in the two-step process at 0 ^oC; plasma conditions are: 60 sccm Cl_2, 20mtorr, RF1=150 W and RF2=1800 W on on 4'' blanket Cu samples (200 nm thick).

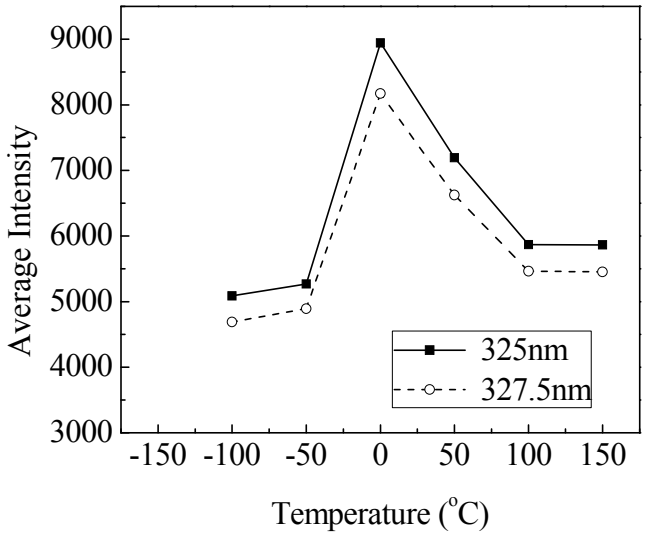

Figure 5.7 Average intensities of the two atomic Cu lines (325nm and 327.5 nm) from optical emission spectra during the H_2 plasma (for the two-step process) etching of Cu (4'' blanket Cu film) at temperatures between -150 ^oC and 150 ^oC; plasma conditions were RF1= 150 W, RF2= 1800 W, 20 mTorr pressure, 60 sccm H_2 flow rate.

5.3.2.3 Role of Cl_2 Plasma in the Two-step Cu Etch Process

In our previous discussion of the two-step Cu plasma etching process [1, 14], the mechanism for Cu removal was assumed to be Cu chlorination to preferentially form $CuCl_2$, followed by $CuCl_2$ reduction to Cu_3Cl_3 by a H_2 plasma, which facilitated Cu removal or etching due to the more volatile (relative to $CuCl_2$) Cu_3Cl_3. The absence of copper chloride emission lines during the H_2 plasma step is inconsistent with this assumption. Furthermore, the similarity between the H_2 plasma emission spectra in the single step process and the two-step process suggests that the role of chlorine and hydrogen species in the two-step process may be different than originally assumed.

During the chlorination step, $CuCl_2$ is formed in the surface region, with a monotonic decrease in Cl concentration as a function of depth into the film [15]. The chlorination depth is controlled by temperature due to diffusion of Cl as a function of time, provided that the incident energy, flux and exposure time from the plasma are essentially constant. Figure 5.8 shows a comparison of chlorination results via SEM images of patterned samples and the corresponding XPS spectra (blanket samples) at temperatures of 0 ^{o}C and -150 ^{o}C. These results indicate that at higher temperature (0 ^{o}C), the 100 nm Cu film was fully chlorinated and only surface $CuCl_2$ (935.7 eV) is detected at least to the detection limit of XPS (~10 nm). At lower temperature (-150 ^{o}C), only a certain depth of the Cu layer was chlorinated and both $CuCl_2$ and CuCl (932.8 eV) are observed (in agreement with [15]), which indicates that only a thin layer (< 10 nm) of $CuCl_2$ was formed.

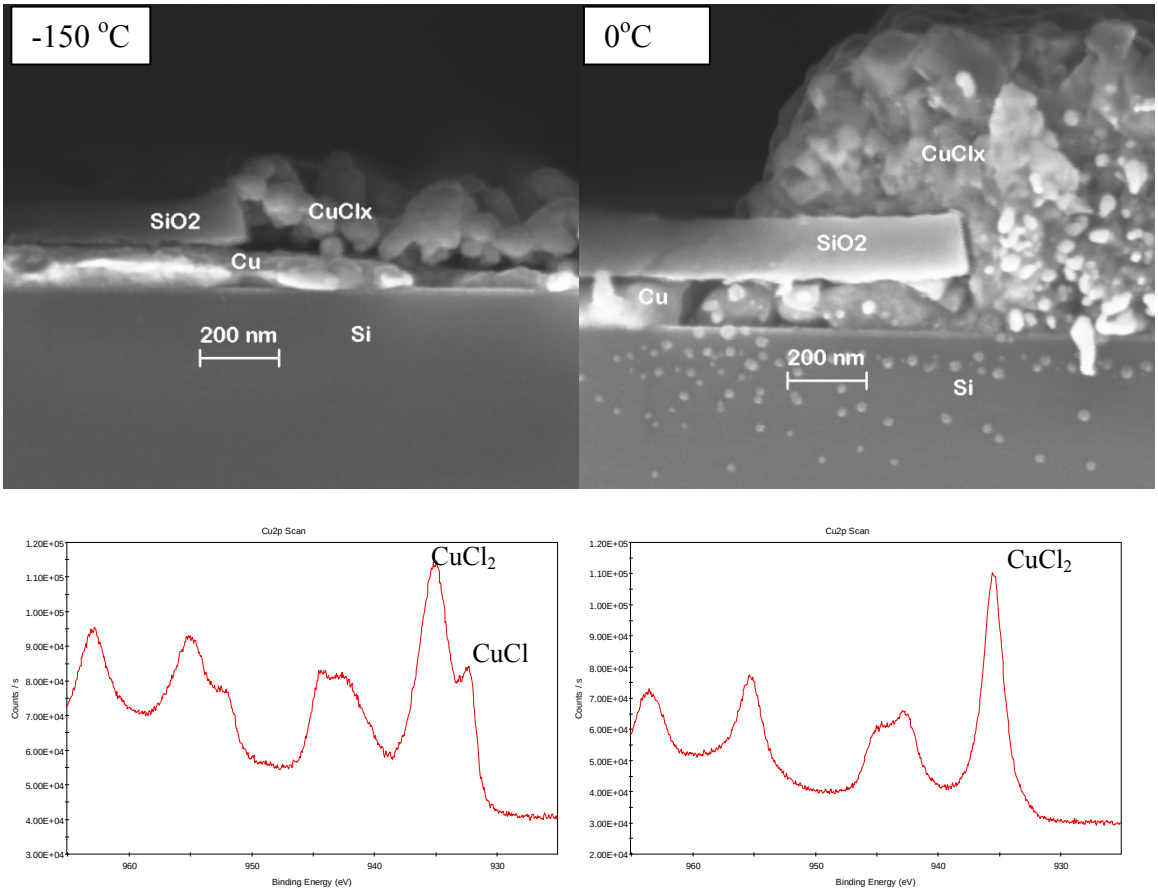

Figure 5.8 Cross-sectional SEM images and the corresponding XPS spectra of a 100 nm Cu film after a 1 min Cl_2 plasma at -150 °C (left) and 0 °C (right); plasma conditions are: 10 sccm Cl_2, 20mtorr, RF1=100 W and RF2=1800 W.

5.3.2.4 Role of H_2 Plasma in the Two-step Process

During the H_2 plasma step, the emission intensities of the two atomic Cu lines (related to Cu etch rate) increased with time as shown in Figure 5.9, for temperatures of 100 °C and -100 °C; however, at -100 °C, after a certain etch time (> 60 sec), the emission intensity reached a constant level. These observations can be compared to the Cu emission intensities vs. time in the single step H_2 plasma etching process (Figure 5.10, at 10 °C), where the emission intensity is essentially constant. Such results indicate that

the presence of Cl inhibits removal of Cu by a H_2 plasma. That is, in the single step etching of Cu by a H_2 plasma, removal of Cu species takes place at a constant rate. However, during the H_2 plasma step in the two-step process, it appears that hydrogen species must first react with Cl in the $CuCl_x$ layers to eliminate Cl, probably through the formation of HCl. Thus the increasing etch rate shown in Figure 5.9 is likely due to the decreasing concentration gradient of Cl in Cu throughout the chlorination depth. This mechanism also explains why the Cu etch rate of a single step pure H_2 plasma is higher than that for the two-step process. For the -100 ^{o}C etch results, the chlorination depth is more shallow at this lower temperature. Thus, when the H_2 plasma finally removes all chlorine present, the etch rate reaches a maximum value and remains at that level because only Cu is being etched from that time onward throughout the remainder of the film.

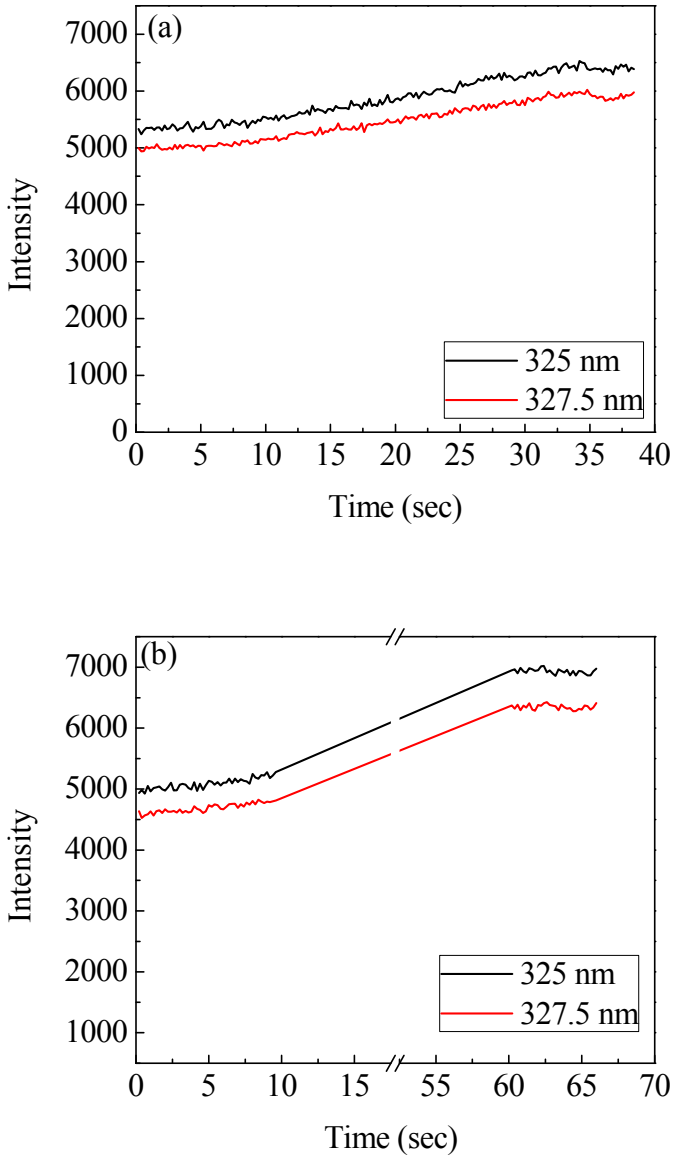

Figure 5.9 Intensities of the two Cu emission lines (325nm and 327.5 nm) from the optical emission spectra during the H_2 plasma (in the two-step process) etching of Cu (4'' blanket Cu film) under (a) 100 ^{o}C and (b) -100 ^{o}C; the plasma conditions were RF1= 150 W, RF2= 1800 W, 20 mTorr pressure, 60 sccm H_2 flow rate.

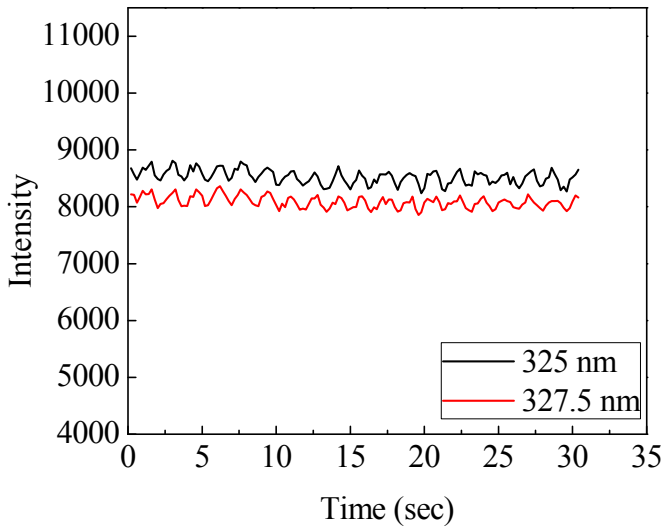

Figure 5.10 Intensities of the two Cu emission lines (325nm and 327.5 nm) from the optical emission spectra during the H_2 plasma (single step process) etching of Cu (4'' blanket Cu film) at 10 ^{o}C; the plasma conditions were RF1= 150 W, RF2= 1800 W, 20 mTorr pressure, 60 sccm H_2 flow rate.

5.4 Conclusion

Optical emission spectroscopy and etch temperature variations have been used to gain insight into the mechanisms involved in the low temperature etching of Cu in a hydrogen plasma (one-step process) or in sequential chlorine and hydrogen plasmas (two-step process). For the single step H_2 plasma Cu etch process, the etch rate initially (-150 ^{o}C to +10 ^{o}C) displayed an increase with temperature, followed by a decrease in etch rate above 10 ^{o}C. These etch rate trends were consistent with Cu optical emission data and were reproducible when performed in a different plasma reactor (in the 10 ^{o} to 40 ^{o}C temperature range). Such observations suggest a change in etch mechanism in the vicinity of 10 ^{o}C. Atomic Cu emission lines were detected in the optical emission spectrum during etching of Cu in a H_2 plasma, which further demonstrates Cu removal from the

etching surface. These data suggest that CuH is a likely etch product, although proof of this conjecture is not available at present.

Studies on the two-step Cu etch process showed no effect of temperature for the chlorination step insofar as Cu etch rate is concerned. Rather, OES analyses suggested that the Cl_2 plasma step in the two-step process inhibited Cu removal by the H_2 plasma. These results are consistent with the need for the H_2 plasma to react with the Cu chlorides generated in the Cl_2 plasma step to form Cu and HCl and thereby expose Cu to the etching plasma; the H_2 plasma can then remove Cu as observed in the single step pure H_2 plasma etch process. Such results indicate that even in the two-step Cu plasma etch process, the etch rates observed cannot be attributed to the formation and volatilization of Cu_3Cl_3. Rather, the H_2 plasma in both the one-step and two-step plasma etch processes appears to be responsible for the etch rates observed.

5.5 References:

[1] F. Wu, G. Levitin, and D. W. Hess, "Patterning of Cu Films by a Two-Step Plasma Etching Process at Low Temperature," *Journal of The Electrochemical Society,* vol. 157, pp. H474-H478, 2010.

[2] N. S. Kulkarni and R. T. DeHoff, "Application of Volatility Diagrams for Low Temperature, Dry Etching, and Planarization of Copper," *Journal of The Electrochemical Society,* vol. 149, pp. G620-G632, 2002.

[3] A. Grill, *Cold plasma in materials fabrication: from fundamentals to applications*. Piscataway, NJ: IEEE Press, 1994.

[4] F. Wu, G. Levitin, and D. W. Hess, "Low Temperature Etching of Cu by Hydrogen-Based Plasmas," *ACS Applied Materials & Interfaces,* vol. 2, pp. 2175-2179, 2010.

[5] N. P. Fitzsimons, W. Jones, and P. J. Herley, "Studies of copper hydride. Part 1.—Synthesis and solid-state stability," *Journal of the Chemical Society, Faraday Transactions* vol. 91, pp. 713-718, 1995.

[6] C. Candler, *Atomic Spectra and the Vector Model*, 2nd ed. Princeton, N. J.: Van Nostrand, 1964.

[7] A. M. Efremov and V. I. Svettsov, "Dry Etching of Copper Using Chlorine: A Review," *Russian Microelectronics,* vol. 31, pp. 179-192, 2002.

[8] J. E. Greene, "Optical spectroscopy for diagnostics and process control during glow discharge etching and sputter deposition," *Journal of Vacuum Science & Technology,* vol. 15, p. 1718, 1978.

[9] R. W. B. Pearse and A. G. Gaydon, *The Identification of Molecular Spectra*, Fourth ed. London: Chapman and Hall Ltd., 1976.

[10] E. V. Lavrov, J. Weber, and F. Borrnert, "Copper dihydrogen complex in ZnO," *Physical Review B,* vol. 77, p. 155209, Apr 2008.

[11] R. Burtovyy, E. Utzig, and M. Tkacz, "Studies of the thermal decomposition of copper hydride," *Thermochimica Acta,* vol. 363, pp. 157-163, 2000.

[12] W. A. Herrmann, *Synthetic methods of organometallic and inorganic chemistry: (Herrmann/Brauer)*. Stuttgart: Georg Thieme Verlag, 1996.

[13] G. P. Kota, J. W. Coburn, and D. B. Graves, "The recombination of chlorine atoms at surfaces," *Journal of Vacuum Science & Technology A* vol. 16, 1998.

[14] P. A. Tamirisa, G. Levitin, N. S. Kulkarni, and D. W. Hess, "Plasma etching of copper films at low temperature," *Microelectronic Engineering,* vol. 84, pp. 105-108, 2007.

[15] W. Sesselmann and T. J. Chuang, "The interaction of chlorine with copper : I. Adsorption and surface reaction," *Surface Science,* vol. 176, pp. 32-66, 1986.

CHAPTER 6

PRELIMINARY STUDIES OF SILICON DIOXIDE ETCHING IN HYDROGEN PLASMAS AND CONTAMINATION ISSUES DURING THE PLASMA ETCHING OF COPPER FILMS

6.1 Introduction

Thin Cu films patterned using a SiO_2 mask have been etched in H_2 plasmas as discussed in previous chapters, and the etching results showed good selectivity of Cu over SiO_2 (Chapter 4). In this chapter, a preliminary study of H_2 plasma effects on SiO_2 mask etching will be described, including the effects of rf power and substrate temperature. Contaminants are unavoidable in our systems since the reactors used are invoked primarily for fluorine-based plasma etching of silicon oxides. Thus, in order to investigate how contaminants such as fluorine and oxygen affect the etch chemistry, small amounts of CF_4 or O_2 were intentionally added into the H_2 etching atmosphere, and etch rates and SiO_2 surface composition were determined for these additives. In addition, since Cu films have oxide layers present after exposure of the samples to air prior to etching, several Cu samples have been intentionally oxidized and subsequently etched in hydrogen-based plasmas to determine the effect of copper oxide on the etch characteristics.

6.2. Experimental

6.2.1 Cu/SiO_2 Sample Preparation

In this chapter, six types of samples were prepared: four inch diameter blanket Cu; 1 cm^2 blanket Cu; 1 cm^2 SiO_2 (on Si substrate); Cu sample masked by an SiO_2 film; four inch diameter blanket oxidized Cu; patterned Cu film that was subsequently oxidized.

100 nm thick Cu films were deposited by e-beam evaporation (CVC E-Beam Evaporator) onto (100) silicon wafers that had been coated with 20 nm of titanium to promote Cu adhesion to silicon. Four inch diameter Cu-coated silicon substrates were used for OES studies or were sectioned into small samples ~1 cm^2 for etch studies. In order to obtain directly the SiO_2 mask ablation rate, a 150nm blanket plasma-deposited SiO_2 film on a Si substrate was etched simultaneously with Cu samples, or was etched separately.

SiO_2 masked Cu films were prepared as described in previous chapters. The SiO_2 film was deposited in a Plasma Therm PECVD (plasma enhanced chemical vapor deposition) system with 400 sccm SiH_4 and 900 sccm N_2O as precursors; the substrate electrode was heated to 250 ^oC, the power applied to the electrode was 25 W, and the pressure was maintained at 900 mtorr during the deposition process. Mask patterns were generated by fluorine-based plasma etching in a Plasma Therm SLR ICP reactor; the etch gas was a mixture of 5 sccm Ar, 28 sccm CO_2, and 15 sccm C_4F_8 , RF1 (power applied to the platen) was 80 W and RF2 (power applied to the coil) was 400 W, while the process pressure was maintained at 5 mtorr.

A thick (~ 350 nm) four inch diameter blanket Cu sample was oxidized in a plasma (barrel) cleaner (YES-R1) by an O_2 plasma at 1.2 torr and 700 W rf power, in order to prepare oxidized Cu samples; SEM images indicated that the 350 nm Cu was

almost fully oxidized. This four inch diameter sample was the Cu used for OES analysis. In addition, a patterned 100 nm Cu sample (described in the above paragraph) was oxidized under the same conditions for the purpose of determining the etch rate.

6.2.2 Plasma Etching of Cu/SiO_2

Since the experiments performed in this chapter utilized two different ICP reactors: Plasma Therm ICP reactor (at Georgia Tech) and Oxford Plasmalab System 100 ICP-RIE (at Oak Ridge National Laboratory), experimental details in the different reactors will be described separately in each section.

6.2.3 Post Etch Characterization

After Cu etching (details described below), the SiO_2 mask layer was removed with a dilute HF: H_2O solution (1:50). Cu film patterns were examined with a scanning electron microscope (SEM, Zeiss SEM Ultra60). Thickness changes of the Cu layers were determined from SEM images, Wyko Profilometer and Dektak 150 Profilometer data, while the thickness changes of the SiO_2 layer were measured by a Nanospec Refractometer. Chemical analysis of the films and surfaces before and after plasma etching was performed using X-ray photoelectron spectroscopy (XPS). XPS spectra were collected using a Thermo Scientific K-Alpha XPS system. Optical emission spectra (OES) of plasmas during the etch processes were obtained with a Verity SD2048DL Spectrography system. Mass spectra of the H_2 plasma atmospheres were obtained with an AccuQuad Model 300D RGA (residual gas analyzer) system.

6.3 H_2 Plasma Etching of SiO_2 Masks

6.3.1 Selectivity of Cu Relative to SiO_2 Masks

This section describes studies performed using the Plasma Therm ICP reactor.1 cm^2 blanket SiO_2 films on Si substrates were utilized to investigate SiO_2 etch rates. Etching of SiO_2 and Cu were performed separately in the Plasma Therm ICP reactor although the same plasma conditions were invoked. The H_2 gas flow rate was 50 standard cubic centimeters per minute (sccm) and the reactor pressure was maintained at 20 mtorr. The radio frequency power applied to the ICP coil was designated RF2, whereas the power applied to the substrate was RF1. The electrode temperature was maintained at 10 ^oC.

Figure 6.1 displays the etch rates of SiO_2 and Cu at different power settings (RF1/RF2): 100W/500W, 100W/700W and 200W/500W; the etch rate ratio between Cu: SiO_2 was 13.7, 5.7 and 11.9, respectively for these conditions. Figure 6.1 indicates good selectivity of Cu over SiO_2, although increases in both platen power (RF1) and coil power (RF2) clearly lower the selectivity. These results indicate that ion flux may be the major contributor to SiO_2 mask ablation during H_2 etching of Cu. The low etch rate of SiO_2 suggests that little if any chemical enhancement is involved in the ablation of SiO_2 masks during Cu etching.

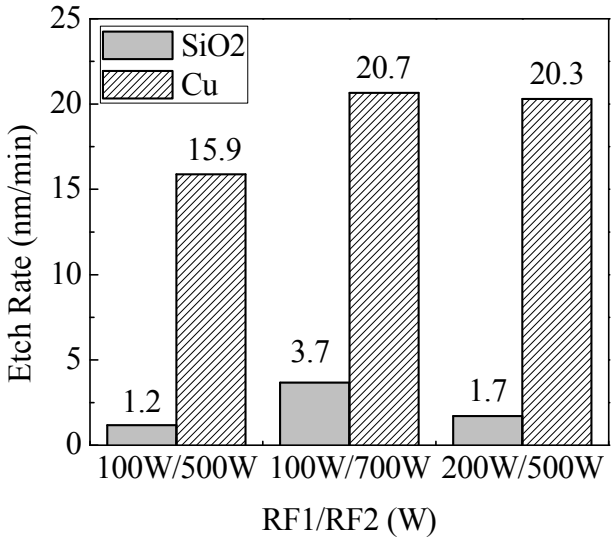

Figure 6.1. Etch rates of SiO_2 and Cu in H_2 plasmas under different power settings; other plasma conditions were: 20 mTorr pressure, 50 sccm H_2 flow rate and 10 ^oC.

6.3.2 Temperature Effects on SiO_2 Films Etched in H_2 Plasmas

This section describes studies performed using the Oxford Plasmalab System 100 ICP-RIE reactor, wherein the etch rate and surface composition of 1 cm^2 plasma deposited SiO_2 films on Si substrates that were exposed to an H_2 plasma are investigated. These results offer further details regarding the robustness of the mask layer that has been used for Cu pattern definition in this thesis.

In section 5.3.1, although we did not discuss the SiO_2 etch rate, the experiments performed utilized a SiO_2 film (sample C), blanket Cu sample A and sample B (SiO_2 masked Cu films) in the same etch run and thus reactor (Oxford Plasmalab System 100 ICP-RIE); etch rate data of SiO_2 were therefore obtained from samples designated as sample C in these experiments, while the etch rate data of Cu were from samples A and B (Cu etch rates in Figure 5.1). SiO_2 etch rates are plotted in Figure 6.2a as a function of

electrode temperature; Cu etch rates are re-plotted (from Figure 5.1) in Figure 6.2b for convenience to the reader. The SiO_2 etch rate trends with temperature (Figure 6.2a) are similar to those observed for Cu etching (Figure 6.2b), in that both have a change in the trend at a particular temperature: 50 ^oC for SiO_2 (10 ^oC for Cu). Below and above that temperature, the etch rates displayed opposite trends with temperature. That is, SiO_2 etch rates decreased as temperature increased in the temperature range -150 ^oC to 50 ^oC, while the rates increased as temperature increased in the temperature range between 50 ^oC and 150 ^oC.

In order to obtain further insight into this phenomenon, XPS analyses were performed on the SiO_2 samples and four elements were detected: F, O, Si and C. Interestingly, no Cu is detected, despite the fact that the SiO_2 (sample C) was positioned next to (less than 1 cm from) Cu samples B and C during the etching process, indicating that no or at least minimal Cu re-deposition occurs on the SiO_2 samples. Fluorine contamination is evident on these surfaces which is due to the fact that the chamber is used routinely for various F-based etch processes; furthermore, the SiO_2 mask layers in our studies have been etched in this reactor using fluorine chemistries. As shown in Figure 6.2a, the atomic percentages of fluorine were very high. Furthermore, the fluorine atomic percentages do not correlate directly with SiO_2 etch rates (Figure 6.2a); however, the Cu etch rates do suggest possible dependence on F concentrations (Figure 6.2b).

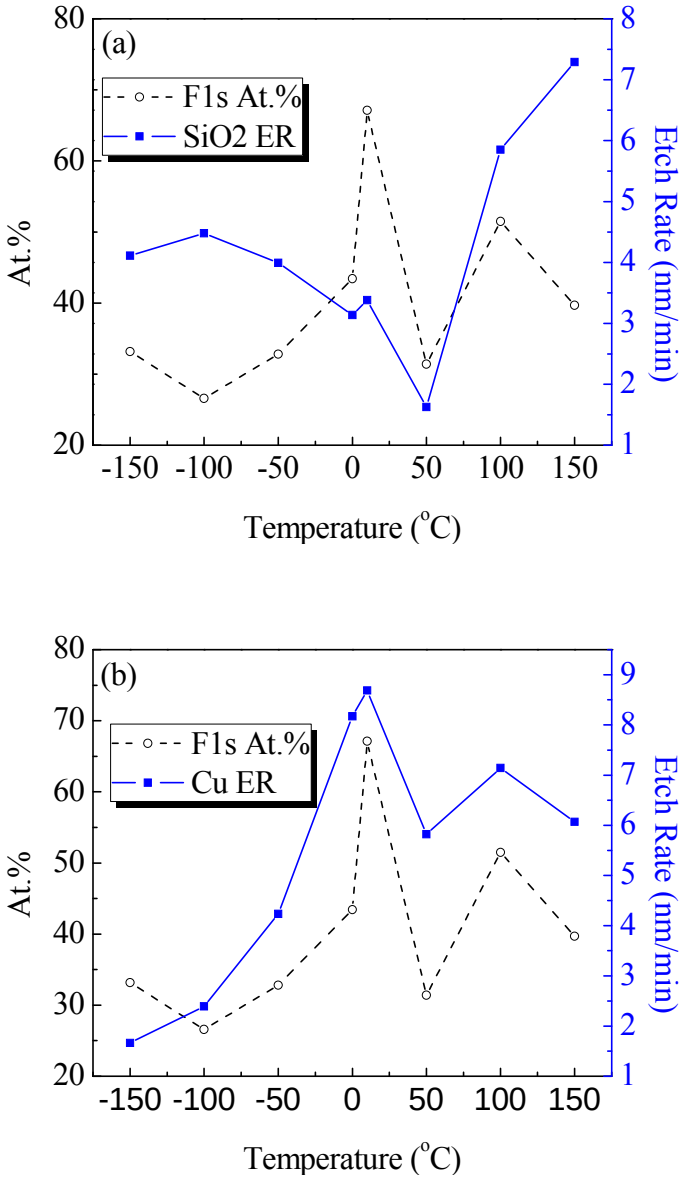

Figure 6.2. (a) SiO_2 (sample C) etch rates; (b) Cu (sample A & B) etch rates and atomic percentage of F on SiO_2 samples (sample C) vs. electrode temperature. Etch conditions were RF1= 100 W, RF2= 1800 W, 20 mTorr pressure, 60 sccm H_2 flow rate. All three samples were etched (simultaneously) in the same etch run.

Despite the high atomic percentage of F on SiO_2 sample surfaces positioned next to the Cu samples during the H_2 plasma etch process, no detectable emission from HF^+ (452.0, 360.0 nm), CuF (493.2 nm), SiF_2 (390.2, 395.5 nm) [1], atomic F (703.7, 712.8

nm), SiF (436.8, 336.3, 334.6 nm), or CF_2 (251.9 nm) [2] was observed. This means that either no F-related species are in the plasma or the intensities of those emission lines were below OES detectability. Comparison of the atomic composition on the SiO_2 sample surface before and after H_2 plasma etching (at 10 ^oC) as shown in Table 6.1, indicates a significant reduction in the O1s and Si2p signals, while the F1s increases. In addition, consideration of the C1s peaks before and after H_2 plasma etching (Figure 6.3) indicates that the primary bonding configuration of C1s moieties changed from C-O and C (284.5 eV) to C-F_x bonding structures (290 - 295 eV) [3]. Apparently, after the etch process, a thin fluorocarbon film is formed on the SiO_2 surface. Since these studies were performed in the Oxford ICP reactor, we will now compare the contamination situation in the two reactors (Plasma Therm ICP at Georgia Tech and Oxford ICP at ORNL). We have less control on the contamination present in the Oxford ICP reactor than in the Plasma Therm ICP reactor that we used in Chapters 2, 3 and 4, since only an O_2 plasma can be utilized to clean the Oxford chamber. That is with the Plasma Therm system, a manual clean (open the chamber and scrape off the polymer deposits) was performed prior to every etch run; with the Oxford system (ORNL), this was not possible, resulting in less efficient cleaning, which leads to enhanced carbon contamination. This is the likely reason why significant fluorocarbon film deposition on SiO_2 samples occurred in the Oxford ICP reactor.

Table 6.1 Comparison of atomic composition (from XPS spectra) on the SiO_2 sample surface before and after H_2 plasma etching (at 10 ^oC) of Cu

Element	At.% (before the H_2 plasma etching)	At.% (after the H_2 plasma etching)
O1s	45.02	14.06
F1s	12.21	67.13
Si2p	29.56	3.57
C1s	9.74	15.25
N1s	3.47	N/A

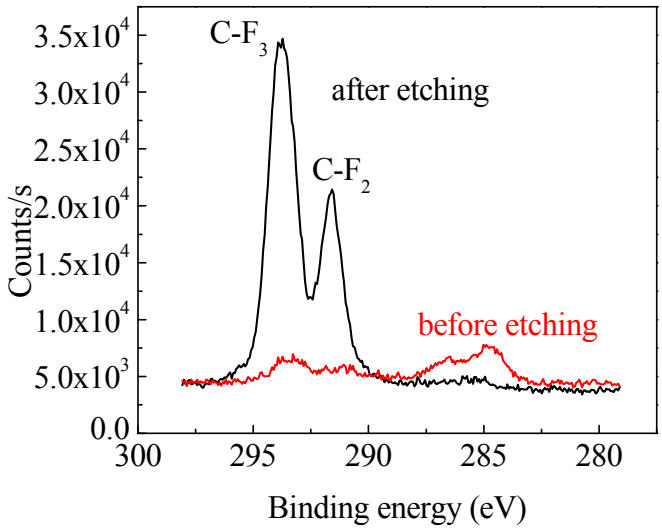

Figure 6.3. C1s peaks in the XPS spectrum of SiO_2 sample surfaces before and after H_2 plasma etching of Cu at 10 ^oC in the Oxford ICP reactor.

Fluorocarbon deposition occurs most prevalently in a fluorine-deficient plasma [3], which is consistent with the absence of F emission lines in our H_2 plasma optical emission spectrum. However, no direct correlation between the SiO_2 etch rate in the H_2 plasma and the F concentration on SiO_2 surfaces is evident. This observation may be

related to the fact that the etch rate depends upon both the F flux to the surface and the amount of F adsorbed, both of which depend upon the release of fluorine species from the chamber walls (outgassing or contamination). If the SiO_2 etch rate is high, little F may remain on the surface, since it is removed as an etch product; when the SiO_2 etch rate is low, then F can accumulate on the surface. As a result, the etch rate may be controlled by a different mechanism depending upon the incident flux of F onto SiO_2 samples. That is, the F concentration on SiO_2 sample surfaces is controlled by both the incident flux of F to this surface (which may be increased due to enhanced outgassing/desorption from reactor surfaces at higher temperatures) and the SiO_2 etch rate, where the higher the SiO_2 etch rate, the lower the residual F concentration on SiO_2 surface. Since the SiO_2 etch rate is a combination effect of ion bombardment flux and F-Si chemistry, we cannot determine at this time, which of these mechanisms (or synergy between them) controls the trend of SiO_2 etch rate within a particular temperature range (decrease between -150 and 50 ^oC, and increase between 50 and150 ^oC). In any case, a change in mechanism would be analogous to the Cu etch rate situation as we proposed previously (Figure 6.2b).

Although possible explanations for the correlation observed between SiO_2 etch rate (sample C) and atomic F concentration (on sample C) after H_2 plasma etching (in Figure 6.2a) have been postulated, the dependence of Cu etch rate (sample A and B) on F atomic concentration (on sample C) shown in Figure 6.2b is not subject to the same issues since CuF has limited volatility. That is, SiO_2 and Cu surfaces offer very different adsorption characteristics with respect to F in that SiO_2 adsorbs F more readily than does Cu – this will be discussed further in Section 6.4.4). One possible consideration is that temperature changes cause a change of incident F flux to the sample surface by

influencing F outgassing/desorption from reactor surfaces, while the temperature also affects Cu etch rates. An additional possibility is that release of F from reactor walls causes increased dissociation of H_2 via formation of HF and thereby enhances the extent of chemical interactions of H with Cu. Clearly such possibilities are speculations since no HF^+ peaks were determined by OES and at present it is unclear how the incident F flux at these low gas phase concentrations impacts Cu etch rates.

The C and F contamination arising from previous F-based etch processes performed in the reactor raises a number of issues for the etching of Cu, such as how the contaminants affect the H_2 or H interactions with Cu, and whether or not the Cu etch rate can be significantly affected by these contaminants. These issues will be addressed in a preliminary fashion in the following sections.

6.4 Contamination Considerations in H_2 Plasma Etching of Cu

All experiments in this section were performed in the Plasma Therm ICP reactor (Georgia Tech, where prior to the etch runs, the reactor chamber was thoroughly manually cleaned, followed by an O_2 plasma clean and H_2 plasma conditioning, in order to remove the contaminants as effectively as possible. Etch conditions for all experiments were: RF1=100 W, RF2=500 W, 50 sccm total flow rate, 20 mtorr pressure and 10 ^oC electrode temperature. The only changes to the etch conditions used was the etch gas composition.

6.4.1 Mass Spectral Analyses of H_2 Plasmas

Mass spectra during the H_2 plasma etching of blanket Cu samples were collected by an AccuQuad Model 300D residual gas analyzer (RGA). Figure 6.4 displays the mass spectrum of the H_2 plasma; as noted previously [4], no Cu-related peaks are detected in this spectrum. In addition to the H_2^+ peak (AMU=2, not shown completely due to the Y axis scaling), Figure 6.4 shows peaks corresponding to H_2O^+ (18), HF^+ (20), N_2^+, CO^+ or Si^+ (28), O_2^+ (32), CO_2^+ (44), turbo pump oil (55, 57, 69) [5], thereby confirming the presence of C, N, O, and F contaminants in the H_2 plasma atmosphere. Si was contributed by the holder on which the Cu sample resides (bare Si wafer), and C is unavoidable due to photoresist contamination on chamber walls from previous etch processes, although another C source could be the pump oil of the RGA system (peaks at 41, 43, 55, 57, 69, 71). N and O are likely present due to small leaks in the vacuum system, although N_2 is the purge gas used prior to the etch process; thus, residual N_2 gas in the chamber is another N source. The presence of F arises due to chamber outgassing from residues generated as a result of previous etch processes. Due to reactor equipment limitations, gas flow control of N_2 in this system is not possible; thus only O and F contamination will be investigated by intentionally adding a small amount of O_2 or CF_4 (2% of the total flow rate; i.e., 1 sccm of O_2 or CF_4 was added to 49 sccm H_2 flow).

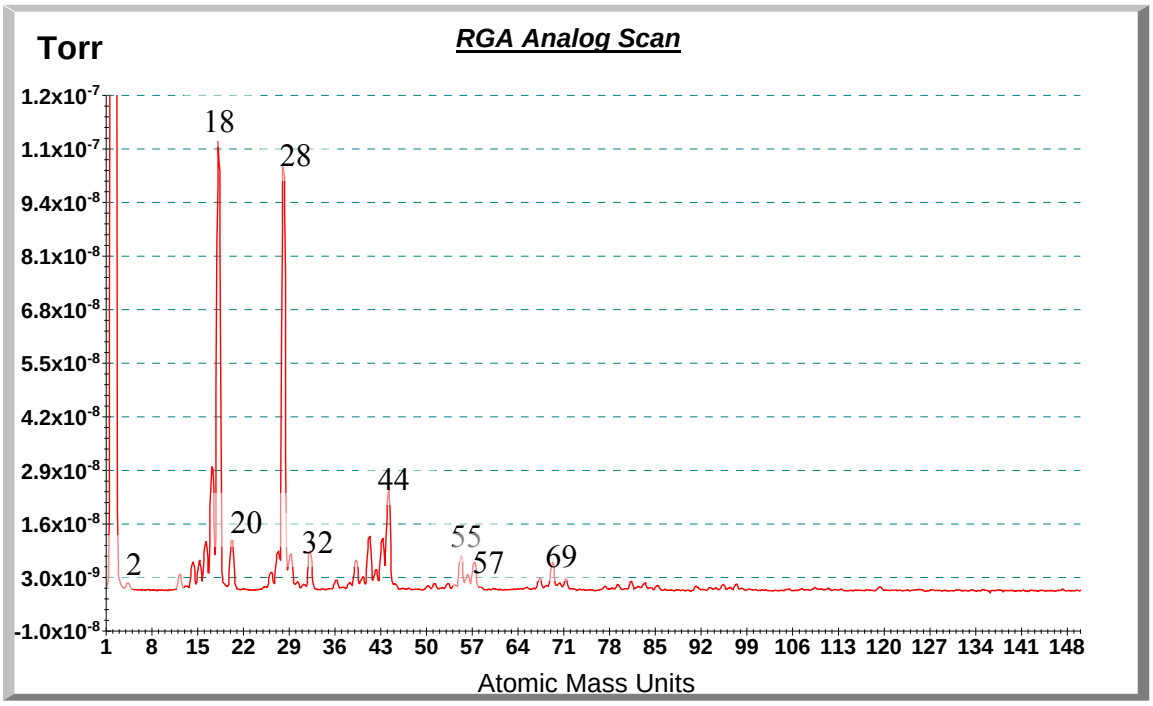

Figure 6.4. Mass spectrum of H_2 plasma during blanket Cu film etching; etch conditions were RF1= 100 W, RF2= 500 W, 20 mTorr pressure, 50 sccm H_2 flow rate and 10 ^{o}C.

6.4.2 Optical Emission Spectra During H_2 Plasma Etching of Cu in Plasma Therm ICP Reactor

6.4.2.1 H_2 Plasma Emission Using a Bare Si Wafer as the Substrate

An optical emission spectrum of an H_2 plasma with a bare Si wafer as a substrate was collected to serve as the reference spectrum (Figure 6.5). Emission lines were identified as: N_2 (296.2, 297.7 nm); OH (308.9 nm) and N_2 (315. 9 nm) overlapped band; NH (336 nm), O_2 (337.0 nm) and N_2 (337.1 nm) combination; N_2 peaks from 350 to 430 nm (353.7, 357.7, 399.8, 409.5, 420.0 nm); H peaks at 434.0 (H_s), 486.1(H_β), 656.3 and 656.5nm(H_α); and likely O_2^+ bands from 600 to 650 nm (which could also be the Fulcher series emission of H) [1-2, 6]. As in the previous spectra, F peaks were not observed

since the strongest F emission peaks (703.7, 712.8 nm) were absent. Therefore, the major contamination sources in this Plasma Therm ICP reactor are O and N.

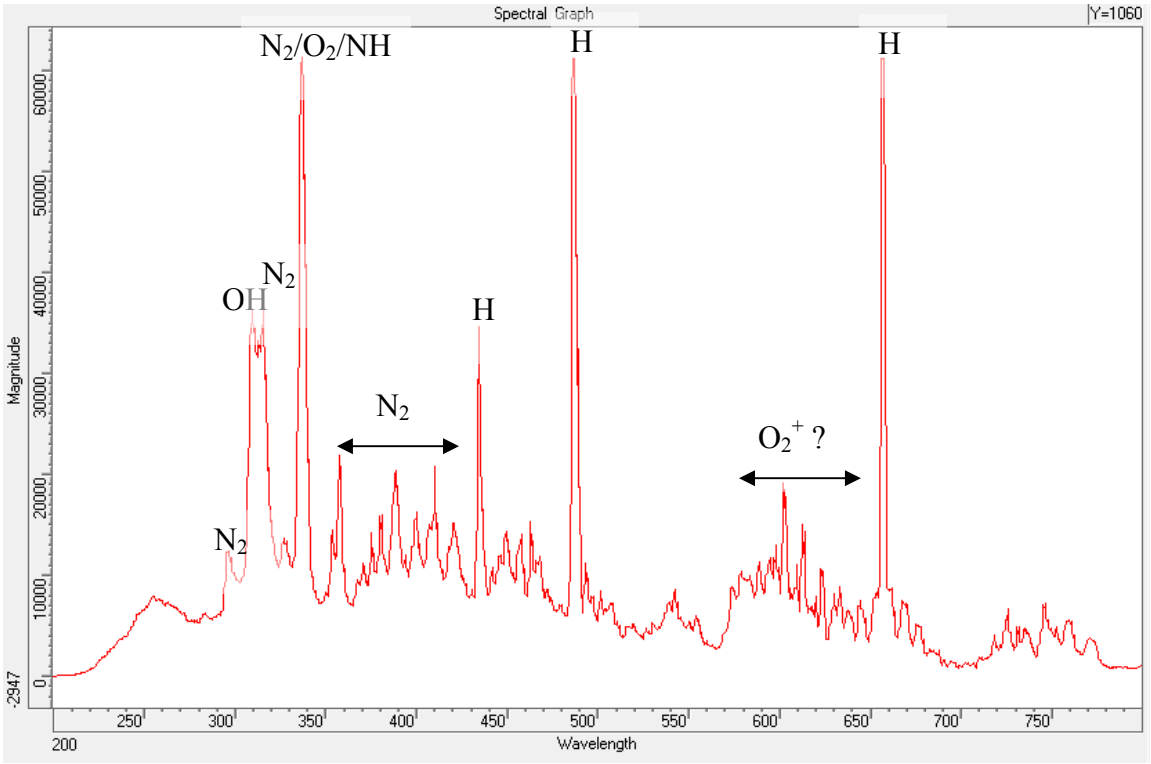

Figure 6.5. H_2 plasma emission spectrum with a bare Si wafer as the substrate; etch conditions were RF1= 100 W, RF2= 500 W, 20 mTorr pressure, 50 sccm H_2 flow rate and 10 ^{o}C.

6.4.2.2 H_2 Plasma Emission on 4'' Blanket Cu Sample

The emission spectrum of an H_2 plasma with a 4'' diameter blanket Cu film as the substrate is shown in Figure 6.6. In comparison to the spectrum in Figure 6.5, two Cu peaks (324.7 and 327.4 nm) are evident. In addition, the relative intensities of two H peaks (434.0, 486.1 nm) and the OH peak (308.9 nm) are reduced. These observations are an indication that H atoms were consumed during the etch process as expected if chemical interactions between H and Cu occur. The absolute peak intensities of Figure

6.5 and Figure 6.6 cannot be compared since the plasma parameters changed (even the DC bias has been altered slightly, from - 360 V for the Si substrate and - 385 V for the Cu substrate). Nevertheless, no significant changes are apparent in the N or O emission intensities.

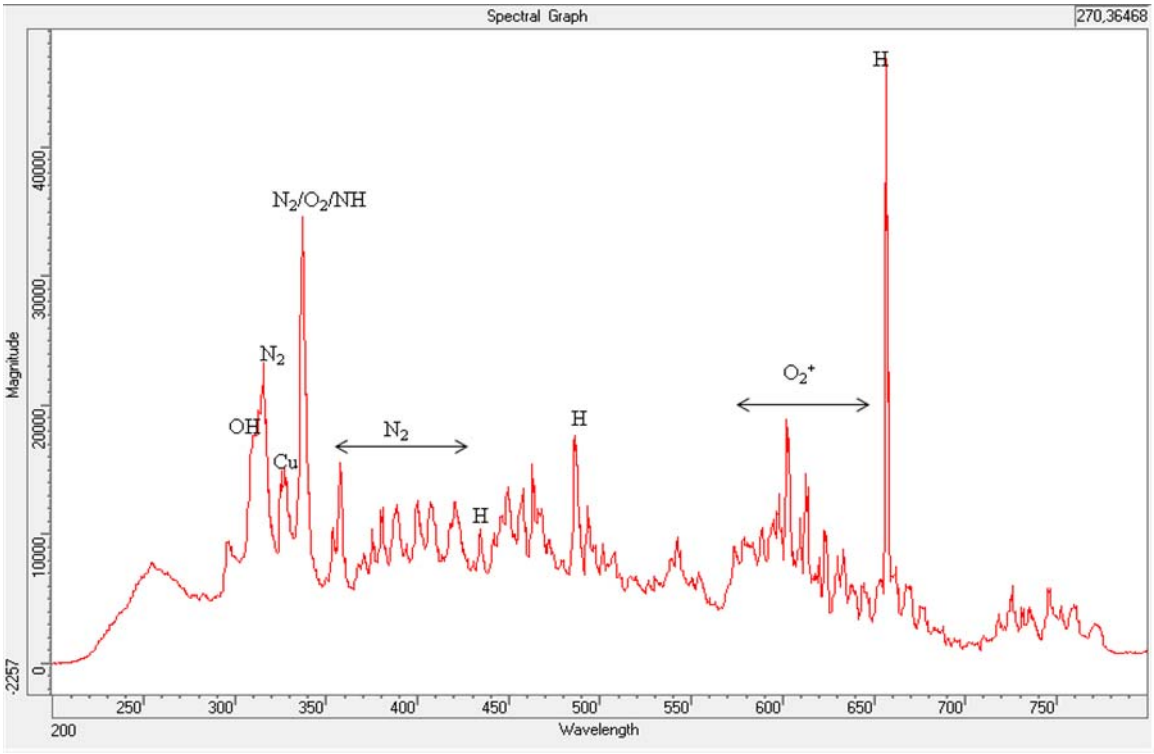

Figure 6.6. H_2 plasma emission spectrum with a 4'' blanket Cu sample as the substrate; etch conditions were RF1= 100 W, RF2= 500 W, 20 mTorr pressure, 50 sccm H_2 flow rate and 10 ^{o}C.

6.4.2.3 H_2/O_2 Plasma Emission

1 sccm of O_2 was added to the 49 sccm H_2 to investigate the effect of oxygen contamination. The resulting emission spectrum of this H_2/O_2 plasma is shown for the situations where a bare Si wafer (Figure 6.7a) and a 4'' diameter blanket Cu sample (Figure 6.7b) served as substrates.

Comparison of Figure 6.7a to Figure 6.5 indicates that the addition of O_2 into the H_2 plasma atmosphere increased the OH band intensity as expected. In addition, the relative intensities of the two higher-energy H emission peaks (434.0, 486.1 nm) were reduced. A new peak appeared at 283.0 nm, which can be assigned to CO emission (283.3 nm [1]). Comparison of Figures 6.7a and b demonstrate that except for the appearance of Cu peaks, no other changes in the emission spectrum are obvious. The studies indicate that the added oxygen interacted with H atoms in the H_2 plasma to form OH, and some of the reactive O may have interacted with C residues in the chamber to form CO, but the OH or CO species do not appear to contribute to the removal of Cu from surface. Cu etch rate changes as a result of O_2 addition will be discussed in Section 6.4.3.

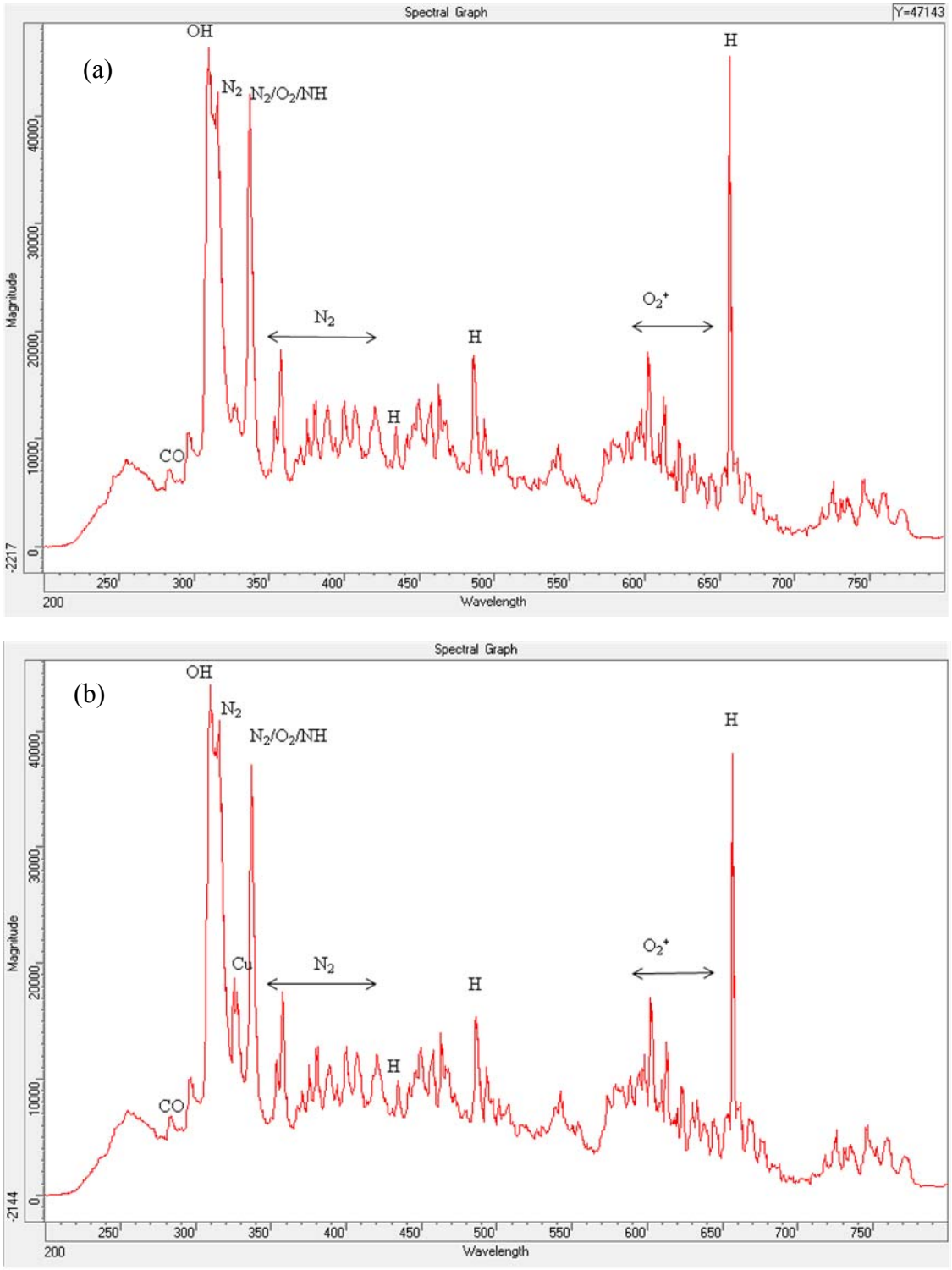

Figure 6.7. H_2 plasma emission spectrum with either a (a) bare Si wafer or a (b) 4'' blanket Cu sample as a substrate; etch conditions were RF1= 100 W, RF2= 500 W, 20 mTorr pressure, 49 sccm H_2 + 1 sccm O_2 flow rate and 10 ^oC.

6.4.2.4 H_2/CF_4 Plasma Emission

1 sccm of CF_4 was added to 49 sccm H_2 to serve as the etch gas mixture. The emission spectrum of this H_2/CF_4 plasma with a bare Si wafer as the substrate is shown in Figure 6.8a and the emission spectrum of the same plasma with a 4'' diameter blanket Cu film as the substrate is shown in Figure 6.8b. Comparison of Figures 6.5 and 6.8a indicate that with the addition of CF_4, a CN peak (388.0 nm, 388.3 nm[1]) appeared, along with a reduction in intensity of H and OH peaks. As noted previously, no F peaks can be identified. These results suggest that CF_x species adsorb/react readily on surfaces to form fluorocarbon layers, and/or react with H to form low (undetectable) concentrations of HF, although mass spectral results indicate the formation of HF (Figure 6.4). In addition, some CF_x fragments can react with nitrogen contamination to form CN.

Although SiF_x species are expected to occur with a Si substrate, SiF emission occurs at 336.3 nm, which is near the NH (336 nm), O_2 (337.0 nm) and N_2 (337.1 nm) emission lines, thereby making definitive assignment of emission peaks difficult. When the 4'' blanket Cu substrate is exposed to the H_2/CF_4 plasma, we expect a reduction in intensity of the 336.5nm peak since no Si is exposed to the plasma. Figure 6.8b does show a slight intensity reduction at this wavelength, at least in comparison with the adjacent CN peak. Finally, Cu peaks appear as a result of Cu etching.

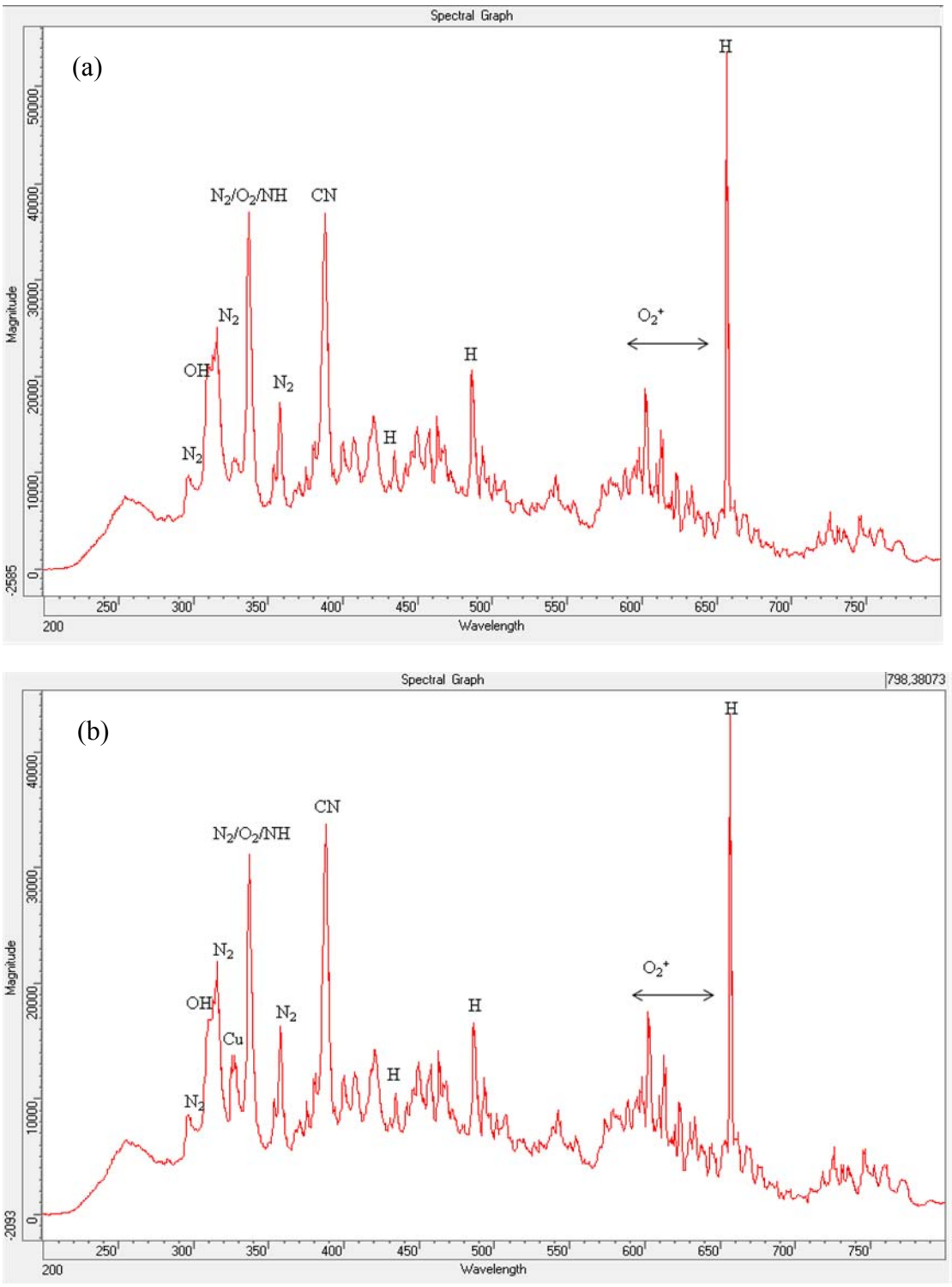

Figure 6.8. H_2 plasma emission spectrum with a (a) bare Si wafer and (b) a 4'' blanket Cu substrate; etch conditions were RF1= 100 W, RF2= 500 W, 20 mTorr pressure, 49 sccm H_2 + 1 sccm CF_4 flow rate and 10 ^oC.

6.4.2.5 H_2 Plasma Emission with an Oxidized Cu Substrate

A blanket Cu sample that had been oxidized by an O_2 plasma was subjected to an H_2 plasma. The H_2 plasma emission spectrum with the oxidized Cu substrate was basically the same as the spectrum in Figure 6.6 where a pure Cu film was the substrate. A plot of the Cu emission intensity at wavelengths 325 nm and 327.5 nm vs. time (Figure 6.9), shows that the Cu emission signal fluctuated significantly at certain time intervals, but overall remained at a constant level. This fluctuation may be caused by minor plasma instabilities, since we observed DC bias, pressure, and flow rate fluctuations during the plasma etching. Corresponding to the Cu emission signal changing, the DC bias varies in a ± 5V range. Furthermore, this fluctuation was not specific to this particular experiment, but was observed in other etch runs. Since the Cu sample was almost fully oxidized before etching (as indicated by Figure 6.10), no O gradient was expected with sample depth. The etch rate results of Cu oxide will be discussed in section 6.4.3.2.

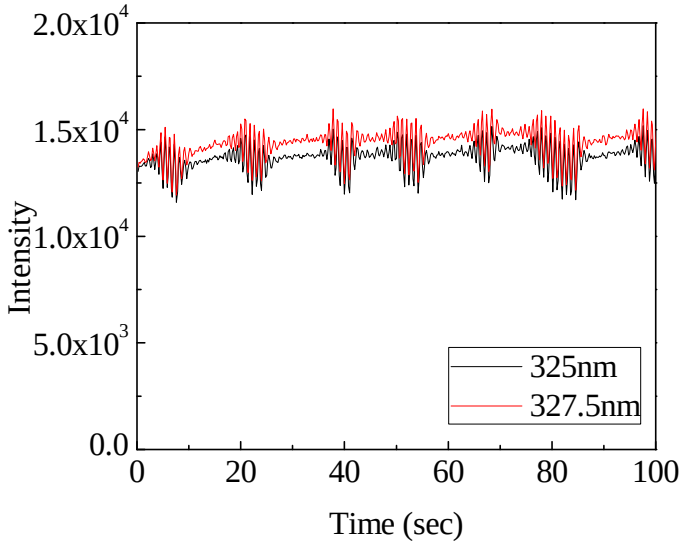

Figure 6.9. Intensities of the two Cu emission lines (325nm and 327.5 nm) from optical emission spectra during the H_2 plasma etching of oxidized Cu (4'' blanket diameter sample) vs. etch time; etch conditions were RF1= 100 W, RF2= 500 W, 20 mTorr pressure, 50 sccm flow rate and 10 ^{o}C.

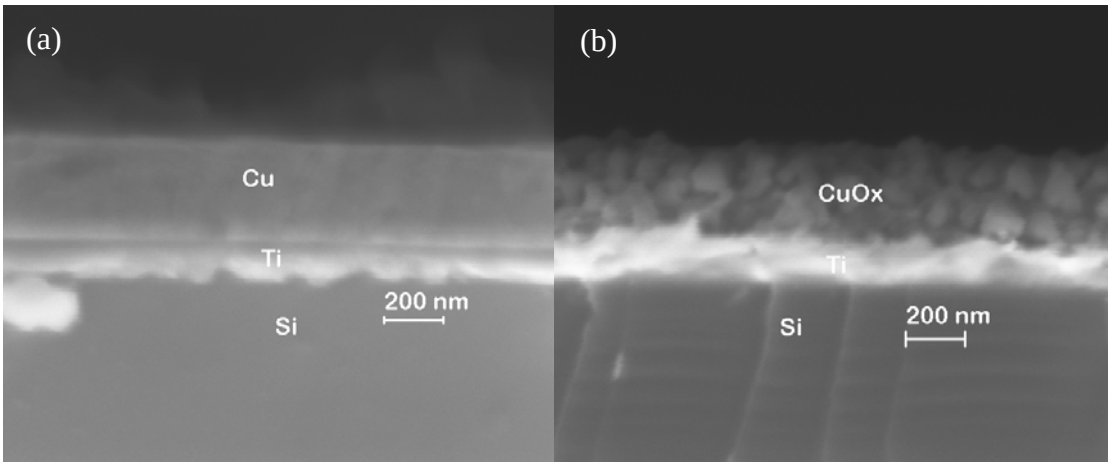

Figure 6.10. Cross-sectional SEMs of blanket Cu samples (~350 nm) (a) before and (b) after oxidation; the sample was oxidized by an O_2 plasma at 1.2 torr and 700 W rf power

6.4.3 Etch Rate Comparisons

6.4.3.1 Cu and SiO_2 Etch Rates

A 1 cm^2 SiO_2 patterned Cu sample, a blanket Cu sample and a blanket SiO_2 sample were etched simultaneously in an H_2 plasma both with and without additives. Figure 6.11 indicates that a 2% O_2 addition resulted in a small reduction in Cu etch rate, but decreased the SiO_2 etch rate more substantially. The DC bias with and without O_2 addition are basically the same (-360 V vs. -369 V). However, as indicated by the OES spectrum (Figure 6.7a), a reduction in the higher emission energy atomic H peaks (H_γ and H_β) and the formation of OH and CO induced by the O_2 addition occurs, which should lead to a decrease in Cu etch rates since H atoms/ions appear to be major contributors to Cu etching. Studies of H_2 plasma etching of SiO_2 in a hollow cathode system have established the importance of hydrogen ions [7]. These results are consistent with our SiO_2 etch rate results (Figure 6.1) in that higher coil power generates higher ion concentrations and increased platen power enhances ion energies.

Generally, addition of electronegative species to an electropositive discharge will profoundly influence the dynamics because of the low-mobility and low-energy of negative ions relative to those of electrons, along with recombination of negative and positive ions [8]. For example, minor additions of O_2, CF_4 or Cl_2 (all highly electronegative species) to low pressure radio frequency Ar (electropositive) plasmas decreased the metastable densities [9]. Since a H_2 plasma is more electropositive than O_2 and CF_4 plasmas, we may also expect a decrease in hydrogen ion density upon addition of these electronegative molecules.

The addition of CF_4 reduced the Cu etch rate to almost half of the original rate, and dramatically increased the SiO_2 etch rate. This result is expected since CF_4 is known to etch SiO_2 [8] efficiently by forming SiF_4. Because polymerization of CFx occurs on

the etching surface, the Cu etch rate will be reduced, even though H can scavenge both C and F. In addition, oxygen from SiO_2 can assist removal of C and thereby reduce the inhibition of Cu etching by C.

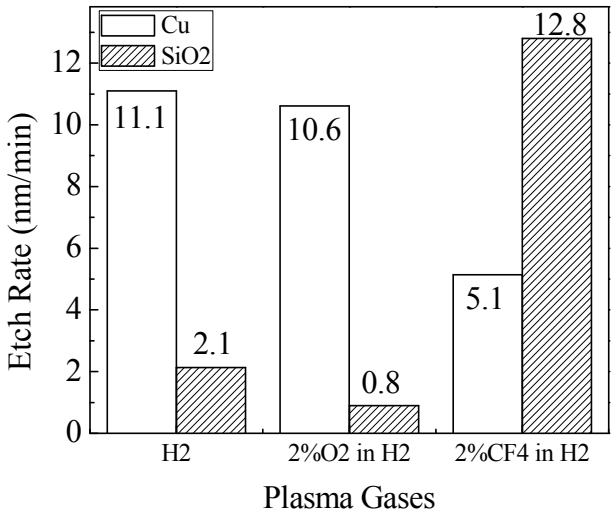

Figure 6.11. Etch rates of SiO_2 and Cu in H_2 plasmas with different additives; the plasma conditions were: RF1=100 W, RF2=500 W, 20 mTorr pressure, 50 sccm total flow rate and 10 ^{o}C.

These contamination studies have also been augmented by SEM evaluation of etched features. Figures 6.12a-c demonstrate that the Cu etch results are similar for a pure H_2 plasma and a 2% O_2 in H_2 plasma. In contrast, a 2% CF_4 in H_2 plasma deposits a CF_x film on the Cu film and sidewall that inhibits etching. However, the H_2 plasma can react with both C and F and thereby remove the CF_x film; thus, even with CF_4 addition, Cu etching still occurs albeit at a reduced etch rate. Furthermore, with CF_4 addition, the remaining SiO_2 mask thickness was reduced due to the higher etch rate relative to that of a pure H_2 plasma.

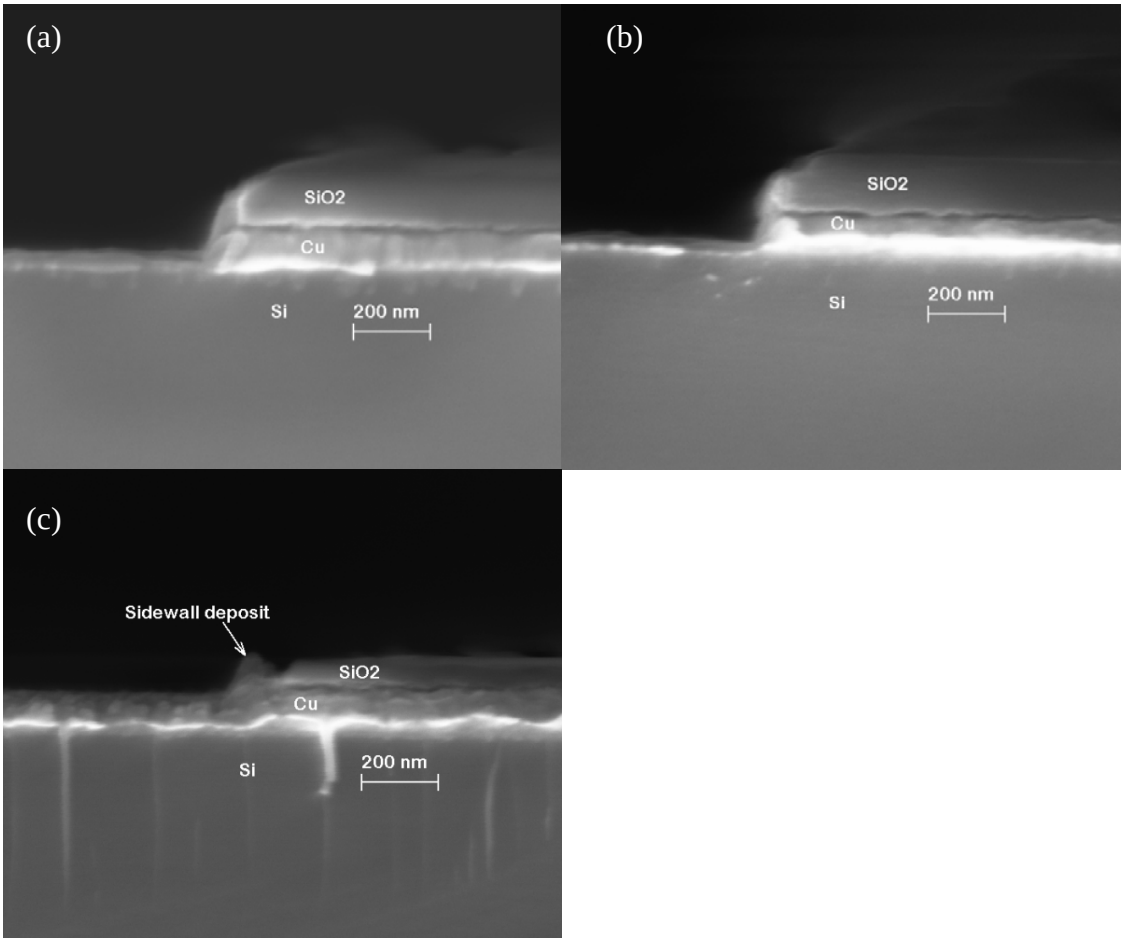

Figure 6.12. Cross-sectional SEMs of patterned Cu samples after etching by (a) H_2; (b) 2% O_2 in H_2; (c) 2% CF_4 in H_2 plasmas. Plasma conditions were: RF1=100 W, RF2=500 W, 20 mTorr pressure, 50 sccm total flow rate and 10 ^oC.

6.4.3.2 Cu Oxide Etch Rates

A patterned Cu sample (masked by SiO_2) was oxidized under the same conditions as in Figure 6.10 and this oxidized sample was subjected to an 8 min H_2 plasma under the following conditions: RF1=100 W, RF2=500 W, 50 sccm total flow rate, 20 mtorr pressure and 10 ^oC electrode temperature. SEM images before and after etching are displayed in Figure 6.13. Etch rate can be estimated from these images; this yields an

etch rate of CuO_x of ~18nm/min. Since volume expansion of the Cu occurs due to film oxidation, the etch rate of the oxidized Cu is much less than that of the Cu etch rate when pure Cu was exposed to H_2 plasma. According to the SEM image, a 3.5 times volume expansion occurs due to Cu oxidation; we thus estimate that the effective oxidized Cu etch rate will be ~18/3.5= 5.1 nm/min, which is an apparent reduction relative to the etch rate of pure Cu under the same conditions (13 nm/min as reported in Chapter 3). These results indicate that the H_2 plasma etching of Cu oxide is similar to the etching of $CuCl_x$, in that Cu etching is impeded by the presence of O in CuO_x. That is, H may first remove O so that the remaining Cu can be etched. Although the etch rate was reduced, a H_2 plasma is able to etch the oxidized Cu sample, indicating the robustness of this plasma etch process.

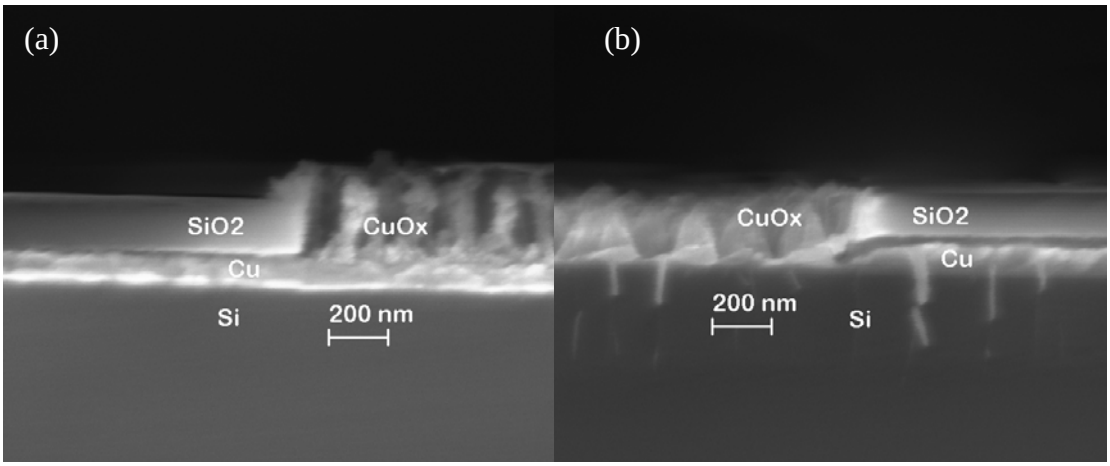

Figure 6.13. Cross-sectional SEMs of oxidized Cu samples (patterned by SiO_2) (a) before and (b) after etching by 8min of H_2 plasma under conditions: RF1=100 W, RF2=500 W, 20 mTorr pressure, 50 sccm flow rate and 10 ^oC

6.4.4 XPS Studies on Blanket Cu/SiO_2 Samples

Post plasma etch XPS results on blanket Cu and blanket SiO_2 samples are shown in Table 6.2. These data demonstrate that the SiO_2 mask reacts with or adsorbs F readily, even with no intentional F addition to the plasma atmosphere. That is, F contamination exists on SiO_2 surfaces, although the SiO_2 etch rate is not directly related to the F concentration on the SiO_2 surface as indicated in Figure 6.2. With a 2% O_2 addition to the etch atmosphere, slight oxidation of the Cu surface took place, while a 2% CF_4 addition incorporates a small amount of F on the blanket Cu surface. All three Cu samples displayed the same C1s peak binding energy at 285.9 eV, which indicates that a CF_x film has not formed on the blanket Cu surface. This result indicates that the H_2 plasma removes the CF_x film during Cu etching, although on patterned Cu samples, a CF_x film did accumulate on the sidewalls (Figure 6.12c). Clearly ion bombardment during the etch assists removal of CF_x on flat surfaces but since essentially no ion bombardment occurs on the sidewall, CF_x residue remains.

It should be noted that with intentional CF_4 addition to the H_2 plasma, lower concentrations of F are observed on SiO_2 sample surfaces than are measured when residual F contamination from the chamber walls is the only F source. Such results suggest that accumulation of F occurs when the concentration is low (resulting in low SiO_2 etch rates) but a higher SiO_2 etch rate induced by the addition of CF_4 leads to the removal of F from surface in the form of SiF_4. These results also indicate that the two ICP reactors that have been employed in this thesis are very different with respect to the dominant contamination present during Cu etching. The Oxford Plasmalab System 100 ICP-RIE (ORNL) has higher concentrations of fluorine, while the Plasma Therm ICP (Georgia Tech) is has more residual nitrogen and oxygen. Nevertheless, both reactors

gave very similar etch results, which demonstrates that at least at the levels present in the respective reactors, these contaminants do not play a critical role in the H_2 plasma etch process for Cu.

Table 6.2 Comparison of atomic composition (from XPS spectra) on Cu and SiO_2 samples after H_2 plasma etching with and without selected additives

Element (on Cu sample)	At.% (H_2 plasma)	At.% (2% O_2 in H_2 plasma)	At.% (2% CF_4 in H_2 plasma)
Cu2p	41.06	33.77	32.12
O1s	34.9	40.46	33.0
C1s	19.18	19.3	19.05
N1s	4.86	5.4	5.29
F1s	N/A	1.07	10.55
Element (on SiO_2 sample)	At.% (H_2 plasma)	At.% (2% O_2 in H_2 plasma)	At.% (2% CF_4 in H_2 plasma)
Si2p	29.51	29.02	33.5
O1s	52.57	54.08	52.26
C1s	4.97	4.17	3.59
N1s	3.09	3.77	4.79
F1s	9.86	8.97	5.85

6.5 Conclusion

Preliminary studies of the effects of a H_2 plasma on SiO_2 masks indicated that although the SiO_2 etch increases with increases in platen or coil power, the etch selectivity of Cu over SiO_2 is between 5 and 10 under the etch conditions investigated, which should allow reasonable control of such a patterning process. SiO_2 etch rate trends with temperature are analogous to those observed for Cu in H_2 plasmas. Although F contamination is present, the correlation between F concentrations (which arise from residue outgassing from chamber walls) and Cu/SiO_2 etch rates are not yet clear. However, both effects will be affected by temperature changes.

Optical emission spectroscopy and XPS detected several contaminants (F, O, N, C) in the H_2 plasma etching system. Intentional addition of small amounts of O_2 or CF_4 into the plasma system allowed preliminary indications of the effect of these species on Cu etching. OES results indicated that only H-related emission lines changed during the Cu etch process. However, the contaminants can inhibit Cu etch rates. That is, oxygen oxidizes the Cu surface and thereby reduces the Cu etch rate, since copper oxide has a lower etch rate than does Cu in a H_2 plasma. Carbon and fluorine contamination results in the deposition of a fluorocarbon film, which also inhibits etching, although a H_2 plasma can remove this film and thereby prevent etch termination. Therefore, despite the fact that some amount of contamination is unavoidable in the etch systems used in our studies, these results have demonstrated the robustness of the H_2 plasma etching process for Cu, since similar etch results are possible in different reactors containing different contaminants.

6.6 References:

[1] R. W. B. Pearse and A. G. Gaydon, *The Identification of Molecular Spectra*, Fourth ed. London: Chapman and Hall Ltd., 1976.

[2] I. P. Herman, *Optical diagnostics for thin film processing*. San Diego, CA: Academic Press, 1996.

[3] T. E. F. M. Standaert, C. Hedlund, E. A. Joseph, G. S. Oehrlein, and T. J. Dalton2, "Role of fluorocarbon film formation in the etching of silicon, silicon dioxide, silicon nitride, and amorphous hydrogenated silicon carbide," *Journal of Vacuum Science & Technology A,* vol. 22, p. 8, 2004.

[4] F. Wu, G. Levitin, and D. W. Hess, "Mechanistic Considerations of Low Temperature Hydrogen-Based Plasma Etching of Copper," *The Journal of Vacuum Science and Technology B,* vol. 29, pp. 011013-1-7, 2010.

[5] R. G. Wilson, *Ion Mass Spectra*: John Wiley & Sons, Inc., 1974.

[6] H. Ohmi, H. Kakiuchi, K. Nishijima, H. Watanabe, and K. Yasutake, "Low-Temperature Crystallization of Amorphous Silicon by Atmospheric-Pressure Plasma Treatment in H2/He or H2/Ar Mixture," *Japanese Journal of Applied Physics,* vol. 45, p. 8848, 2006.

[7] O. Peña, S. Muhl, W. López, L. Rodríguez-Fernández, and J. L. Ruvalcaba-Sil, "Hydrogen plasma etching of silicon dioxide in a hollow cathode system," *Thin Solid Films,* vol. 518, pp. 3156-3159, 2010.

[8] M. A. Lieberman and A. J. Lichtenberg, *Principles of plasma discharges and materials processing*, 2nd ed. Hoboken, N.J.: Wiley-Interscience, 2005.

[9] B. K. McMillin and M. R. Zachariah, "Two-dimensional laser-induced fluorescence imaging of metastable density in low-pressure radio frequency argon plasmas with added O-2, Cl-2, and CF4," *Journal of Applied Physics,* vol. 79, pp. 77-85, Jan 1 1996.

CHAPTER 7

CONCLUSIONS AND FUTURE WORK

7.1 Conclusions

Damascene technology has been the dominant method for patterning of Cu metallization in IC fabrication due to the inability to develop a fully plasma-based subtractive etch process for Cu at low temperatures. But a critical "size effect" problem has arisen that cannot be solved by the traditional damascene process. In this thesis, we investigated possible approaches to a fully plasma-based etch process for Cu. Specifically, we described low temperature (below room temperature) Cu etch processes that use either (i) a two-step plasma etch sequence that involved a Cl_2 plasma followed by a H_2 plasma , or (ii) a one step H_2 plasma process.

In the two-step Cu etch process at 10 ^oC, Cu chlorinated rapidly during the 1^{st} step (Cl_2 plasma) to form a mixture of CuCl and $CuCl_2$ that resides at the Cu surface. The subsequent H_2 plasma (2^{nd} step) removed a certain depth of the $CuCl_x$ formed. XPS analyses indicated that the concentration of CuCl on the Cu surface increased greatly after the H_2 plasma treatment. Both of these observations were consistent with the thermodynamic premise that only $CuCl_2$ was removed as a result of reduction by the H_2 plasma to form the more volatile Cu_3Cl_3, as described by Eqn (1.1). Although patterning of large (several micron) feature sizes was possible using this two-step process with an SiO_2 mask layer, the patterns displayed line edge roughness and sidewall/edge residues. In order to mitigate these issues, plasma parameters such as the Cl_2 plasma exposure time, applied substrate power and residence time of the H_2 plasma were altered. Although

these changes improved the pattern definition, residue removal was more effective upon the addition of Ar to the H_2 plasma (2^{nd} step). Despite the obvious improvement in pattern definition by Ar addition, a pure Ar plasma was unable to effectively remove $CuCl_x$ in the second (post chlorination) step. These results indicate that the H_2 plasma was the limiting step in Cu removal and that chemical effects were critical to Cu removal during the H_2 plasma step.

Since the H_2 plasma played an essential role in the two-step etch process, use of an H_2 plasma to etch Cu (without prior chlorination) was investigated. These studies demonstrated that a single step process using an H_2 plasma etches Cu at a reasonable etch rate (~13 nm/min) at 10 ^{o}C with good selectivity to the Ti adhesion layer as well as to the SiO_2 hard mask. Although, a pure Ar plasma did not etch Cu effectively, addition of Ar (50%) to the H_2 plasma improved the Cu etch rate to 16 nm/min; unfortunately, the anisotropy of the etch degraded with this addition. These observations indicated that the H_2 plasma etching of Cu must involve both physical and chemical components since physical sputtering (Ar plasma) alone cannot remove Cu without leaving etch residues under these etch conditions. However, when enhanced ion bombardment is supplied by addition of Ar to the H_2 plasma, the Cu etch rate increased by more than 20%.

Possible chemical and physical mechanisms that could account for the H_2 plasma etching of Cu films have been considered. From the standpoint of chemical considerations, no detectable Cu re-deposition during the etching of a 4” diameter substrate indicates that the Cu etch product(s) has (have) sufficient volatility to readily leave the surface under the etch conditions explored; this process is not strictly a physical (sputtering) process because pure Ar plasma etching under the same etch conditions gave

extensive residues. However, no Cu related species were detected by mass spectroscopy of H_2 plasmas during the etch process, indicating that whatever Cu etch product desorbs is either unstable or deposits readily within the chamber or tubing leading to the mass spectrometer. These facts suggest that the etch product is a Cu hydride, although no direct evidence has been obtained for this conclusion.

With regard to physical components of the etch process, ion bombardment plays a critical role as evidenced by the fact that the Cu etch rate is proportional to the rf power applied to the electrode which alters ion energy and to the rf power supplied to plasma (through the coil in the ICP reactor system) which alters ion density. In addition to ion bombardment effects, photon flux may be involved in the H_2 plasma Cu etch mechanism. This possibility arose from the ability to etch Cu in a He plasma. Although both He and Ar could etch Cu films, the etch processes left residues on the etching surface and substrate. These results further confirm the importance of a chemical component to an effective etch process and indicate that H_2 plasmas possess unique chemical and physical attributes that allow effective and efficient Cu etching at low temperatures. Experiments that employed zero bias (electrode) power and zero coil (plasma generation) power indicated that both ion bombardment and chemical reaction are critical to successful H_2-based plasma etching of Cu, although ion bombardment appears to be the primary contributor to the etch rate increase. These studies suggested that the mechanism(s) accounting for the H_2 plasma etching of Cu involved a combination of UV photon impingement, ion bombardment and H interaction with Cu surfaces.

Optical Emission Spectroscopy (OES) and temperature variation were used to gain further insight into both the two-step (Cl_2 + H_2) and the single step H_2 plasma Cu

etch processes. Atomic Cu emission lines were observed in the H_2 plasma (for single step H_2 plasma and the H_2 plasma step in the two-step process), but no other Cu species emission (i.e., etch products that might have desorbed) were detected. Cu hydrides are the likely etch products, given the plasmas used. However, Cu hydrides are reported to be unstable, which may explain why Cu hydride emissions were not detected in OES spectra. That is, if CuH_x desorbed from the etching surface, these species likely dissociated upon electron impact collisions, resulting in the detection of only atomic Cu emission. Such assertions are also consistent with the abnormal behavior of Cu etch rates as a function of temperature. In the single step H_2 plasma etch process, Cu etch rate displayed two different trends in the temperature range between – 150 ^{o}C and 150 ^{o}C; specifically, the etch rate increased with temperature up to 10 ^{o}C and decreased with increasing temperature above 10 ^{o}C. Furthermore, this same trend was observed with Cu emission intensities dependence on temperature. These results suggest a change in etch mechanism that is induced by the unstable nature of Cu hydrides. That is, below a certain temperature (10^{o}C under these etch conditions), Cu was removed in the form of Cu hydrides; above this temperature, Cu was removed mainly through physical sputtering although enhanced by the chemical interactions with H.

The results using the single step H_2 were compared to those of the two step process by evaluation of the OES spectra. Cu emission intensities as a function of time in the 2nd step of the two-step process (H_2 plasma step) indicated that the 1st step (Cl_2 plasma step) contributed minimally, if at all, to the removal of Cu. In contrast, the Cu chlorides formed during the 1st step (chlorination) interfered with the etch (removal) of Cu by the H_2 plasma, apparently because H needed to remove the Cl, through the

formation of HCl. Although this conclusion has not yet been proven conclusively, this interpretation establishes a consistent mechanistic connection between the single step and the two-step H_2 plasma-based Cu etch processes.

Because photoresist degrades readily in the H_2 plasma, a hard mask, SiO_2, has been used for Cu patterning. For the most part, SiO_2 is a good choice with respect to selectivity since etch rates in H_2 plasmas are controlled by ion bombardment flux. A number of preliminary experiments were performed in an attempt to gain insight into the etching of SiO_2 in the Cu etch plasmas. Unfortunately, we currently are unable to propose a complete explanation for the observed (unexpected) SiO_2 etch rates trends as a function of temperature. This inability to more fully understand the SiO_2 etch results relates to the fact that all three reactors that have been used for our etch studies have a complex gas phase chamber environment that is induced by the contaminants within the etch chamber that arise from the use of these chambers/reactors for the fluorine-based etching of oxide materials. The studies and results we obtained therefore revolve around consideration of the F, O, N and C contaminants observed. By intentionally adding CF_4 or O_2 into the H_2 plasma, the influence of F, O and C were investigated by OES, etch rates and XPS analysis. Although these contaminants did affect the H_2 plasma etching of Cu to some extent by forming fluorocarbons or oxides, the H_2 plasma can remove these impurities; therefore, the etching process proceeded and minimal interference with the overall process was observed. Furthermore, the fact that the H_2 plasma etching of Cu was performed successfully in several different reactors with different configurations and impurity content demonstrated the robustness of this unique etch process.

7.2 Future Work

This thesis described the development of a novel, simple, fully plasma-based low temperature Cu etch process, which displays very promising results and offers the potential of subtractive etching for Cu interconnect fabrication and manufacture; whether this process can be implemented in a manufacturing process and thereby replace the current damascene technology is unclear at this time. The results obtained have identified several future needs and directions necessary to assess the suitability of this process for Cu metallization in IC fabrication.

Although we gained insight into some of the mechanistic considerations of etching Cu in H_2 plasmas, a clear understanding of this mechanism has not been established. In particular, the Cu etch products, i.e., species desorbing from the etching film have not been identified. Probing the relevant etch products/species will require in-situ monitoring of the surface during the etch process, perhaps using FTIR. Alternatively, analysis of the surface by XPS after etch but before the surface is exposed to atmospheric conditions could offer information regarding bonding structures and product formation. These approaches will require an integrated system that either allows real-time monitoring or transfer of samples for analyses under UHV conditions. In order to investigate specific chemical interactions, downstream plasmas may allow pure chemical information to be generated (i.e., without ion, electron or photon bombardment) so that H interaction/reactions with Cu can be probed. Again, this may require in-situ or at least controlled atmosphere transfer of samples after the etch process.

OES is still the most simple and informative way to explore plasma characteristics real time. Although OES analyses were performed in this thesis, quantitative information regarding the relative species concentrations has not been obtained. Actinometry is a method wherein an inert tracer gas such as Ar is added to the plasma atmosphere. The tracer is selected so that it exhibits a similar electron excitation threshold and cross section to that of the species of interest, in this case H, to assist quantitative changes in species concentration as a function of plasma parameters [1-2]. Such studies may permit a quantitative relationship between Cu emission intensities and etch rates and contamination issues to be established.

An etching process that is suitable for large scale manufacturing must meet several requirements: selectivity, anisotropy, adequate etch rates, uniformity, surface quality and reproducibility [3-4]. Based on these requirements, further works need to be performed in order to investigate the feasibility of developing a suitable Cu metallization process for future device generations.

Our investigations used SiO_2 as the etch mask material and Ti as the underlying adhesion layer; good selectivity was observed. However, other mask choices need to be considered, since SiO_2 has its own limitations, for example, the deposition process of SiO_2 may oxidize Cu. Current photoresists cannot withstand exposure to H_2 plasmas; thus "hard masks" such as SiNx, metal masks or even carbon masks should be investigated. Tantalum (Ta) is the barrier layer that is used extensively in the IC industry for Cu metallization; therefore, the etch characteristics and selectivity of Ta in H_2 plasmas also needs to be investigated.

Control of the etched profile through the control of anisotropy is another important factor especially for current very small (<50 nm) geometries. In particular, we discussed previously the two major contributors of resistivity increase in the sub-100 nm regime; in addition to electron scattering at grain boundaries, the electron scattering at surfaces also plays an important role especially for rough surfaces. Thus the line edge roughness needs to be carefully controlled by optimizing the plasma conditions.

Currently, the highest etch rate that we have obtained was ~ 20 nm/min at high applied power levels; this rate may still not be sufficient for the throughput needed for large scale manufacturing. Additives to the H_2 plasma may allow higher etch rates to be obtained.

Cu re-deposition on the reactor chamber walls will be a critical issue for continuous operation of production equipment, since plasma/reactor potentials, currents, and thus control of plasma processes depend upon wall coatings. Thus “coupon” studies, performed by sticking substrate (coupon) samples to the chamber wall should be performed to investigate the re-deposition of etch products during the etch process.

Because H is very reactive species, potential damage to the surface of other materials involved in IC fabrication will need to be investigated, this is particularly important for barrier materials beneath the Cu layer.

Finally, since the purpose of replacing damascene technology with a subtractive plasma-based process is to ensure lower Cu resistivity at small feature size, resistivity measurements must be performed to confirm this advantage. However, such measurements must be performed on Cu patterns with good anisotropy and low edge roughness; thus such studies must await further etch process development.

7.3 References:

[1] J. W. Coburn and M. Chen, "Optical emission spectroscopy of reactive plasmas: A method for correlating emission intensities to reactive particle density," *Journal of Applied Physics*, vol. 51, pp. 3134-3136, 1980.

[2] I. P. Herman, *Optical diagnostics for thin film processing*. San Diego, CA: Academic Press, 1996.

[3] M. A. Lieberman and A. J. Lichtenberg, *Principles of plasma discharges and materials processing*, 2nd ed. Hoboken, N.J.: Wiley-Interscience, 2005.

[4] A. Grill, *Cold plasma in materials fabrication: from fundamentals to applications*. Piscataway, NJ: IEEE Press, 1994.

APPENDIX A

AUTHOR'S PUBLICATIONS

[1] F. Wu, G. Levitin, and D. W. Hess, "Mechanistic Considerations of Low Temperature Hydrogen-Based Plasma Etching of Copper," The Journal of Vacuum Science and Technology B, vol. 29, pp. 011013-1-7, 2010.

[2] F. Wu, G. Levitin, and D. W. Hess, "Subtractive Etching of Cu with Hydrogen-based Plasmas," in ECS Transactions, Las Vegas, 2010, pp. 157-162.

[3] F. Wu, G. Levitin, and D. W. Hess, "Low Temperature Etching of Cu by Hydrogen-Based Plasmas," ACS Applied Materials & Interfaces, vol. 2, pp. 2175-2179, 2010.

[4] F. Wu, G. Levitin, and D. W. Hess, "Patterning of Cu Films by a Two-Step Plasma Etching Process at Low Temperature," Journal of The Electrochemical Society, vol. 157, pp. H474-H478, 2010.

VITA

FANGYU WU

Fangyu Wu was born in Panzhihua, south of Sichuan province, China. She attended PanGangYiZhong high school, and received both her B.S. and M.S. in Chemical Engineering from Tsinghua University, Beijing, China in 2001 and 2004, respectively. Before coming to Georgia Tech to pursue a doctorate in Chemical Engineering, she was working in a company making animations. She joined the school of ChBE at Georgia Tech in August 2006, under the supervision of Dr. Dennis Hess. When she is not working on her research, Fangyu still enjoys the fun from animations.